1967 Annual Progress Report
of
Palaeogeophysics Research in Japan

1 9 6 7

Osaka

Preface

Paleogeophysics is the study to determine some of the Earth's intrinsic properties using information retained in rocks and other terrestrial materials. One of the most appropriate studies worthy of this name is Paleomagnetism, in which the remanent magnetization of rocks is utilized as a fossil of the past geomagnetic field. In these investigations many concepts and hypothesis have been fruitfully established. Thus it was desired by many scientists in Japan that study along the above mentioned line of thought be extended to much broader aspects in geophysics, not being merely restricted to geomagnetism alone.

Such fossil information as that revealing the gravity field on the past Earth's surface, past pressure and temperature prevailing in the Earth's crust, velocity of the Earth's rotation in geologic past, distribution of the past continents, the frequency and magnitude of the past earthquakes, or the past volcanic activities of the Earth, could probably be found in many rocks, if a careful investigation was made. In this short report are gathered several contributions with the purpose mentioned above, although the greater part of the report is concerned still with results of Paleogeomagnetism and its relevant studies.

Naoto Kawai

Toyonaka, Osaka

February, 1968

C o n t e n t s

1. A Method for Palaeogravity

K. Yaskawa

Geological Institute, Fukui University

(I) Introduction

Although information on ancient gravity is very important from the view point of the theory of the evolution of the earth, it has not been collected because of the difficulty in finding means reflecting the ancient gravity. Since sediments have been deposited in the gravitational field, they should indicate the gravity at the time of deposition. Aqueous deposits, however, are usually subject to too many factors effective during the deposition, and are so complicated that for the present it is almost hopeless to distinguish the effect of gravity from the others. On the other hand, aeolian deposits are much simpler and seem better for giving information on the ancient gravity. In particular, as aeolian sandstone is subject to only two major factors, i.e. the wind and the gravity, at the time of deposition, it seems to be most suitable for this purpose.

(II) Aeolian cross-stratification

Cross-stratification, cross-lamination or false-bedding is a well-known feature of aeolian sandstone, and it is believed to be the remnant of the successive foreslopes of sand dunes advancing with the dominant wind. The sand grains are transported up on the back slope of sand dune by the dominant wind and fall down over the foreslope. Therefore, the angle of the foreslope of sand dunes is the angle of repose of dry sand (about 33°). Sometimes cross-stratification shows the backslope of sand dunes, the angle of which is usually less than 12°. The cross-stratification is very well-known as an indicator of the ancient wind direction (Reiche 1938, Shotton 1937, Opdyke 1961), as the direction of the maximum angle of cross-stratification shows the direction of the dominant wind direction at the time of deposition. It may also show us the other factor, the gravity, at the time of deposition.

(III) The angle of repose

According to the result of Fowler et al. (1959), the angle of slide of powder on a solid plane is given by the following equation:

$$\phi \tan \phi_s = \frac{A}{\psi^2} + B\left(\frac{\varepsilon}{d}\right)^{\frac{1}{2}} + C \cdot s + D,$$

where ϕ_s , ψ , ε , d and s are the angle of slide of powder on a solid plane, the roundness of grains, the roughness of plane, the typical diameter of grains and the specific gravity of grains respectively. The constants A, B, C and D were determined as follows from the experiments using various kinds of grains such as several kinds of sands, lead shots, wheat grains, rice grains, rapeseed, sugar etc.. That is; in the ranges of $d = 0.27$ to 4.00 mm, $\psi = 0.67$ to 1.00,

$s = 1.103$ to 11.340, and $\varepsilon = 0.272$ to 3.134 mm,

A, B, C and D were 0.2110, 0.3436, -0.0171 and 0.1834 respectively.

Regarding the angle of repose (ϕ_r), no systematic and quantitative relation with these factors has been given such as ϕ_s . So, let us use the maximum of ϕ_s on ε as ϕ_r , that is;

$$\phi_r = (\ \phi_s\ (\ \varepsilon\ )\ )_{max}.$$

This approximation is acceptable from the fact that ϕ_s is usually smaller than ϕ_r , or more precisely ϕ_s increases with ε but not in excess of ϕ_r . In this case, as ε is constant, the equation is to have the form of

$$\tan \phi_r = \frac{A}{\psi^2} + \frac{B}{\sqrt{d}} + C \cdot s + D,$$

where A, B, C and D are the constants to be determined by experiments.

The following fact is wellknown about aeolian sands; they are usually very well sorted and show very high sphericity and roundness values due to their mode of transport (Opdyke 1961). Therefore, for ϕ_r of aeolian sands or dune sandstones, ψ can be regarded as a constant and, if we use only the sandstones whose grain sizes are nearly equal, d also may be regarded as a constant. Finally, we have the equation for the angle of repose of aeolian sands;

$$\tan \phi_r = C \cdot s + K,$$

where C and K are the constants to be determined by experiments. If it is admissible to use the same value of C as in the equation of ϕ_s, i.e. $C = -0.0171$, we can roughly estimate the rate of change of the angle of repose with the gravity. In the equation of ϕ_s, evidently $C \cdot s$ being the term relating to the pressure of grains to the plane, s has to be greater when the gravity is greater. In other words, s is a function of the gravity and not of the usual specific gravity. That is;

$$s(g) = \left(\frac{m}{m_0 \; g_0}\right) g.$$

Replacing s in the equation of ϕ_r with $s(g)$, we have

$$\tan \phi_r = -0.0171 \left(\frac{m}{m_0 \; g_0}\right) g + K,$$

where m_0 and m are the mass of water and the mass of sand grains of the unit volume at the standard condition respectively, and g_0 represents the gravity in situ at the present, and g represents the ancient gravity having acted on the sand grains at the time of making a slope. Assuming that $m = 3.0$ and $\phi_{r0} = 33.0^{\circ}$ when $g = g_0$, we can estimate ϕ_r for $g = 2g_0$ as follows:

$$\tan \phi_{r0} = -0.0171 \left(\frac{m}{m_0 \; g_0}\right) g_0 + K$$

$$\tan \phi_r = -0.0171 \left(\frac{m}{m_o \; g_o}\right) (2g_o) + K$$

$$= \tan \phi_{ro} - 0.0171 \; m$$

$$= 0.6494 - 0.0513 - 0.5981$$

$$= \tan 30^\circ \; 53'$$

and we obtain

$$\phi_r = 30^\circ \; 53'.$$

(IV) Discussion

There are the following three difficulties in this method, and so, in some cases we may be unable to reconstruct the angles of ancient sand dunes from that of cross-stratification:

(1) As shown above, the difference of angles seems to be rather small compared with that of gravities. It is required to measure the angles of cross-stratifications with an accuracy of 1 minute for the 1 % difference of the present gravity.

(2) The second problem is knowing the ancient horizontal plane. The base of sand dunes is not always flat and also not always horizontal. Without knowing the ancient horizontal surface, it is impossible to obtain the correct angles of sand dunes.

(3) The third is whether the ancient dunes have kept the same shape, or whether the ratio of unit length of the vertical axis of dunes to that of the horizontal axis is unchanged. It is very probable that any sedimentary rock has been squeezed along its vertical axis, and as a result, the ratio has been changed.

In these three difficulties, the first and the second are not so serious for the rough estimation of the ancient gravity that we cannot say anything. However, without overcoming the third difficulty, it is almost impossible to say anything about the ancient gravity.

In the equation deduced approximately from the equation of the angle of slide, ϕ_r is an arctangent function of g as shown above. Actually, it seems to be an exponential function of g, i.e.

$$\phi_r = A \cdot e^{-B \cdot g} + C$$

on the analogy of the relation between the fluidity and the shearing stress in the structural viscosity (Reiner 1960) and of the lateral shape of volcanos (Takizawa 1931). To determine the equation experimentally, the author tried to measure the angle of repose for various gravity values using a centrifuge, but the result was unsuccessful because of the disturbance due to the acceleration or the shock at the start or stop.

References

Reiche, Parry, (1938), An analysis of cross-lamination, the Coconino sandstone, J. Geol., 46, 905-932.

Shotton, F.W., (1937), The lower Bunter sandstones of North Worcestershire and East Shropshire, Geol. Mag., 74, 534-553.

Opdyke, N.D., (1961), The palaeoclimatological significance of desert sandstone, Descriptive Paleoclimatology, edited by A.E.M.Nairn, Interscience Publishers Inc., 45-60.

Fowler, R.T. and W.B.Chodziesner, (1959), The influence of variables upon the angle of friction of granular materials, Chem. Eng. Scie., 10, 157-162.

Reiner, Markus, (1960), Deformation, strain and flow, H.K.Lewis & Co. Ltd.

Takizawa, T., (1931), Lateral shape of volcanos, Geogr. Rev. Japan, 7, 799-811, in Japanese.

2. The Gravity in the Geological Past

K. Yaskawa

Geological Institute, Fukui University

(I) Introduction

Was the ancient gravity smaller than at present? Or larger? Unchanged? Some suppose it to be smaller because the annihilation of the giant reptiles, dinosaurs, might be caused by increasing gravity[1]. Some may suppose it to be larger as would be deduced from a smaller paleoradius. But none give the direct and quantitative value of paleogravity. In this paper actual paleogravity values will be brought to light using the aeolian sandstones of the Triassic and the Permian ages.

(II) Method

In the previous paper[2] the author discussed the method by which the paleogravity values are expected to be obtained. That is, the maximum value of the angle of cross-stratification (ϕ_r) is the angle of repose of dry sand and it is a function of the gravity being expressed by the equation

$$\tan \phi_r = -0.0171 \left(\frac{m}{m_o} \right) \left(\frac{g}{g_o} \right) + K,$$

where m_o and m are the mass of water and that of sand grains of the unit volume at the standard condition respectively. g_o represents the present gravity and g the ancient gravity.

Assuming $m_o=1.0$, $m=3.0$ and $\phi_r = 32^\circ$ at $g=g_o$, we get

$$K = 0.6762$$

$$\therefore \tan \phi_r = -0.0513 \left(\frac{g}{g_o} \right) + 0.6762.$$

At the same time the author pointed out the 3 problems in this method, namely, (1) The error due to the fact that the small difference of angle corresponds to the large difference of gravity. (2) The difficulty of determining the ancient horizontal plane in the aeolian sandstone. (3) The difficulty of obtaining the ratio of lateral and vertical deformations without which we cannot rebuild the original angle of dunes. Among these 3 problems the first one should be settled by the statistical method. If we measure numerous numbers of the maximum leeward angles (the maximum angle of the foreslope of dunes) at as many localities as possible, we may expect to get a resonable value of the leeward angle. The only way to know the ancient horizontal plane without which we cannot determine the angle of the ancient dunes is to find a layer of aqueous sediments with which the aeolian sandstone layer is covered or on which it is spread. The most difficult problem is the third one. To know the difference between lateral and vertical deformations, generally it is necessary to find out some characteristics like the anisotropy of physical constants or mineral composition corresponding to the difference of the deformations. If it is possible, however, to get the data about the angle of the windward slope of the ancient dunes, we can estimate the original angle of leeslope as follows:

$$\tan \phi_r = \frac{\tan\phi_m \cdot \tan\theta_r}{\tan\theta_m},$$

where ϕ_r and θ_r are the original angles of the leeslope and the windward slope respectively, and ϕ_m and θ_m are those angles obtained from the field data. The windward slope of the dune is regarded as a wind erosion surface and to suffer little effect of gravity, the angle of which is usually believed to be 12° or 13° for active sand dunes.

(III) The Triassic paleogravity

In 1937, Shotton[3] reported very precisely his investigations of the Lower Bunter Sandstones. He examined at 476 exposures and took 1142 readings of the maximum angles, in which 793 readings were taken on bedding planes (i.e. leeslope) and 349 readings were on erosion planes (i.e. windward slope). His result is shown in Fig. 1. The upper diagram shows the frequency distribution of the dip angle of bedding planes and the lower shows that of erosion planes. From these diagrams we can get 26° and 11.5° for the maximum angle of bedding plane (leeslope) and that of erosion plane (windward slope) respectively, as the most probable value. Then, if we adopt 12.5° as the angle of windward slope of modern sand dunes, as the original angle of bedding plane, we obtain

$$\tan \phi_r = \frac{\tan\theta_r \cdot \tan\phi_m}{\tan\theta_m}$$

$$= \frac{\tan 12.5^\circ \times \tan 26^\circ}{\tan 11.5^\circ}$$

$$= \frac{0.2217 \times 0.4877}{0.2035}$$

$$= 0.5365$$

$$\therefore \phi_r = 28^\circ 20',$$

as mentioned in the previous section. If we take 32° as the angle of leeslope of modern sand dunes, we can calculate the paleogravity (g) in the early Triassic period as follows:

$$\tan \phi_r = -0.0513 \left(\frac{g}{g_0}\right) + 0.6762$$

$$\tan 32^\circ = 0.5365 = -0.0513 \left(\frac{g}{g_0}\right) + 0.6762$$

$$\frac{g}{g_0} = \frac{0.1397}{0.0513} = 2.72$$

(IV) The Permian paleogravity

Fig. 2 shows the frequency distribution of the dip angle of bedding plane of the Coconino Sandstones, the Lower Permian aeolian sandstones of North America, and was drawn using the results of Reiche[4] who had introduced the use of the stereographic polar net for representation of cross-bedding attitudes. From the curve we can determine 22° as the most probable angle of leeslope. He did not take, however, any readings on erosion planes or did not distinguish them from those on bedding planes. Therefore, in this case we have not the angle of windward slope and hence we cannot determine the original angle of leeward slope. So, let us assume that the rate of compression of the Permian rock is equal to that of the Triassic rock, and we can obtain a result for Permian as follows:

$$\tan \phi_r = \frac{\tan 12.5^\circ \times \tan 22^\circ}{\tan 11.5^\circ}$$

$$= \frac{0.2217 \times 0.4040}{0.2035} = 0.4444$$

$$\therefore \phi_r \fallingdotseq 24^\circ$$

As mentioned already, ϕ_r is a function of g expressed by the equation

$$\tan \phi_r = -0.0513 \left(\frac{g}{g_o}\right) + 0.6762.$$

Therefore, we obtain

$$\frac{g}{g_o} = \frac{0.6762 - 0.4444}{0.0513} = 4.51.$$

This value seems to be too large. Reiche took 277 readings over the Coconino Sandstones, and it does not seem to be sufficient for this statistical treatment as is seen in Fig. 2. If we have many more readings at more exposures, we may have the maximum peak of the frequency curve at around 24°. In this case we will obtain 3.63 as g/g_o.

(V) Paleoradius of the Earth

If we regard the mass of the Earth as constant through geological time, we can directly calculate the paleoradius of the Earth using these paleogravimetric data. That is, for the early Triassic period,

$$\frac{r}{r_o} = \frac{1}{\sqrt{2.72}} = 0.61,$$

where r and r_o are the paleoradius and the present radius of the Earth, respectively.

For the early Permian period,

$$\frac{r}{r_0} = \frac{1}{\sqrt{4.51}} = 0.47,$$

or if we use 3.63 as g/g_0,

$$\frac{r}{r_0} = \frac{1}{\sqrt{3.63}} = 0.53.$$

Creer[5),6)] described precisely the Earth's expansion theory connecting with the continental drift. If the radius of the Earth was about 0.55 times the present value, all the Earth's surface would be covered with the sialic continental shell. The Earth of about 4 billion years ago, he thinks, would be in this state. The paleoradius calculated from the data of paleogravity, however, shows us that the Earth of the early Permian was in this state.

This result is not necessarily unacceptable, but we should recalculate it after obtaining the more exact relation between the angle of repose and the gravity. The equation used here in these calculations may not be perfect and it may only give us approximations in a short range, because it is impossible that the angle of repose becomes negative under the finite gravity as in this equation.

(VI) Discussion

Shotton[3)] mentioned that as the Lower Bunter cannot be assumed to have a level base, the Middle Bunter Pebble Beds including parallel beds of clay and silt occurring immediately beside the Lower Bunter were used for tilting correction of the readings. The latter inclines in a general eastward direction (4° or 5° at most), and that transport and deposition was affected by a prevailing east wind. Therefore, each angle of leeward slope is not larger than the corrected value and that of windward slope is not smaller. It means that the gravity value calculated above gives the lower limit of this age.

In this paper, the angle of leeward slope of the active dune is regarded as 32°, but it should be checked. For this purpose, it is necessary to make frequency distribution curves of leeward slope and of windward slope in the modern dune field.

References

1) Colbert, E.H. (1961)

Dinosaurs, E.P.Dutton & Co., Inc., New York.

2) Yaskawa, K.

A method for paleogravity

1967 Ann. Progress Rep. Palaeogeophysics Res. Japan, 1-5.

3) Shotton, F.W. (1937)

The Lower Bunter Sandstone of North Worcestershire and East Shropshire

Geol. Mag., vol. 74, 534-553.

4) Reiche, P. (1938)

An analysis of cross-lamination, the Coconino Sandstone

J. Geol., vol. 46, 905-932.

5) Creer, K.M. (1965)

An expanding Earth?

Nature, vol. 205, 539-544.

6) Creer, K.M. (1965)

Tracking the Earth's continents

Discovery.

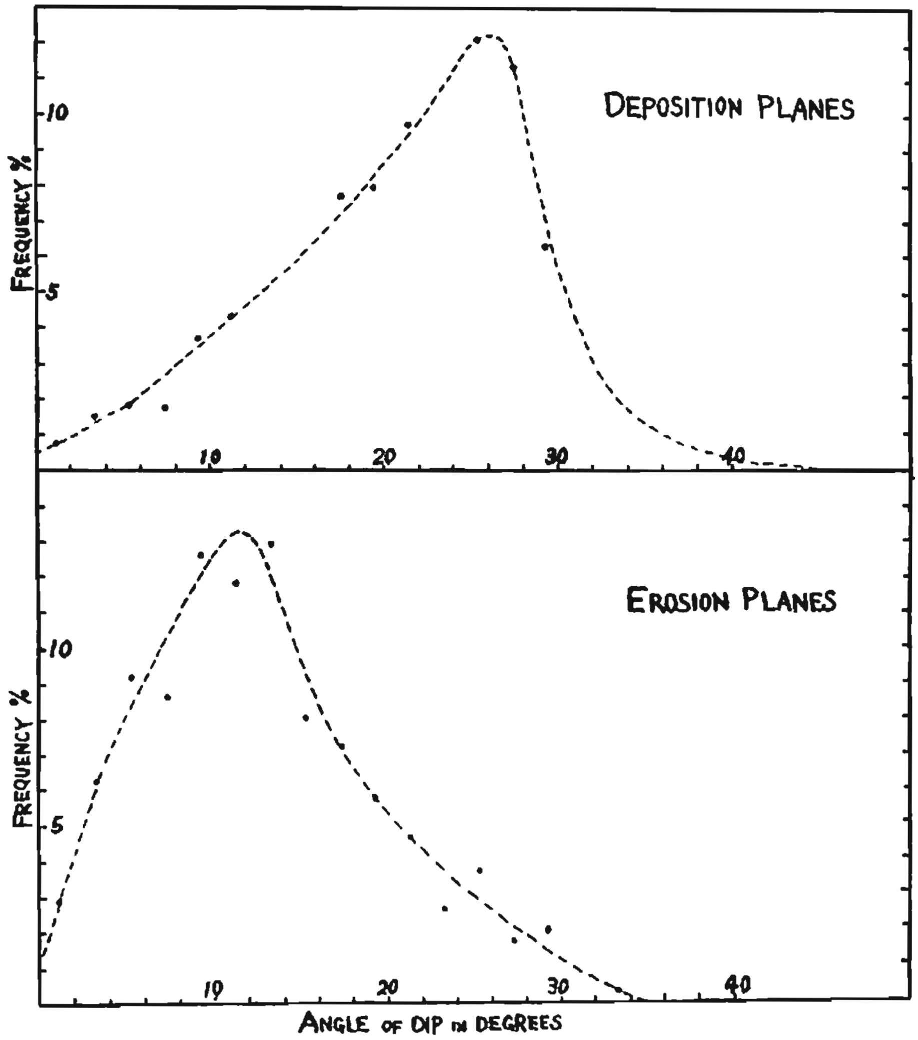

DEPOSITION PLANES
FREQUENCY %
10
5
10
20
30
40
EROSION PLANES
FREQUENCY %
10
5
10
20
30
40
ANGLE OF DIP IN DEGREES

Fig. 1

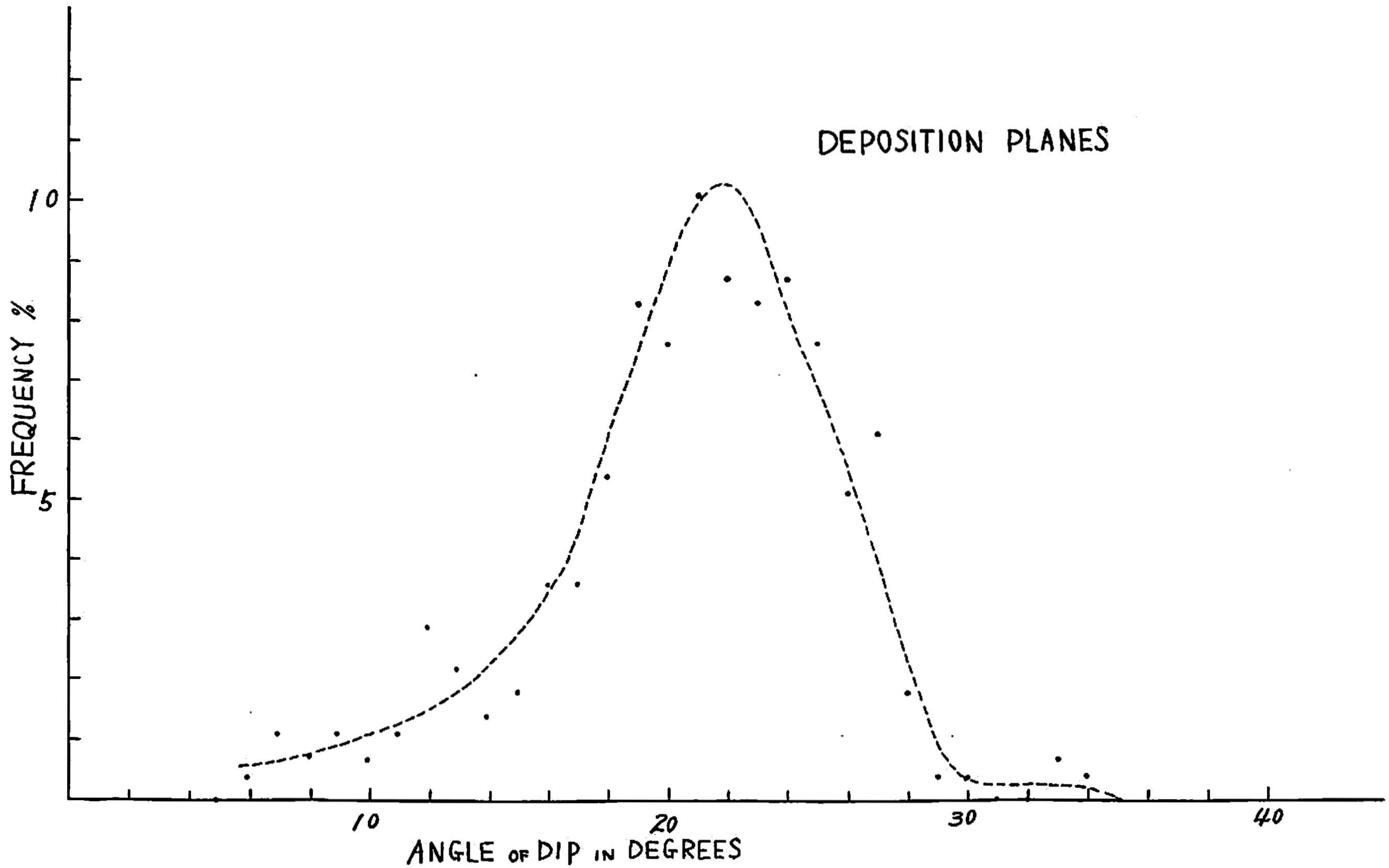
DEPOSITION PLANES
FREQUENCY %
10
5
10
20
30
40
ANGLE OF DIP IN DEGREES

Fig.2

3. Archaeo-Aurora' and Geomagnetic Secular Variation in Historic Time

Mitsuo Keimatsu

College of Liberal Arts, Kanazawa University

Naoshi Fukushima and Takesi Nagata

Geophysics Research Laboratory, University of Tokyo

Abstract

In order to trace the secular variation of the geomagnetic field in historic time, the documents of ancient aurorae can be utilized. In China, Korea and Japan there are a number of valuable records, which can be reasonably supposed to describe the events of auroral appearance. After a comparison of these descriptions with those in Europe, the archaeosecular variation in the geomagnetic field can be inferred. A preliminary examination of the auroral appearance on the same day in the Occident and Orient suggests that the geomagnetic dipole axis might have been inclined towards China around 11-12th centuries AD.

1. Introduction

Since the location of auroral appearance is subjected to the geomagnetic field distribution over the earth, the study of archaeo-secular variation in the geomagnetic field is possible through the comparison of the historical aurorae observed at different places. Though the study is still in progress, a preliminary report is presented to show the usefulness of this work.

In China unusual events on the earth and in the sky have been described by specialists in the royal astronomical observatories established by the central government, and the documents have been carefully preserved for thousands of years. Therefore, we can trace ancient events in China as to their exact dates and details, though descriptions are sometimes given in poetic or exaggerated expressions. These Chinese records as well as those from the Korean and Japanese literatures (Keimatsu, 1965) are compared with the Occidental records taken from lists compiled by Fritz (1873), Seydl (1954) and Link (1962).

2. Latitude defference of the southern boundary of aurorae simultaneously observed in Europe and Asia

From a comparison of simultaneous aurorae, we have estimated the latitude difference in the southern boundary of aurorae borealis seen in Europe and China (or sometimes Korea and Japan), and it is plotted against year in Fig. 1. In this diagram the point for the event of 6 October, 1138, has the largest reliability compared with other points, because the southern boundaries of the auroral appearance on that day in Europe and China are most definitely known. In order to obtain as many points as possible for Fig. 1, the following conventional method was adopted. For events recorded in early centuries, some aurorae in the same year are assumed to be of the same date, even when there is no definite evidence for this assumption. For aurorae in the later centuries, only those which appeared on exactly the same day were used. The southern boundaries of aurorae inferred may have an error of several degrees in latitude.

3. Archaeo-variation of the geomagnetic axis

In the geomagnetic field distribution at the present time, the geomagnetic latitude in China is definitely lower than that of Central Europe, so that the appearance of aurorae is much less frequent in China than in Central Europe at present. However, the appearance of an aurora on the same day, e.g., on 6 October, 1138, in Bohemia (geographic latitude about 50°), and Hangchow in China (geogr. lat. 30°) suggests that the geomagnetic field distribution at that time might be quite different from that of the present time, i.e., the geomagnetic dipole axis might have been inclined towards the Asian side of the earth. This conclusion is obtained under some idealized assumptions, e.g., (1) the auroral appearance depends on the geomagnetic latitude of the observing location; (2) the geomagnetic field distribution has been mainly of a centered dipole type; (3) the size of the auroral zone was almost the same at the times when the aurora was observed in Europe and in Asia.

Kawai et al. (1965) have shown that the axis of the earth's main dipole field might have rotated counter-clockwise in archaeologic time, and the axis might have been inclined towards Asia in the 10th - 12th centuries, as illustrated in Fig. 2. They arrived at this conclusion after examining the archaeosecular variation in the virtual geomagnetic pole positions (assuming a dipole approximation of the geomagnetic field), based on the remanent magnetization of rock and cley samples measured by research workers in England, France, Iceland, U.S.A., U.S.S.R. and Japan. The geomagnetic dipole axis appears to have been inclined towards China around the 12th century. The curve in Fig. 1 obtained from a comparison of Occidental and Oriental aurorae seems to be in accordance with the result obtained by Kawai et al. (1965), though our preliminary result is still of insufficient accuracy to test the wobbling motion of the geomagnetic field in historic time as suggested by Kawai and Hirooka (1967). The writers hope that the future extension of this work can make an appreciable contribution to the study of archaeomagnetism. The full paper of the preliminary results is now under press in the Journal of Geomagnetism and Geoelectricity (1968).

References

Fritz, H., Verzeichniss beobachteter Polarlichter, Wien, 1873.

Kawai, N., and K. Hirooka, (1967), Wobbling motion of the geomagnetic dipole field in historic time during these 2000 years, J. Geomag. Geoelectr., 19, 217-227.

Kawai, N., K. Hirooka and S. Sasajima, (1965), Counterclockwise rotation of the geomagnetic dipole axis revealed in the world-wide archaeo-secular variations, Proc. Japan Acad., 41, 398-403.

Keimatsu, M., (1965), Documentary catalogue of northern lights observed in China, Korea and Japan from 7BC to 10AD (Preprint, College of Liberal Arts, Kanazawa University, 1965).

Link, F., (1962), Observations et Catalogue des Aurores Boreales Apparues en Occident de -- 626 à 1600. Travaux de l'Inst. Géophys. Acad. Sci., No. 173, Geofysikalni Sbornik, 297-387.

Seydl, O., (1954), A list of 402 northern lights observed in Bohemia, Moravia and Slovakia from 1013 till 1951. Travaux de l'Inst. Géophys. Acad. Sci., No. 17, Geofysikalni Sbornik, 159-194.

Figure Captions

Fig. 1. Latitude difference of the southern boundary of aurorae borealis seen on the same days in Europe and China. The ordinate is: (geographic latitude of the auroral southern boundary in Europe) -- (that in China). Abscissa is years AD.

Fig. 2. Mean virtual pole position at 700, 1000, 1100, 1200, 1300, 1400 and 1500 AD. Broken circles indicate the region of 95% confidence. (after Kawai et al.)

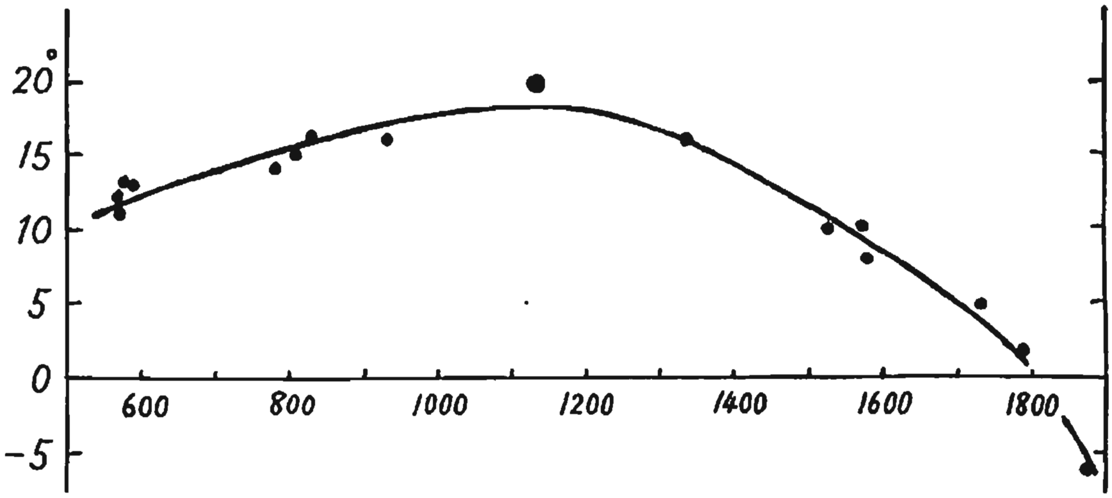

Fig. 1. Latitude difference of the southern boundary of aurora borealis seen in Europe and China. The ordinate is: (geographic latitude of the auroral southern boundary in Europe) — (that in China). Abscissa: years in AD.

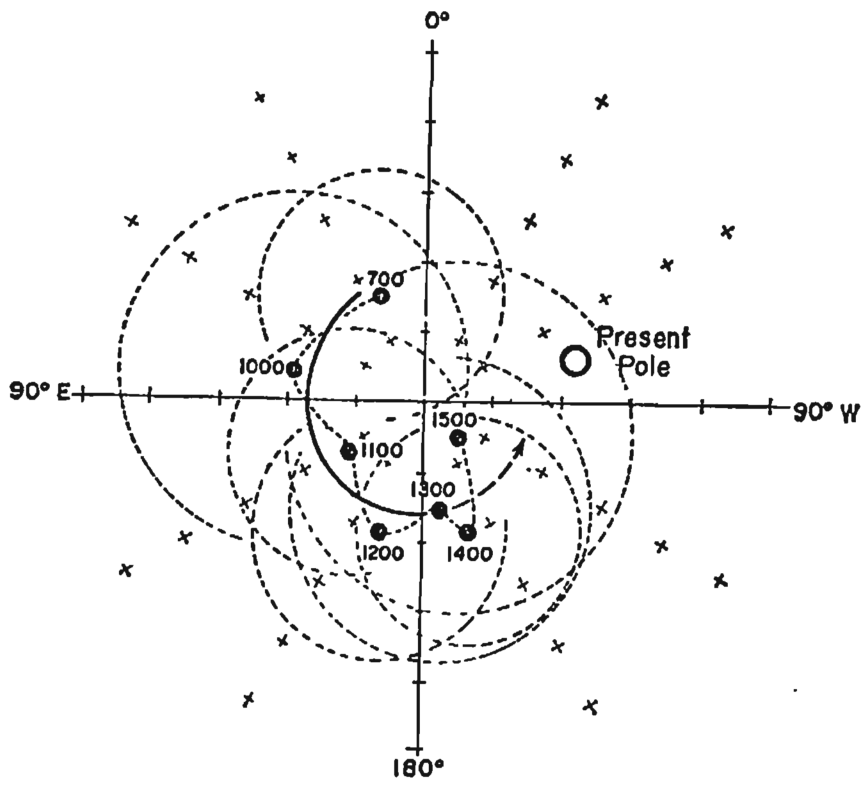

Fig. 2. Mean virtual pole position at 700, 1000, 1100, 1200, 1300, 1400, and 1500 A.D. Broken circles indicate the region of 95% confidence. (after Kawai et al.)

4. Self-reversal of Remanent Magnetization in Some Dredged Submarine Basalts*

Mituko Ozima and Minoru Ozima

Geophysical Institute, University of Tokyo

Several cases of self-reversal of remanent magnetization in ferromagnetic minerals and rocks are known (Uyeda, 1958; Carmichael, 1961; Everitt, 1962; Yama-ai et al, 1963). Self-reversal in basalts, however, is extremely rare in spite of numerous reports on their magnetic properties (Meitzner, 1963; Havard and Lewis, 1965; Schult, 1965).

This report deals with the results of a study of eight basalts dredged from deep sea mounts in the Pacific Ocean (Table 1) in which three of the dredged samples showed self-reversal of remanent magnetization. Although the magnetic properties of dredged basalts are not well known (Ade-Hall, 1964; Ozima et al, 1968), the high percentage of self-reversed samples would imply that the ferromagnetic minerals in submarine basalts differ significantly from those in continental basalts. The results of our preliminary experiments on self-reversal in dredged basalts are now reported.

Fig. 1 indicates self-reversal of thermoremanent magnetization in sample WPDR-2; The ordinate represents an intensity of thermoremanent magnetization produced by cooling the sample to room temperature in the geomagnetic field in air from various temperatures (as shown on the absissa). Thermoremanent magnetization produced below 300°C has a direction parallel to the ambient geomagnetic field, whereas that produced between 300°C and 330°C has a direction antiparallel to the field. When

* Submitted for Earth and Planetary Science Letters.

the sample is cooled from above 330°C, the thermoremanent magnetization again parallels the geomagnetic field.

The occurrence of the self-reversal is sensitive to the duration of heat-treatment. When the sample is kept at 300°C in air for more than 150 minutes it no longer shows self-reversal upon cooling.

The Curie temperature also changes on heating. Fig. 2 shows the thermomagnetic curves obtained for sample WPDR-2 in air at H=3000 Oe. During the initial heating, the magnetization almost linearly decreases and finally disappears at 250°C, indicating that original sample has a single magnetic phase with Curie temperature of 250°C. When sample is heated at 400°C for several minutes and then cooled, magnetization appears at 300°C indicating a development of a new magnetic phase with Curie temperature of 300°C. The temperature change of magnetization is more gradual than in the initial heating as seen in Fig. 2. On further heating at higher temperatures, the sample becomes a single magnetic phase with Curie temperature of 560°C.

Fig. 3 shows a magnetization curve obtained on sample WPDR-2 which was once heated at 300°C for 10 minutes in air and shows self-reversal of remanent magnetization. In the same figure, magnetization curve for unheated sample WPDR-2 is compared. A smooth hysteresis curve for the unheated sample indicates that the sample consists of a single magnetic component in accordance with a monotonous decreasing thermomagnetic curve in an initial heating (see Fig. 2), whereas kinks in the magnetization curve suggest the existence of two magnetic components in the self-reversed heated sample.

In summary, when the sample is heated to 300°C, the original ferromagnetic component with a Curie temperature of 250°C is gradually transformed to another component with a Curie temperature of 300°C and there exists momentarily two magnetic components. Magnetic interaction between these two components seems to be responsible for self-reversal of the remanent magnetization, since self-reversal is only observed in a sample which is heated at 300°C for less than 150 minutes and has two magnetic components. With prolonged heating at 300°C the original magnetic component will be exclusively changed to the component with a Curie temperature of 300°C and self-reversal is no longer observed.

In order to understand the nature of the magnetic interaction between the two phases, the sample was heated at 300°C for 10 minutes and then cooled in various intensities of magnetic field up to 120 Oe. 120 Oe was not sufficient to suppress self-reversal. Inas-much as a few tens of oersteds of magnetic field should generally be sufficient to suppress magnetostatic coupling (Nagata, 1961), it is unlikely that the magnetostatic interaction is responsible for the observed self-reversal phenomena. However, it is necessary to examine the self-reversal in much higher field (say, more than 10^4 Oe) to definitely conclude that the self-reversal is truly due to exchange interaction such as in the case of the Haruna dacite (Uyeda, 1958).

Whether the change of the magnetic component on heating is due to oxidation or to other causes such as rearrangement of the ionic configuration is not yet clear. However, as there is no significant differences between the thermomagnetic curves obtained in air and in vacuo of 10^{-3} torr, rearrangement of ionic configuration seems to be a more preferable explanation. Microscopic observation on original and the heated one would possibly resolve this question.

Sample WPDR-8 and EPDR-2 show essentially identical magnetic behaviour as WPDR-2, including self-reversal. This would imply that self-reversal of remanent magnetization is rather common in submarine basalts and its consideration may be important in understanding the magnetization of the ocean floor.

References

Ade-Hall, J.M., (1964), The magnetic properties of some submarine oceanic lavas, Geophysical Journal, 8, 85-92.

Carmichael, C.M., (1961), The magnetic properties of ilmenite-hematite crystals, Proc. Roy. Soc., A 263, 508-530.

Everitt, C.W.F., (1962), Self-reversal of magnetization in a shale containing pyrrhotite, Phil. Mag., 7, 831-842.

Havard, A.D. and M. Lewis, (1965), Reversed partial thermo-magnetic remanence in natural and synthetic titano-magnetites, Geophys. J., 10, 59-68.

Meitzner, W., (1963), Der Einfluss von Entmischung und Oxydation auf die magnetischen Eigenschaften der Titanomagnetit in Basalten bei 250 und 350°C, Beitrage Mineralogie und Petrographie, 9, 320-352.

Nagata, T., (1961), Rock Magnetism, Maruzen, Tokyo.

Ozima, M., M. Ozima, and I Kaneoka, (1968), K-Ar ages and magnetic properties of some submarine basalts and their geophysical implications, J. Geophys. Res., 73.

Schult, A., (1965), Über die Umkehr der remanenten Magnetisierung von Titanomagnetiten in Basalten, Beitrage zur Mineralogie und Petrographie, 11, 196-216.

Uyeda, S., (1958), Thermo-remanent magnetism as a medium of paleomagnetism with special reference to reverse thermo-remanent magnetism, Jap. J. Geophys., 2, 1-123.

Yama-ai, M., M. Ozima, and T. Nagata, (1963), Self-reversal of remanent magnetization of magnetite at low temperatures, Nature, 198, 4886.

Table 1

Sample	Rock Type	Dredged Station Lat.	Dredged Station Long.	Depth to the Dredged Site(m)
WPDR-1	basalt	38°00' N	145°58' E	3000
WPDR-2	basalt	37°03' N	163°45' E	3000
WPDR-5	basalt	28°22' N	148°14' E	2000
WPDR-7	basalt	27°03' N	148°39' E	1000
WPDR-8	basalt	27°57' N	147°37' E	2000
EPDR-2	basalt	20°45' N	112°47' W	1712
EPDR-9	basalt	21°07' N	119°22' W	2985
EM7*	basalt	28°59' N	117°30' W	3750

* basalt in Hole EM7, Mohole Project

Figure Captions

Fig. 1. Production of thermoremanent magnetization. When sample heated at 300 ~ 350°C in air for less than 10 minutes and then cooled to room temperature in the geomagnetic field, the thermoremanent magnetization is reversed.

Fig. 2. Thermomagnetic curves obtained at H=4000 Oe in air. On initial heating (curve 1), magnetization disappears at 250°C. When sample is heated to 400°C and then cooled (curve 2), magnetization appears at 300°C. On subsequent heating (curve 3), magnetization changes reversibly and disappears at 300°C. When sample is heated above 600°C, magnetization changes reversibly on cooling (curve 4) and on heating (curve 5) indicating a single magnetic component of Curie temperature of 560°C.

Fig. 3. Magnetization curves for original and heated sample (heated at $300^{\circ}C$ for 15 minutes). Magnetizations were measured up to H=2000 Oe, but only part of the magnetization curves for a field range of H=400 Oe are shown in Fig. 3.

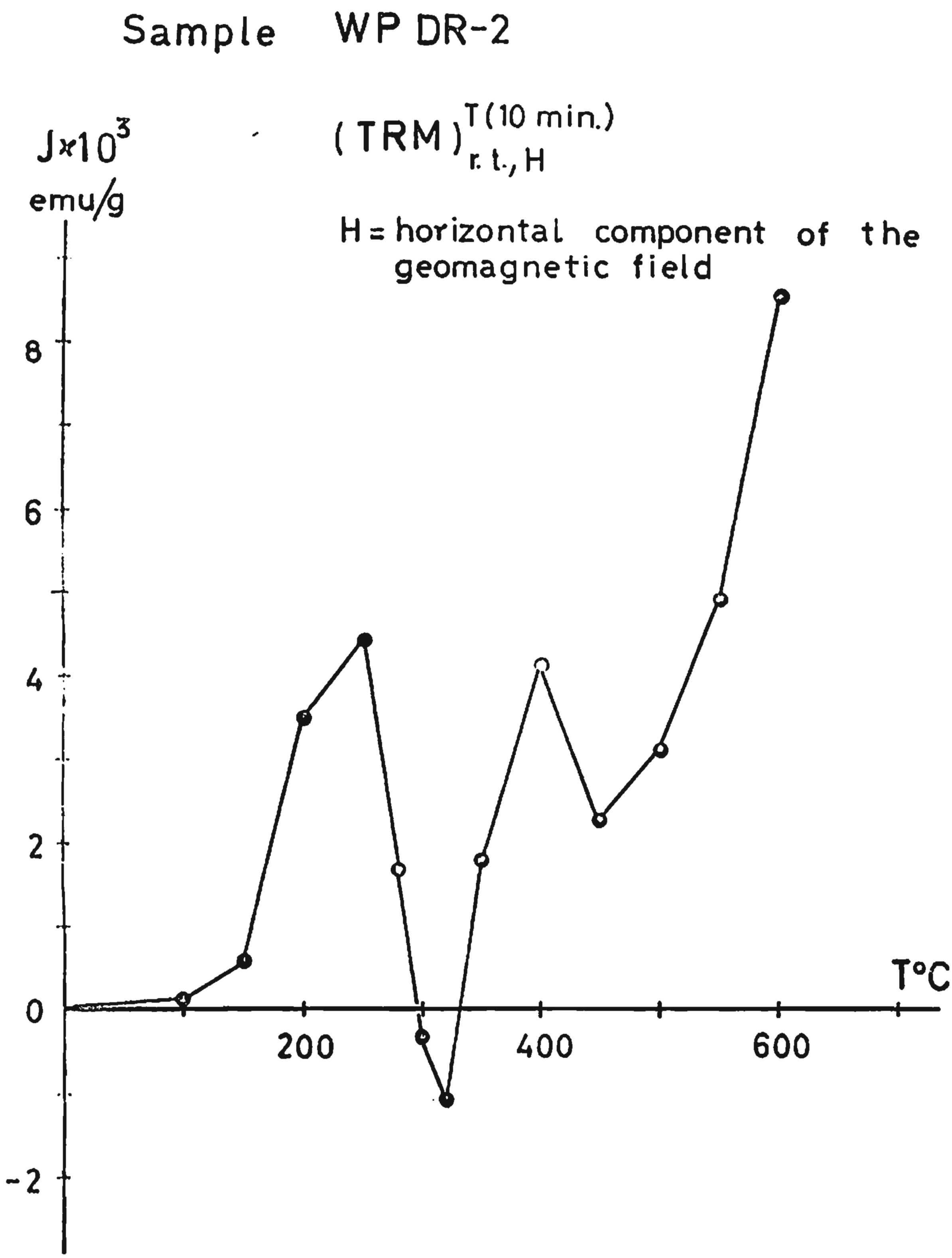
Sample WP DR-2
$(TRM)^{T(10\ min.)}_{r.t.,H}$
$J \times 10^3$
emu/g
H = horizontal component of the geomagnetic field
8
6
4
2
0
-2
200
400
600
T°C

Fig.1

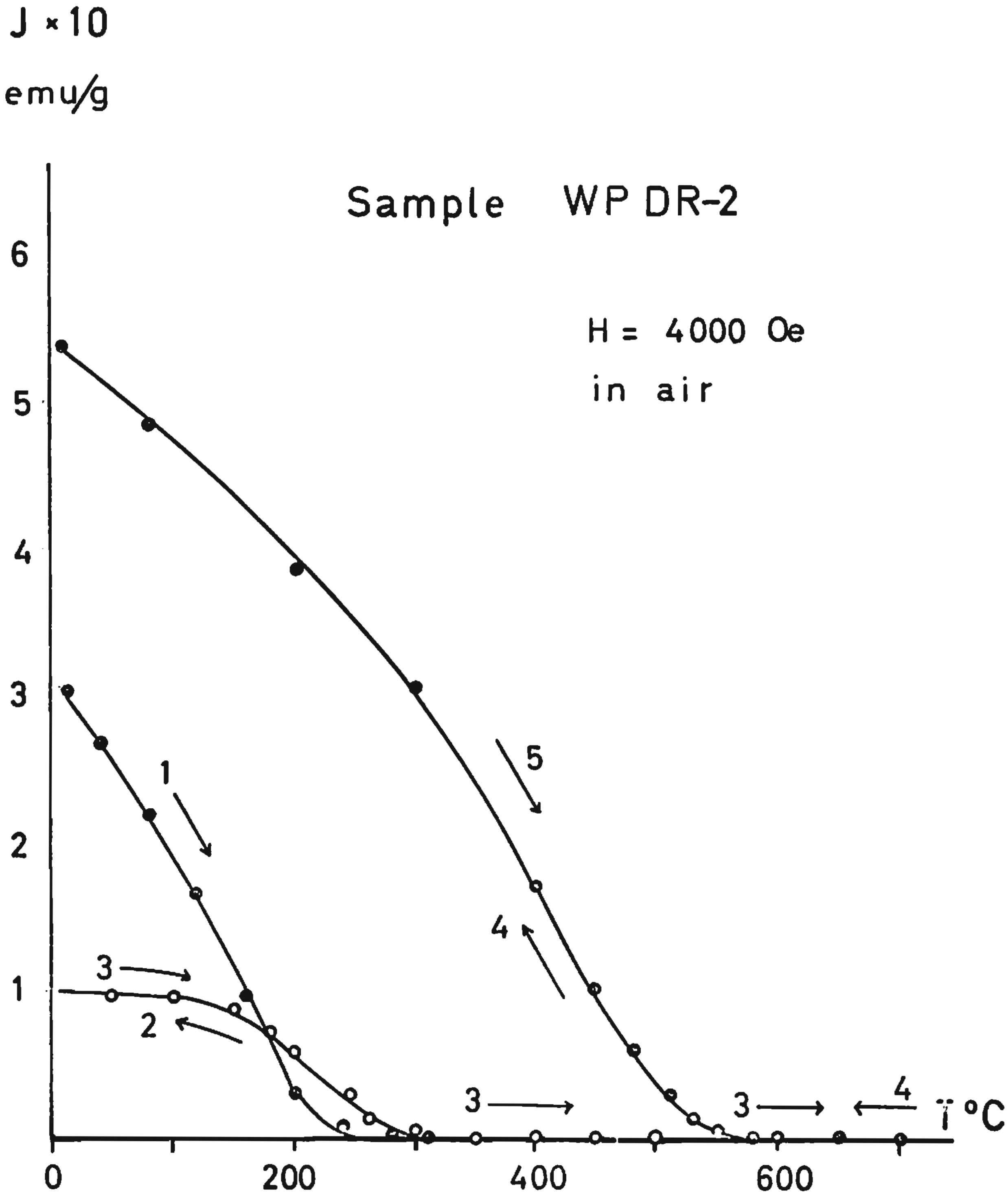

J ×10
emu/g
Sample WP DR-2
H = 4000 Oe
in air
6
5
4
3
2
1
0
200
400
600
T °C
1
2
3
4
5

Fig.2

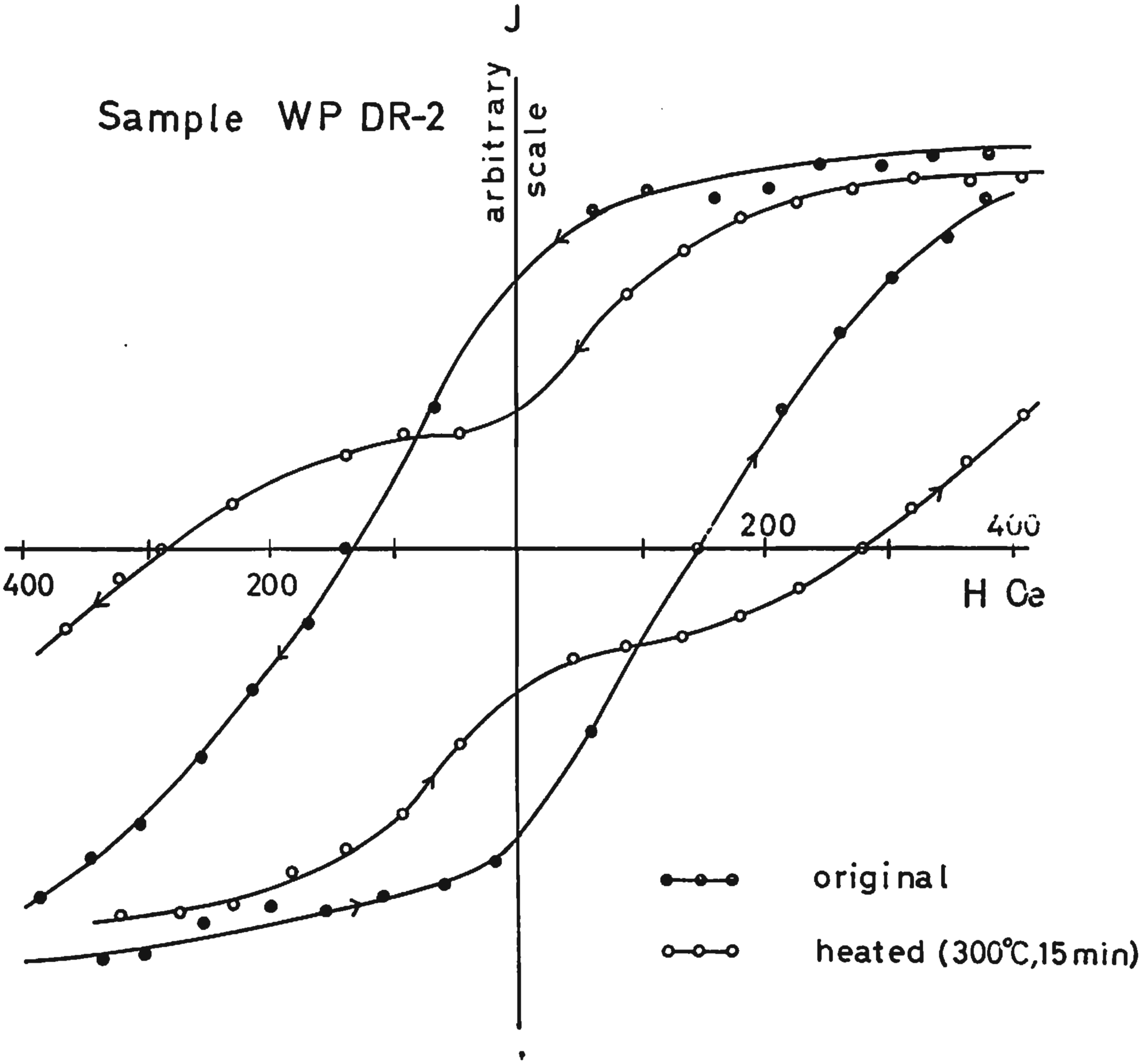
J
arbitrary scale
Sample WP DR-2
400
200
200
400
H Oe
original
heated (300℃,15 min)

Fig. 3

5. Palaeomagnetism of Nine Seamounts in the Western Pacific and of Three Volcanoes in Japan

Seiya Uyeda,

Earthquake Research Institute and Geophysical Institute,

University of Tokyo

and

Victor Vacquier,

Marine Physical Laboratory of the

Scripps Institution of Oceanography,

University of California, San Diego

Assuming uniformity of magnetization, the direction and intensity of magnetization of nine seamounts in the Western Pacific off the coast of Japan (Fig. 1) have been computed from their topographic and magnetic surveys (Uyeda et al., 1967). From the estimated directions of magnetization, assuming a high Konigsberger ratio, palaeomagnetic pole positions were calculated as shown in Fig 2. Results of computations are listed in Table 1. The goodness ratio in the tables is defined as $r = \sum_{j=1}^{n} |\Delta T_j| / \sum_{j=1}^{n} |R_j|$, where n is the number of points where the observed anomaly ΔT_j and the residual anomaly R_j are given (see Vacquier and Uyeda, 1967). The average position of the palaeomagnetic poles from the three seamounts in the Pacific Basin (4-2, 4-3, 4-4 in Figs. 1 and 2) is at 56°N 66°W, which agrees in latitude with the average pole position of 51°N 14°W obtained previously (Uyeda and Richards, 1966) from another group of four seamounts (A, B, S, R in Figs. 1 and 2) in the Pacific Basin off Hokkaido. A group of three seamounts west of the Izu-Bonin Arc (Shikoku Basin) (4-5, 4-6, 4-7 in Figs. 1 and 2) gave an average pole position of 76°N 44°W. The difference in latitude between the pole positions of the groups within and outside the Pacific Basin can be interpreted as caused by a northerly drift of the Pacific Ocean floor. Such a drift of the Pacific floor is in agreement with the results of other seamount palaeomagnetic studies (Uyeda and Richards 1966, Richards et al. 1967) and also with the idea of the Ocean floor spreading hypothesis (e.g. Vine, 1966). The radiometric age of the dredged rock samples (Ozima et al. 1967) indicates that the seamounts in the Paicifc Basin originated in the Cretaceous. The same method of analysis has been applied to three active Japanese volcanoes (Oshima, Sakurajima and Aso), over which aeromagnetic surveys had been made (Kato et al. 1965, Matsuzaki and Utashiro 1966, Blank 1965). Of the three volcanoes, two volcanic islands gave palaeomagnetic poles not far from the present geographic pole, but the inland volcano Aso gave a pole at low latitude (Fig. 2 and Table 2). Low-latitude poles were also obtained from two undated seamounts on the NW Pacific (Shatsky) Rise (3-1 and 3-2). Detailed account of this work can be found in Vacquier and Uyeda (1967).

References

Blank, R., (1965), private communication.

Kato, Y., A. Takagi and T. Muroi, (1965), private communication.

Ozima, M., M. Ozima, and I. Kaneoka, (1968), K-Ar ages and magnetic properties of some dredged submarine basalts and their geophysical implications, Jour. Geophys. Res., 73, No.2.

Richards, M. L., V. Vacquier and G. D. Van Voorhis, (1967), Calculation of the magnetization of uplifts from combining topographic and magnetic surveys, Geophysics, 32, 678-707.

Uyeda, S. and M. L. Richards, (1966), Magnetization of four Pacific seamounts near the Japanese Islands, Bull. Earthq. Res. Inst., 44, 179-213.

Uyeda, S., V. Vacquier, M. Yasui, J. Sclater, T. Sato, J. Lawson, T. Watanabe, F. Dixon, E. Silver, Y. Fukao, K. Sudo, M. Nishikawa and T. Tanaka, (1967), Results of geomagnetic survey during the cruise of R/V Argo in Western Pacific 1966 and the compilation of magnetic charts of the same area, Bull. Earthq. Res. Inst., 45, 799-814.

Vacquier, V., and S. Uyeda, Palaeomagnetism of Nine Seamounts in the Western Pacific and of three Volcanoes in Japan, Bull. Earthq. Res. Inst., 45, 815-848.

Vine, F. J., (1966), Spreading of the ocean floor: new evidence, Science, 154, 1405-1415.

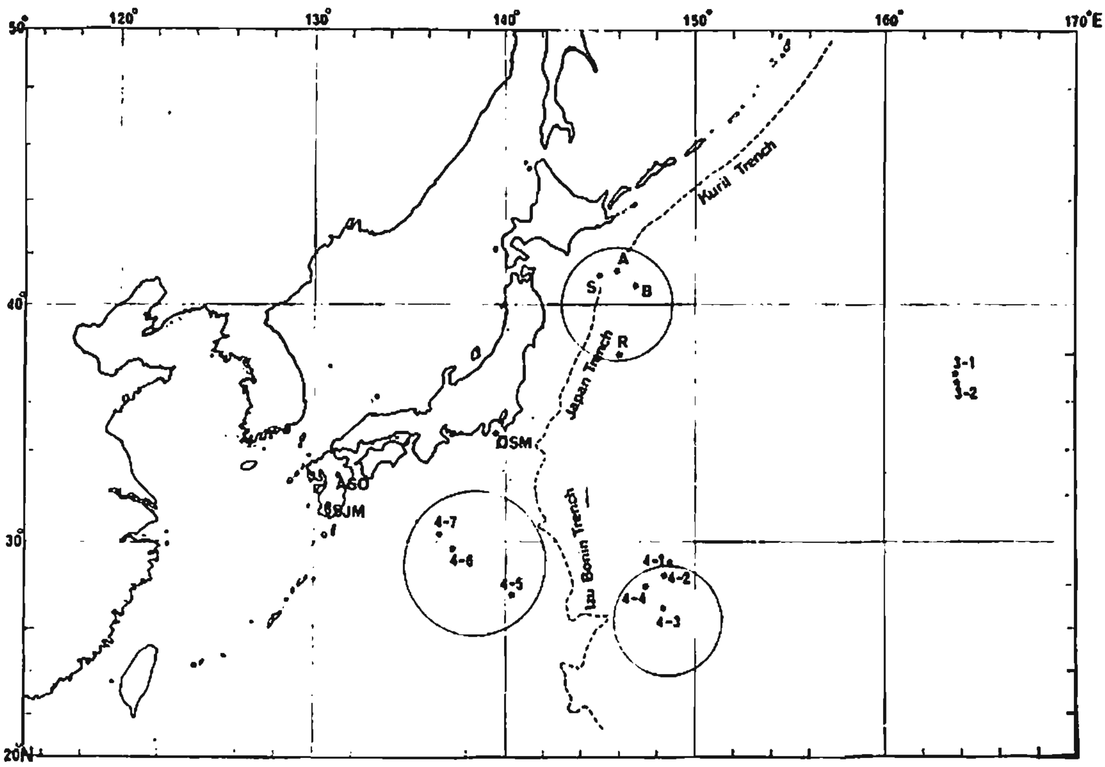

Fig. 1 Localities of seamounts and volcanoes studied. A, B, R and S are the seamounts studied previously (Uyeda and Richards, 1965), and symbols 3-1, 4-2 etc. stand for the seamounts No. 1 of ZETES III, No. 2 of ZETES IV, *etc.* Large circles define group of seamounts of which palaeomagnetic pole positions are averaged in Fig. 18.

OSM ...... Oshima Island (Mihara Volcano)
ASO ...... Aso Volcano
SJM ...... Sakurajima Island

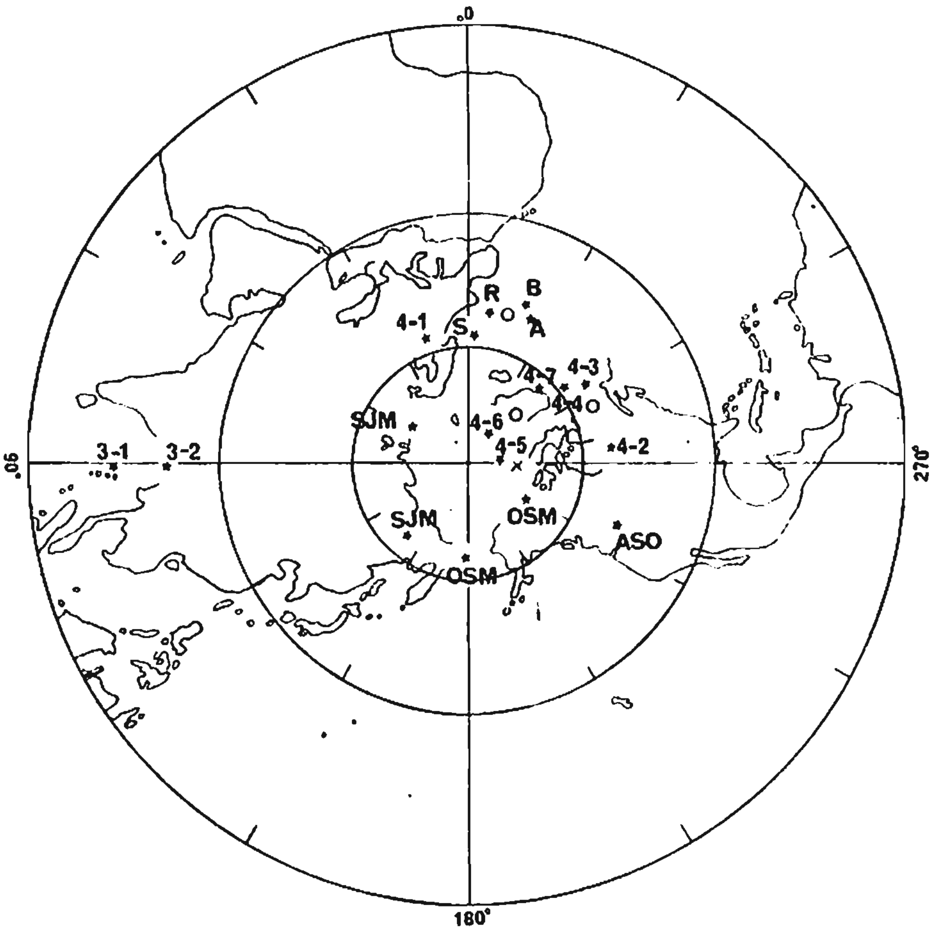

Fig. 2 Palaeomagnetic pole positions of the Western Pacific seamounts and Japanese Volcanoes. Hollow circles are the average pole positions for each group of seamounts encircled in Fig. 1.

× ...... present geomagnetic pole

Table 1. Result of Computation on Seamounts.

Seamount No. Zetes	Latitude	Longitude	(emu/cc)×10⁻² A	B	G	Intensity	(Degree) Geomagnetic Declination	Geographic Declination	Inclination	(γ) Mean of Abs. Residual	(γ) Mean of Abs. Anomaly	Goodness Ratio, R	Palaeomagnetic Latitude	Palaeomagnetic Pole Position Lat.	Long.
III-1	37°03'N	163°45'E	−0.014	−0.268	0.210	0.341	267	268	38	70	81	1.16	21°N	11°N	92°E
III-2	36°33'N	163°53'E	0.058	−0.513	0.502	0.720	276	278	44	98	242	2.48	26	21	91
IV-1	28°48'N	148°21'E	0.165	−0.074	0.029	0.183	336	334	9	18	40	2.25	4	55	19
IV-1'	28°48'N	148°21'E	0.132	−0.132	−0.129	0.226	315	313	−35	58	82	1.41	−20	24	17
IV-2	28°22'N	148°14'E	0.364	0.203	0.035	0.419	9	28	5	44	114	2.61	2	53	−82
IV-3	27°03'N	148°39'E	0.597	0.007	−0.145	0.643	17	16	−13	99	408	4.12	−7	53	−58
IV-4	27°57'N	147°34'E	0.202	0.064	−0.006	0.299	12	11	−1	57	100	1.75	−1	60	−54
IV-5	27°41'N	140°24'E	0.244	0.031	0.197	0.315	7	5	39	33	128	3.88	22	82	−78
IV-6	29°37'N	137°03'E	0.433	0.026	0.262	0.507	3	−1	31	43	80	1.88	17	77	−40
IV-7	30°09'N	136°40'E	0.120	0.007	0.014	0.121	3	−1	7	53	75	1.42	4	63	−41

Table 2. Palaeomagnetic Results from Three Volcanoes in Japan.

Name and Description	Lat.	Long.	(emu/cc) $\times 10^{-3}$ A	B	G	Intensity	(Degree) Geomagnetic Declination	Geographic Declination	Inclination	(γ) Mean of Abs. Residual	(γ) Mean of Abs. Anomaly	Goodness Ratio, R	Palaeomagnetic Pole Position Lat.	Long.
Sakurajima No. 1	31°35′N	130°40′E	0.045	0.010	0.143	0.151	13	8	72	26	63	2.41	64°N	140°E
No. 2	31°35′N	130°40′E	0.095	−0.029	0.142	0.178	343	338	55	28	69	2.49	71°N	58°E
Oshima 6000 ft	34°42′N	139°24′E	0.831	0.442	1.065	1.421	28	22	49	76	244	3.21	71°N	121°W
4000 ft	34°42′N	139°24′E	0.450	0.269	1.301	1.403	31	25	68	132	306	2.32	66°N	179°E
Aso Volcano: A Cone Base at 600 m	32°53′N	131°06′E	0.0076	−0.0181	0.523	0.0558	−61	−67	69	154	235	1.52	89°N	86°E
Cone Base at 800 m	32°53′N	131°06′E	−0.0408	−0.0119	0.0778	0.0788	257	251	81	161	222	1.38	26°N	112°E
Dipole at −6400 m $x=3.9$ $y=5.21$	32°53′N	131°06′E	0.0688	0.0273	0.0261	0.0785	28	22	19	102	307	3.01	60°N	95°W
Dipole with Mountain: Dipole	32°53′N	131°06′E	0.0359	0.0270	0.0150	0.0474	43	37	19	77	278	3.59	49°N	113°W
Dipole with Mountain: Aso Volcano	32°58′N	131°06′E	−0.0216	−0.0807	0.0236	0.0868	−99	−105	16					

6. Rb-Sr and K-Ar Isotopic Investigations of Granodiorites and Associated Metamorphic Rocks of the Abukuma Plateau

N. Ueno, M. Ozima

Geophysical Institute, University of Tokyo

and

H. Kuno

Geological Institute, University of Tokyo

The present short note is to report the results of Rb-Sr and K-Ar isotopic studies on granodiorites and associated metamorphic rocks in the Abukuma Plateau. It is particularly intended to resolve if there is significant time gap in the intrusions of two types of granodiorites, the younger and the older, which were identified on the basis of field geology. In addition, it is also hoped that initial Sr isotopic ratio $(Sr^{87}/Sr^{86})_0$ for the granodiorites and the associated metamorphic rocks would yield information as to whether the granodiorites and the metamorphic rocks are cogenetic or not.

Regional metamorphic rocks are widely exposed in the Gosaisyo-Takanuki district, central Abukuma Plateau. Though no fossil has been found in this district, the metamorphism is generally considered to have taken place in late Paleozoic or early Mesozoic time since there are Devonian Sediments in the adjacent northern part of the plateau. (Miyashiro, 1958)

Plutonic rocks of the Abukuma Plateau, intruded into the metamorphic rocks to form several separate masses, have been divided into two groups; older and younger. From the geological and petrological studies (Gorai 1944, Watanabe 1955, Shido 1958), the intrusion of the older group probably took place at or immediately after the culmination of the regional metamorphism, that is, in late Paleozoic or early Mesozoic time. On the other hand, the younger group has been considered to have intruded in early or middle Cretaceous time.

As shown in Fig. 1, we sampled the granodiorites of the plutonic masses named "Tabito", "Miyamoto", "Samegawa", and "Isikawa" composite masses, which are supposed to belong to the older group, and "Kadono" composite mass from the younger one. Biotite schist was also taken from the regional metamorphic rocks.

Rb-Sr measurements were carried out with a Mitsubishi 22cm radius, 60 degree, single filament solid source mass spectrometer with an electron multiplier. All measured (Sr^{87}/Sr^{86}) ratios were normalized against (Sr^{86}/Sr^{88})=0.1194. Potassium analyses were made by a flame photometer with Li internal standard. Argon analyses were made by a Reynolds type 15cm radius mass spectrometer using a static operation.

Table 1 shows the results of analyses. Rb-Sr ages are shown also graphically in Fig. 2. We conclude from these analytical results;

1) The regional metamorphism and plutonic activity took place both in Mesozoic time.

2) "Tabito" mass is considered to belong to the younger group

3) "Isikawa" mass was intruded in the upper Jurrasic or in the lower Cretaceous, but suffered of thermal disturbances on the occasions of the later metamorphism and/or the intrusions of the granodiorites to result in the younger K-Ar age.

4) The initial Sr ratios $(Sr^{87}/Sr^{86})_0$ for granodiorites are low, the value being about 0.7044 ± 0.0025, and it is supposed that they are not psammitic rocks. But, considering the experimental errors, it is difficult to state the genetic relation between the granodiorites and the biotite schist.

References

Gorai, M. (1944), Petrological study on the plutonic rocks of Gosaisho-Takanuki district, sourthern Abukuma Plateau. Mem. Fac. Sci. Kyushu Imp. Univ., Ser. D, 2, 239-321.

Watanabe, Gorai, Kuroda, Ono, Togawa (1955), Igneous activities of the Abukuma Plateau. Chikyu-Kagaku No. 24, 1-11.

Shido, F. (1958), Plutonic and metamorphic rocks of the Nakoso and Iritono districts in the control Abukuma Plateau. Jour. Fac. Sci. Univ. Tokyo, Sec. II, 11, 131-217.

Miyashiro, A. (1958), Regional Metamorphism of the Gosaisyo-Takanuki District. Jour. Fac. Sci., Univ. Tokyo, Sec. II, 11, 219-272.

Table 1. Analytical data

Sample		$(Ar^{40})_{rad}$ 10^{-10} mole/g	$(Ar^{40})_{rad}$ / $(Ar^{40})_{total}$	K %	K-Ar age*** m.y.	Sr^{87}/Sr^{86}	Sr^{86} $\times 10^{-7}$ mole/g	Rb^{87} $\times 10^{-7}$ mole/g	Rb-Sr age**** m.y.
Tabito	6609 W*	3.991	92.6	2.10	104	0.7083	4.25 ±0.09	2.68 ±0.08	87±3
	b**	10.37	84.4	6.38	89	0.7443 ±0.0001	0.37 ±0.00	11.29 ±0.28	
	6609Xe.W	3.037	35.0	2.13	78	0.7066 ±0.0030	4.85	3.44	
	b					0.7246 ±0.0020	0.96 ±0.00	10.65 ±0.55	124±6
Kadono	6610 W	4.454	70.4	2.35	108	0.7020 ±0.0030	3.37	3.06	101±10
	b					0.7622 ±0.0001	0.27 ±0.01	11.85 ±0.75	
Biotite schist	6612 W	3.54	19.0	1.78	109	0.7142 ±0.0004	1.70	2.88	102±3
	b					1.2266 ±0.0082	0.03 ±0.00	11.15 ±0.09	
Miyamoto	6613 W	5.394	89.3	3.08	96	0.7058	3.32	4.09	
Isikawa	6616 W	2.870	79.0	2.35	67	0.7053	3.10	2.81	163±16
	b					0.7344 ±0.0007	1.02 ±0.14	14.04 ±0.16	

* whole rock
** biotite

*** $\lambda e = 0.585 \times 10^{-10}$ yr^{-1}
$R = 0.124$
$K^{40}/K = 1.19 \times 10^{-4}$ mole/mole

**** $\lambda = 1.39 \times 10^{-11}$ yr^{-1}

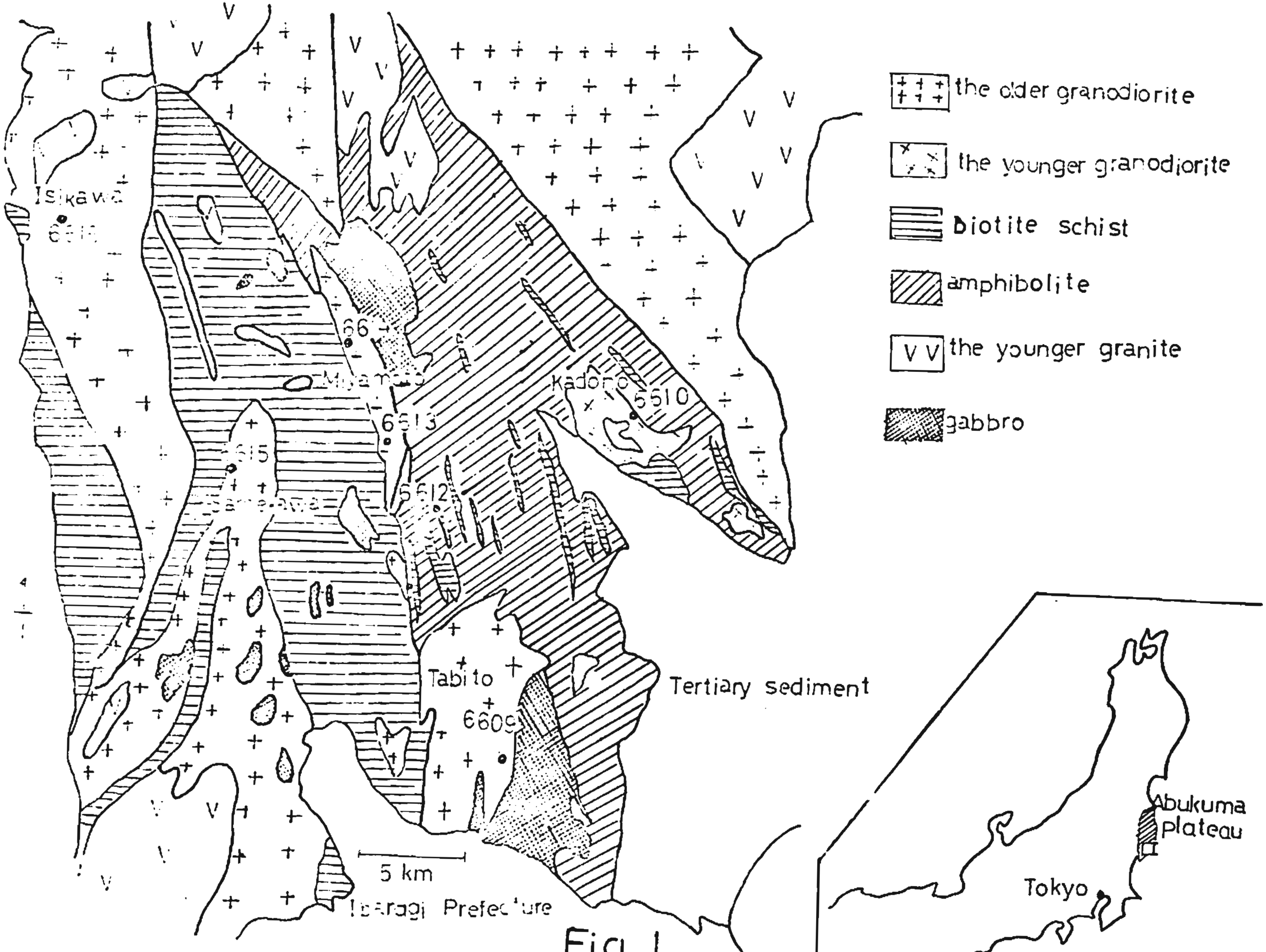

the older granodiorite
the younger granodiorite
biotite schist
amphibolite
the younger granite
gabbro
Isikawa
6613
6612
6610
Tabito
6609
Tertiary sediment
5 km
Abukuma
plateau
Tokyo

Fig. 1

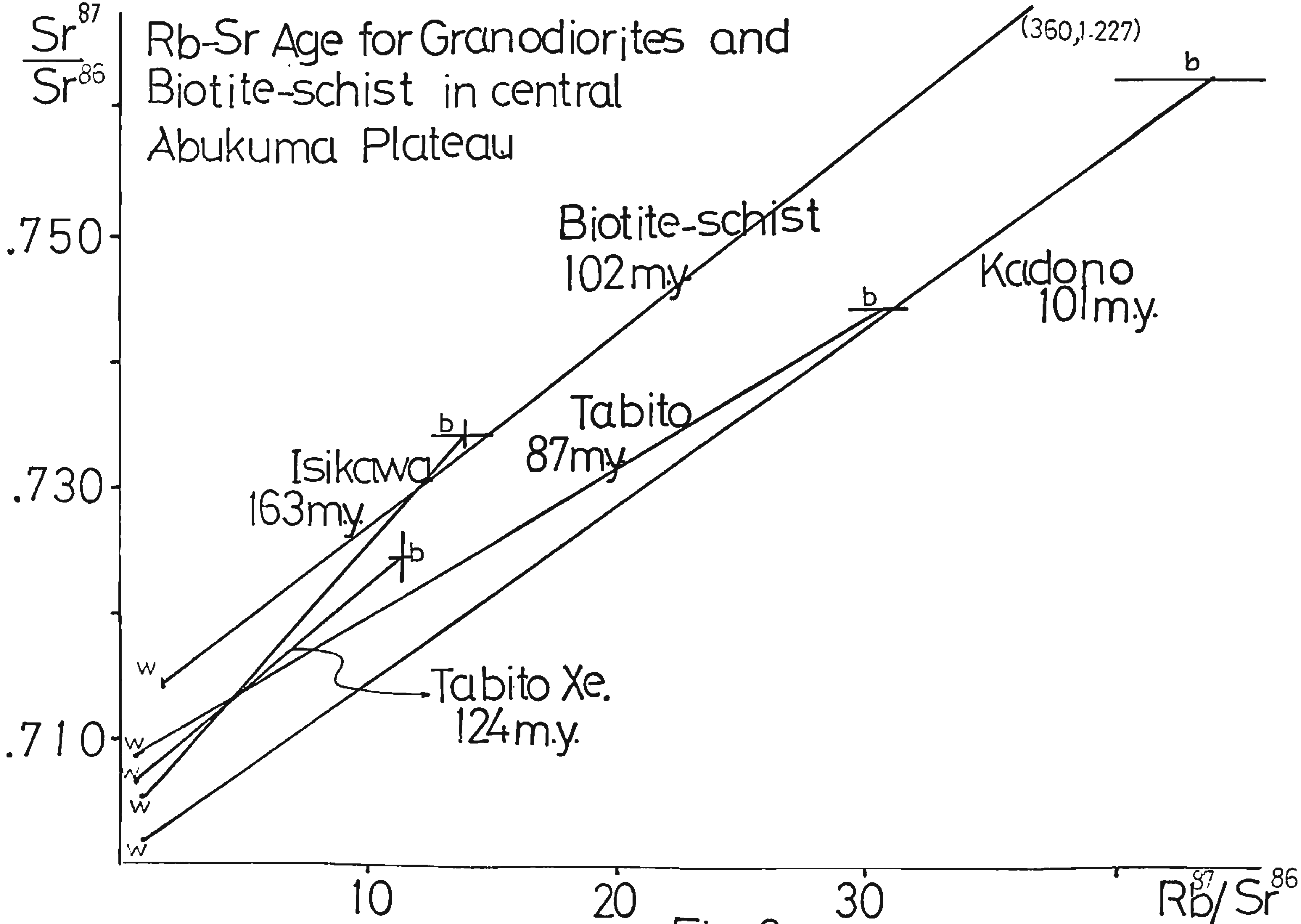

Rb-Sr Age for Granodiorites and Biotite-schist in central Abukuma Plateau
Sr87/Sr86
.750
.730
.710
(360,1.227)
b
Biotite-schist 102m.y.
Kadono 101m.y.
Tabito 87m.y.
Isikawa 163m.y.
Tabito Xe. 124m.y.
w
10
20
30
Rb87/Sr86

Fig. 2

7. K-Ar Ages and Palaeomagnetic Studies on Rocks from the East Coast of Lutzow-Holm Bay, Antarctica

I. Kaneoka, M. Ozima, Mituko Ozima, M. Ayukawa

and

T. Nagata

Geophysical Institute, University of Tokyo

It seems desirable that palaeomagnetic studies and radiometric age determinations are made on the same rock samples for the purpose of systematic research of possible relative movements of Antarctic continent with respect others in geologic time as well as of the palaeogeomagnetic field.

Several rock samples were collected from the Syowa Base area on the East Coast of Lützow-Holm Bay, Antarctica during the period of the 7th Japanese Antarctic Research Expedition, 1965-1966. Sampling sites are shown in Fig. 1 and it was reported that most of this area are composed of high grade metamorphic rocks (Tatsumi and Kikuchi, 1959). K-Ar age determinations and palaeomagnetic studies were made on the same rocks obtained from this area.

K-Ar ages were determined for the samples A02 and AS. For the sample A02, K-Ar ages were also obtained for the separated mafic and felsic minerals. The results of K-Ar age determinations are listed in Table 1. Ages of this area were previously obtained by the Rb-Sr method (Nicolaysen et al., 1961) and the U-Pb method (Saito et al.,1961). They obtained the ages of about 500 m.y.. In comparison with these ages, K-Ar ages in the present study show generally younger ages. However, geology in this region is very complicatad (Tatsumi and Kikuchi, 1959) and it is not possible to identify whether samples dated in the present study belong to the same geological unit as those studied previously by other authors. Therefore, we cannot decide whether the difference in age values are due to the difference of samples or due to some other reasons such as argon loss from the rocks during geological period.

As shown in Table 1, the K-Ar ages for different minerals from the same rock AO2 show different ages; felsic minerals (mostly feldspar and quartz) show the youngest age, whereas the mafic (mostly hornblende and biotite) the oldest age. As it is generally accepted that hornblende and biotite have higher argon retentivity than feldspar (e.g. Hart, 1964), the observed pattern of the order of the age values among different minerals may suggest the argon loss from the felsic minerals. Moreover, it is interesting to note that the whole rock gives the average age between those of felsic and mafic minerals. Considering its high argon retentivity, mafic minerals would show the most reliable age among them.

Since the entire region in which samples were obtained was very intensely metamorphosed, the ages determined in this region should be regarded to represent the ages of the metamorphism. The same conclusion was obtained by Nicolaysen et al. (1961).

Palaeomagnetic measurements were made only for the sample AO2, since sample AS has too weak magnetization (less than 10^{-8} emu/cc) to be measured. The AC magnetization test shows that NRM of these samples is very stable. The average values of declination and inclination of NRM are tabulated in Table 2, in which palaeomagnetic results obtained previously for rocks from the same area (Nagata and Shimizu 1959, 1960, Nagata and Yama-ai, 1961) are also included. According to Tatsumi and Kikuchi (1959), metamorphism in this region was of high temperature type. Therefore, it is most likely that the magnetic mineral (Curie temperature = 560°C) of these samples may have acquired the remanent magnetization (TRM) during the metamorphism. For this reason, no bedding correction was made for the estimation of the virtual pole positions. The average intensity of NRM of 4 samples are 5.4×10^{-4} emu/cc.

The palaeomagnetic data on Antarctic rocks have been summarized from the table compiled by Irving (1964) and they are plotted in Fig. 2 together with the present result. The most remarkable feature is that only the virtual pole determined from the Ongul Island is situated around the equator, while other virtual poles obtained from rock samples of other area located in the middle to higher latitude. As pointed out by Nagata and Yama-ai (1961), it seems that the virtual pole shifted from the equator to the present pole position during the geological period from several hundred million years ago to the present time. However, there still remains the possibility of the relative displacement of the Syowa Base area with respect to the rest of the Antarctic continent, because there are some uncertainties in the absolute ages of other data which were estimated simply on the basis of field observations. It is hoped therefore that more systematic research of palaeomagnetism will be made on radiometrically dated samples collected from many localities of different geologic ages in Antarctica.

We are grateful to Dr. S. Kokubun who collected the rock samples used in the present study.

References

Hart, S. R., the Petrology and Isotopic Mineral Age Relations of a Contact Zone in the Front Range, Colorado (1964), Jour. Geology, 72, 493-525.

Irving, E. (1964), Paleomagnetism, John Wiley and Sons, 399.

Nagata, T. and Y. Shimizu, Paleomagnetic Studies on Precambrian Gneiss of Ongul Island, Antarctica (1960), Antarctic Record, 10, 661-668, (1959), Nature, 184, 1472.

Nagata, T. and M. Yama-ai, Paleomagnetic Studies on Rocks on the Coast of Lutzow-Holm Bay (1961), Antarctic Record, 11, 945-947.

Nicolaysen, L. O., A. J. Burger, T. Tatsumi and L. H. Ahrens, Age Measurements on Pegmatites and a Basic Charnockite Lens occuring near Lützow-Holm Bay, Antarctica (1961), Geochim. Cosmochim. Acta, 22, 94-98.

Saito, N., T. Tatsumi and K. Sato (1961), Absolute Age of Euxenite from Antarctica, Antarctic Record, 12, 1057-1062.

Tatsumi, T. And T. Kikuchi (1959), Report of Geomorphological and Geological Studies of the Wintering Team (1957-1958) of the First Japanese Research Expedition, Part 2, Antarctic Record, 8, 1-21.

Table 1. K-Ar ages of rocks from the east coast of Lützow-Holm Bay

Sample	Locality	Rock type	Ar^{40} ($\times 10^{-9}$ moles/g)	$\frac{(Ar^{40})air}{(Ar^{40})total}$ (%)	K(%)	$(Ar^{40})/(K^{40})$ ($\times 10^{-2}$)	Age (m.y.)
AS	East Coast of Lützow-Holm Bay Skarvshes	Garnet-biotite gneiss (whole rock)	3.423	14.8	4.81 (4.90, 4.72)	2.341	363
A02	East Ongul Is.	Biotite-hornblende gneiss (whole rock)	2.351	3.3	3.08 (3.13, 3.03)	2.511	387
"	"	" (biotite+hornblende)	2.134	11.5	2.54 (2.53, 2.55)	2.764	421
"	"	" (feldspar+quartz)	2.805	13.0	4.09 (4.07, 4.11)	2.257	350

$\lambda_e = 0.585 \times 10^{-10}\ yr^{-1}$

$R = 0.124$

$K^{40}/K = 1.19 \times 10^{-4}$ mole/mole

Table 2. Palaeomagnetic results of rocks from the Ongul Island

Author	Locality	Number of specimen	Direction of NRM: Declination	Direction of NRM: Inclination	Virtual geomagnetic pole (uncorrected): Lat.	Virtual geomagnetic pole (uncorrected): Long.
Nagata and Shimizu (1959)	East Ongul Is.	18	-23°	51°	19°N	163°W
Nagata and Yama-ai (1961)	Ongul Is.	5	-10°	49°	9°N	148°W
Present work	East Ongul Is.	4	$-7^{\circ}0'$	$46^{\circ}36'$ *	7°N	147°W

* . All samples have reverse NRM.

Fig. 1 Map of the East Coast of Lützow-Holm Bay area
AO and AS show the sampling localities

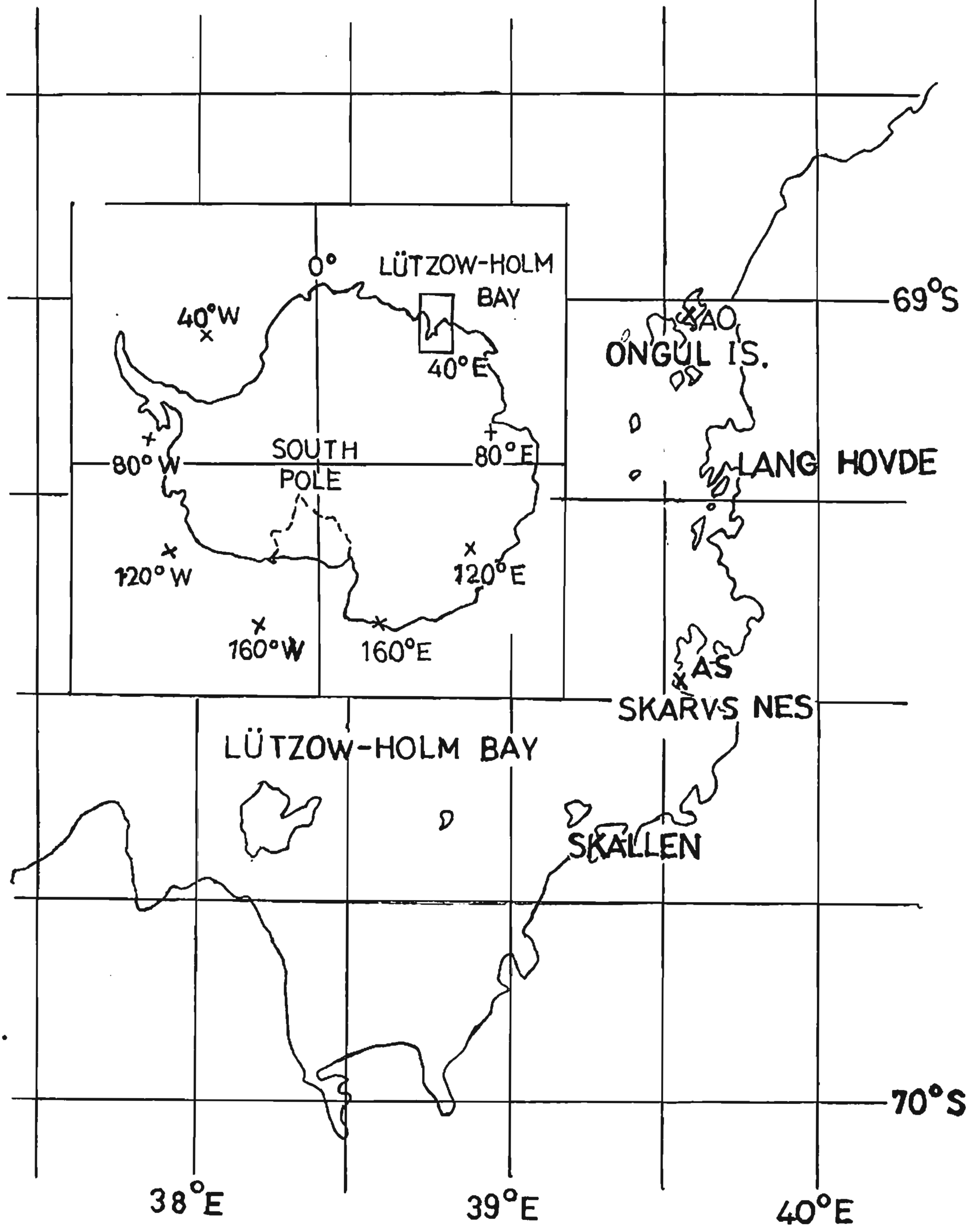

Fig. 2. Palaeomagnetism in the Antarctica
Cross symbol shows the present geomagnetic pole

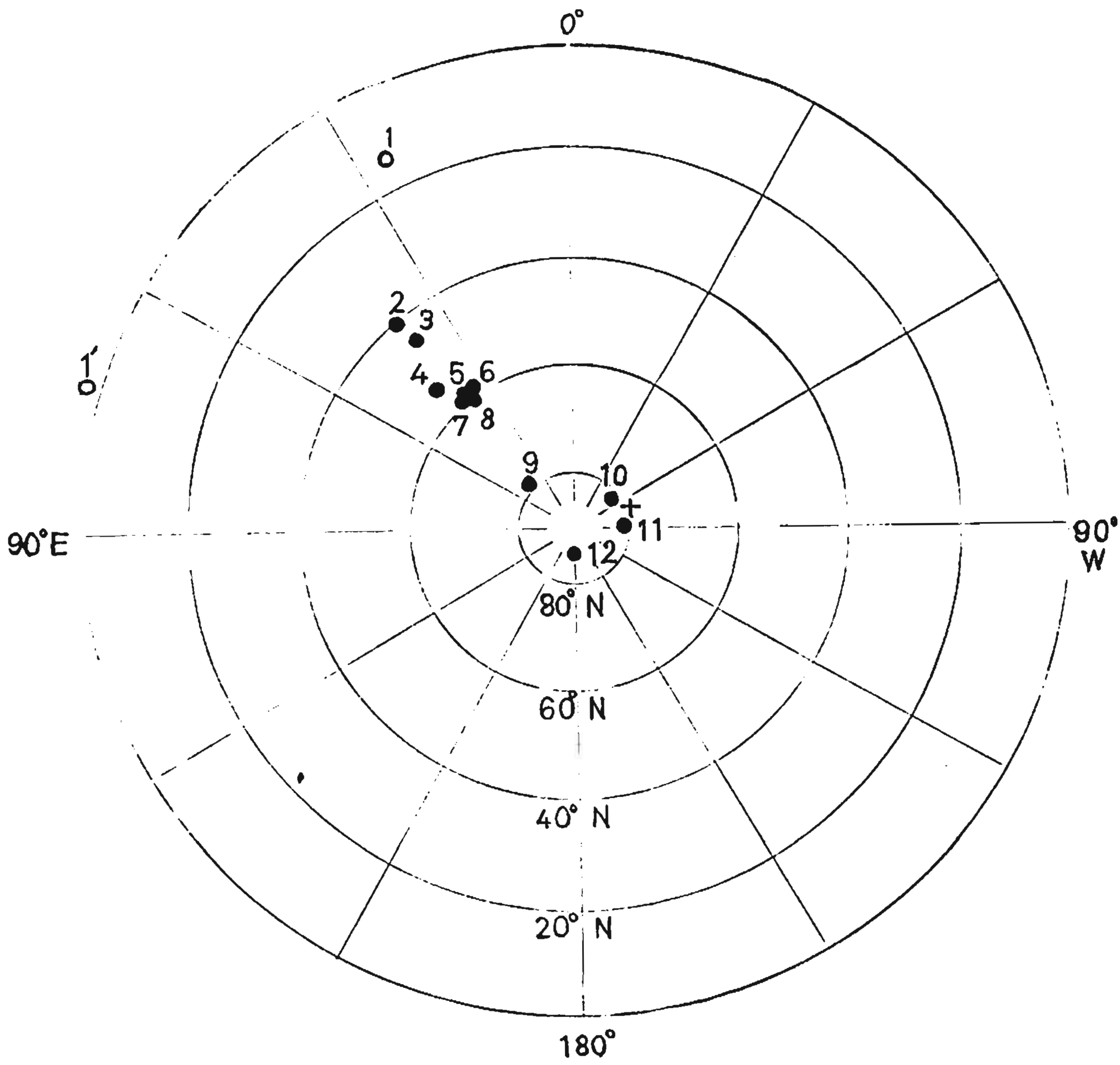

1. Ongul Island (421)
2. Basement Dikes (Є-C)
3. Ferrar Dolerite (163 - 127)
4. Dolerite Intrusions (Tr-J)
5. Ferrar Dolerite (163 - 127)
6. Beacon Sediments (D-Tr)
7. Ferar Dolerite (163 - 127)
8. Admiralty Granite (Є)
9. Volcanics (T-Q)
10. Volcanics (Q)
11. Lavas, Cape Hallet (T-Q)
12. Andean Intrusive Suite (95 - 43)

8. Paleomagnetism and K-Ar Ages of Successive Lava Flows (2)

--- Kita-Matsuura Basalts, Kyushu, Japan ---

Minoru Ozima, I. Kaneoka, M. Kono, H. Kinoshita, K. Kobayashi,
N. Ohnaka, T. Nagata
Geophysical institute, University of Tokyo

and

H. Kurasawa
Geological Survey of Japan

Paleomagnetism and K-Ar ages were studied on two lava flow successions from Kita-Matsuura area, northwestern Kyushu. At Tsujinodo site, there are five successive lava flows, in which the upper and lower flows have normal polarity, whereas the middle flow has reversed polarity. At Ningyo-ishiyama site, eight successive lava flows were identified, in which the upper three flows show normal polarity. whereas the lower five flows show reversed polarity. These are schematically illustrated in Figure. The relationship between the two lava flow successions are not clear on the basis of field geology.

The results of paleomagnetic measurements and K-Ar ages are given in Table 1 and Table 2. Except flow KM 32, NRMs show good grouping and also good stability against a-c demagnetization (Table 1). Hence, we conclude that the measured directions of the NRMs represent the paleomagnetic field. K-Ar ages obtained for four samples at Tsujinodo site and five samples at Ningyo-ishiyama site range from 7 m.y to 10 m.y, the average are being about 8.0 m.y. It can be concluded that the Kita-Matsuura basalts were erupted 8.0 m.y+1.0 ago.

However, K-Ar ages are not generally consistent within a single lava flow and among successive lava flows. There should be no significant difference in the analytical precision between the present analyses and those in New Mexico samples previously reported, in which K-Ar ages are generally consistent within 5 percent (Ozima et al., 1967). In addition, air contamination in the present analyses are generally lower than in the case of New Mexico samples. Hence, it is unlikely that the observed inconsistencies in the age results are merely due to the analytical errors. The inconsistent ages in the present analyses must be due to alteration of samples and/or the presence of glassy parts in the samples. It is therefore not possible to estimate the transition time intervals of the geomagnetic field switching.

With regards to the inconsistent K-Ar ages, we would like to emphasize the necessity to establish criteria for reliability of K-Ar age. To obtain reliable K-Ar age, it is customary to examine thin sections of each sample (Dalrymple, 1963). However, as there is no objective standard in thin section examination to judge the suitability of samples for K-Ar dating, there still remains some ambiguity as to reliability of K-Ar ages even after the severest choice of samples under a microscope. Considering that in the case of dating young basaltic rocks, there is no available dating methods which can be used to check K-Ar ages, it is particularly important to establish a more objective criterion of the reliability of K-Ar ages. Internal consistencies within a single flow and among flows whose successions are geologically well established may be one of the most practical and objective criteria of the reliability of K-Ar ages.

References

Dalrymple, G. B., (1963), Potassium-argon dating of some Cenozoic volcanic rocks of the Sierra Nevada, California, Geol. Soc. America Bull., 74, 379-390.

Ozima, M., M. Kono, I. Kaneoka, H. Kinoshita, K. Kobayashi, T. Nagata, E. E. Larson and D. Strangway, (1967), Paleomagnetism and potassium-argon dating of some volcanic rocks from the Rio Grande Gorge, New Mexico, Jour. Geophys. Res., 72, 2615-2621.

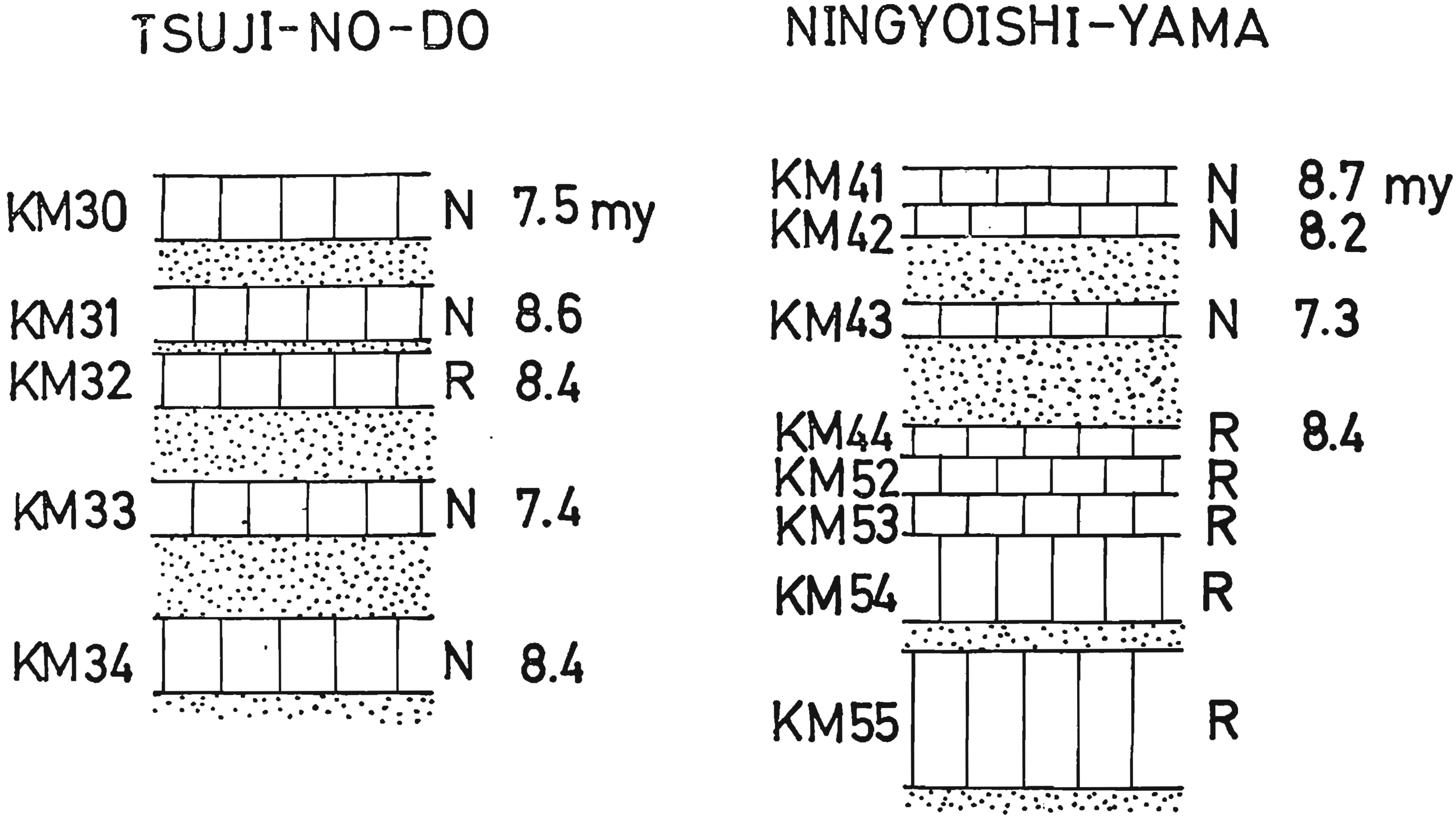
TSUJI-NO-DO
KM30 N 7.5 my
KM31 N 8.6
KM32 R 8.4
KM33 N 7.4
KM34 N 8.4
NINGYOISHI-YAMA
KM41 N 8.7 my
KM42 N 8.2
KM43 N 7.3
KM44 R 8.4
KM52 R
KM53 R
KM54 R
KM55 R

Table 1

Sample	a-c demagnetization*	N	NRM I	NRM D	k	α_{95}	Virtual pole lat.	Virtual pole long.	Intensity (emu/g)
				Tsujinodo site					
KM30	$\tilde{H}$ = 0	5	72.5	47.0	8.03	28.8	50.2	166.8	2.11×10^{-4}
	$\tilde{H}$ = 150 Oe	5	42.2	122.7	9.5	26.1	-10.6	180.5	8.30×10^{-5}
KM31	$\tilde{H}$ = 0	5	68.6	0.0	27.6	14.8	71.3	129.4	3.21×10^{-4}
	$\tilde{H}$ = 150 Oe	5	65.9	57.3	15.4	20.1	45.2	182.1	1.82×10^{-4}
KM32	$\tilde{H}$ = 0	5	1.2	-149.4	5.5	36.0	-45.5	82.6	2.70×10^{-4}
	$\tilde{H}$ = 150 Oe	5	7.8	164.3	1.2	142.5	-49.9	154.1	1.24×10^{-4}
KM33	$\tilde{H}$ = 0	5	47.3	- 2.5	183.4	5.7	84.7	334.4	9.42×10^{-4}
	$\tilde{H}$ = 150 Oe	5	51.3	- 1.9	58.2	10.1	87.9	1.3	5.29×10^{-4}
KM34	$\tilde{H}$ = 0	5	48.3	- 19.1	173.6	5.8	73.3	30.8	1.38×10^{-3}
	$\tilde{H}$ = 150 Oe	5	49.8	- 12.4	184.6	5.6	79.1	28.6	1.07×10^{-3}
				Ningyo-ishiyama site					
KM41	$\tilde{H}$ = 0	4	52.1	-146.5	4.29	50.5	-16.9	100.3	1.55×10^{-4}
	$\tilde{H}$ = 150 Oe	4	35.0	-143.7	3.7	55.4	-27.0	90.4	9.30×10^{-5}
KM42	$\tilde{H}$ = 0	4	42.4	- 21.6	66.5	11.3	69.3	20.0	1.35×10^{-3}
	$\tilde{H}$ = 150 Oe	4	43.3	- 21.4	80.8	10.3	69.7	21.6	1.12×10^{-3}
KM43	$\tilde{H}$ = 0	5	38.8	- 13.2	59.9	10.0	73.8	358.4	7.50×10^{-4}
	$\tilde{H}$ = 150 Oe	5	36.8	- 9.1	39.5	12.3	74.9	344.0	4.22×10^{-4}
KM44	$\tilde{H}$ = 0	8	-46.3	173.9	52.1	6.9	-82.5	173.5	1.36×10^{-3}
	$\tilde{H}$ = 150 Oe	8	-46.6	174.5	67.8	6.0	-82.7	173.3	1.25×10^{-3}
KM52	$\tilde{H}$ = 0	4	-46.0	179.9	127.1	8.2	-84.1	130.4	1.49×10^{-3}
	$\tilde{H}$ = 150 Oe	4	-46.9	-179.5	127.6	8.2	-84.8	124.4	1.28×10^{-3}
KM53	$\tilde{H}$ = 0	5	-50.1	-173.0	210.2	5.3	-83.6	59.4	1.75×10^{-3}
	$\tilde{H}$ = 150 Oe	5	-50.4	-172.3	212.7	5.3	-83.1	55.4	1.59×10^{-3}
KM54	$\tilde{H}$ = 0	5	-44.0	170.6	53.5	10.6	-78.9	179.4	2.40×10^{-3}
	$\tilde{H}$ = 150 Oe	5	-46.0	171.8	66.0	9.5	-80.8	181.7	1.99×10^{-3}
KM55	$\tilde{H}$ = 0	5	-44.7	-173.6	55.2	10.4	-81.1	89.2	1.80×10^{-3}
	$\tilde{H}$ = 150 Oe	5	-47.0	-172.9	75.0	8.9	-82.1	77.2	1.33×10^{-3}

*, H = 0 denotes an original NRM. H = 150 Oe denotes the NRM after a-c demagnetization with H = 150 Oe.
N, number of samples. I, Inclinations of mean direction of NRM. D, Declinations of mean direction of NRM.
k, Fisher's precision parameter. α_{95}, Semiangle of cone of 95% confidence for mean direction.

Table 2

Tsujinodo site

Sample	wt(g)	Ar^{40} rad(mole/gr)	(Ar^{40})air/(Ar^{40})total × 100	k(%)	t (m.y.)
KM3001-a	8.553	1.712×10^{-11}	72.5	1.28	7.52
KM3104-a	7.782	2.050×10^{-11}	56.2	1.47	7.82
KM3104-b	7.788	2.459×10^{-11}	45.7	1.46	9.44
KM3203-a	11.32	1.516×10^{-11}	63.7	1.08	7.87
KM3203-b	7.033	1.740×10^{-11}	84.0	1.07	9.12
KM3203-b	5.934	1.566×10^{-11}	81.6	1.07	8.20
KM3301-b	8.033	6.717×10^{-12}	95.2	0.512	7.35
KM3403-a	7.227	8.136×10^{-12}	91.2	0.543	8.40

Ningyo-ishiyama site

Sample	wt(g)	Ar^{40} rad(mole/gr)	(Ar^{40})air/(Ar^{40})total × 100	k(%)	t (m.y.)
KM4101-a	10.74	2.37×10^{-11}	51.0	1.71	7.77
KM4101-b	11.327	2.732×10^{-11}	81.5	1.63	9.39
KM4101-b	9.523	2.620×10^{-11}	87.3	1.63	9.01
KM4202-c1	7.944	3.314×10^{-11}	70.6	2.29	8.11
KM4202-c2	9.684	3.361×10^{-11}	79.5	2.27	8.30
KM4303-a	7.076	4.548×10^{-11}	42.4	2.23	7.92
KM4303-b	6.086	4.044×10^{-11}	74.6	3.22	7.04
KM4303-b	6.871	4.136×10^{-11}	40.2	3.26	7.11
KM4403-a	8.029	1.502×10^{-11}	91.6	0.791	10.6
KM4403-b	7.381	1.037×10^{-11}	84.1	0.824	7.05
KM4403-b	8.306	1.202×10^{-11}	79.0	0.824	8.18
KM4404-a	9.486	1.087×10^{-11}	81.0	0.777	7.84

$\lambda_e = 0.585\times10^{-10}\ y^{-1}$, $\lambda_\beta = 4.72\times10^{-10}\ y^{-1}$, $K^{40}/K = 1.19\times10^{-4}$ mole/mole

9. K-Ar ages and paleomagnetism of successive lava flows (3)*

--- Hanamagari and Kirizumi andesites, Gumma Prefecture*, Japan ---

Minoru Ozima, I. Kaneoka, M. Kono, H. Kinoshita, K. Kobayashi,
Y. Ohnaka, T. Nagata
Geophysical Institute, University of Tokyo

and

S. Aramaki
Earthquake Research Institute, University of Tokyo

The northeastern part of Nagano Prefecture and western part of Gumma Prefecture belong to the extensive Miocene-to-Quarternary volcanic province of the "Fossa Magna" in central Japan. A partly destroyed Quaternary strato-volcano, Hanamagari (Aramaki, 1963) lies on the boundary between Nagano and Gumma Prefectures and is underlain by a thick pile of volcaniclastic materials and lava flows. This pile is collectively called the Kirizumi group (Iijima et al. 1958, Aramaki 1963). The Kirizumi group is more or less flat-lying and made up of essential tuff, lapilli tuff, tuff breccia, lava flow, and smaller amounts of sandstone, shale, conglomerate, etc. A few geological evidences indicate that the Kirizumi group is Pliocene. The rocks of both the Hanamagari volcano and the Kirizumi group are calc-alkali andesites with common phenocrysts of plagioclase, hypersthene, augite, and opaque minerals (Aramaki, 1963).

Within the drainage area of the Kirizumi River, both the Hanamagari and Kirizumi pyroclastics and lavas are exposed and their stratigraphic succession can be clearly traced. Along one of the branch stream flowing

*) Contribution No. 241 from Division of Geomagnetism and Planetary Physics, Geophysical Institute, University of Tokyo, Series II.

from west to east to join the main course of the Kirizumi River, five successive lava flows of the Hanamagari volcano are underlain unconformably by more than 15 lava flows of the Kirizumi group. Sampling was made on these lava flows as shown schematically in Fig. 2. The lava flows are intercalated with loose to semi-consolidated pyroclastic materials. The altitude of the boundary surface of the unconformity between the Hanamagari volcano and Kirizumi group changes more than 50m within the horizontal distance of 300m. The top of the Kirizumi group has been weathered to the depth of 10m or more. The alternation of lava flows and loose pyroclastic materials of the Hanamagari volcano bears features characteristic to volcanic products of subaerial origin. The volcaniclastic materials intercalated with lava flows of the Kirizumi group are variagated, more or less equigranular tuff, lapilli tuff and tuff breccia with matrix of finely divided materials of the same nature as those composing coarser fractions. Many outcrops are interpreted as part of autobrecciated lava or thick mantle of brecciated part of the lava flow. All of these features indicate that the Kirizumi group is of subaqueous (submarine) origin and the Hanamagari volcano subaerial, and a large time gap existed between the two.

The interface between lava flows and volcaniclastic layers of the Kirizumi group appear to be always conformable indicating successive deposition within a short period.

3-5 cores are drilled from each lava flow. After measuring the NRMs, all samples were subjected to a-c demagnetization with a peak field up to 400 Oe. All flows belonging to the Hanamagari group have a normal polarity. Since the grouping of the NRMs is generally good and there is no marked change in the NRMs after the a-c demagnetization (Table 1), we conclude that the NRMs of the Hanamagari lava flows represent the paleomagnetic field, or the geomagnetic field had a normal polarity when the Hanamagari lavas was erupted. In contrast to the Hanamagari lavas, the lava flows of the under-lying Kirizumi group have either a very shallow positive inclination or negative inclination. Although the NRMs before and after the a-c demagnetization have poor grouping, all the NRMs show a negative inclination after the a-c demagnetization. Hence, it is likely that the geomagnetic field was reversed at the time the Kirizumi was deposited. As will be discussed below, this conclusion is further substantiated by the comparison of the K-Ar ages with N-R geomagnetic polarity time table (Dalrymple et al. 1967, McDougall and Chamalaun 1967). The results of the paleomagnetic measurements are listed in Table 1.

Thin sections were examined for all the lava flows. Except for flows KH 04, KH 06 and KH 10, they carry considerable amounts of alteration of minerals such as chlorite, montmorillonite etc. Hence, K-Ar dating was attempted only for the three flows, KH 04, KH 06 and KH 10. Petrographic descriptions of these flows are given in the appendix. The results of the K-Ar age determinations are given in Table 2. Experimental procedures for Ar and K analyses are the same as those described somewhereelse (Ozima et al, 1967).

Because of high air conatamination in the determination of radiogenic argon-40 and also of the poor reproducibility in the ages of the Hanamagari lava flows, the values of the K-Ar ages should be taken with some reservation. Hence, it is not possible to identify only from the present results to which normal event or epock the Hanamagari lava flows belong. However, it seems to be at least certain that there is a large time span between the Hanamagari and the Kirizumi groups. The latter conclusion is in good accordance with the geological evidences described in the foregoing.

In the case of the Kirizumi lava flows, K-Ar ages can be considered to be internally consistent within a flow and between the flows within the experimental error, the latter being estimated to be about 0.15 m.y. at 3 m.y. Hence, we conclude that the K-Ar ages of the Kirizumi flows represents the time when the flows were erupted. Considering the paleomagnetic results mentioned above and also the normal-reverse geomagnetic polarity time table proposed by Dalrymple et al. (1967) and by McDougall and Chamalaun (1966), it is most likely that the Kirizumi flows were erupted during the Mammoth reversed polarity event.

References

Aramaki, S., (1963), Geology of Asama volcano, Jour. Fac. Sci. Univ. Tokyo, Sec. II, 14, 229-443.

Dalrymple, G.B., A. Cox, R.R. Doell and C.S. Gromme, (1967), Pliocene geomagnetic polarity epochs, Earth and Planetary Sciences, Letters, 2, 163-173.

Iijima, N., Taguchi, K., Ishiwa, K., Koda, M., Nakamura J., Kigune, K., Kobayashi, M., Yano, K. and Yamagishi, I., (1958), The volcanoes and the basement of the eastern part of Fossa Magna (in Japanese). Jour. Assoc. Geol. Collaboration Japan, No. 62, 622-635.

McDougall, I. and F.H. Chamalaun, (1966), Geomagnetic polarity scale of time, Nature, 212, 1415-1418.

Ozima, M., M. Kono, I Kaneoka, H. Kinoshita, K. Kobayashi, T. Nagata, E.E. Larson and D. Strangway, (1967), Paleomagnetism and potassium-argon dating of some volcanic rocks from the Rio Grande Gorge, New Mexico, Jour. Geophys. Res., 72, 2615-2621.

Figure Captions

Fig. 1. Geological map of sampling site. Sampling sites are indicated by crosses.

Fig. 2. Schematic representation of lava flow successions. N. and R indicate normal and reversed polarities of NRM's in each flow. Mean K-Ar ages (m.y.) are also indicated.

Table 1. Paleomagnetic data of Hanamagari and Kirizumi lava flows

Sample	a-c demagnetization*	N	NRM I	NRM D	NRM k	NRM 95	Virtual pole lat.	Virtual pole long.	Intensity (e.m.u/gr)
KH01	$\tilde{H}$ = o	7	47.1	0.1	56.4	8.1	81.9	318.3	2.14×10^{-3}
	$\tilde{H}$ = 200 Oe	7	47.4	1.7	45.4	9.1	82.1	308.0	1.19×10^{-3}
KH02	$\tilde{H}$ = o	6	55.1	8.6	33.9	11.7	83.0	231.8	1.06×10^{-3}
	$\tilde{H}$ = 200 Oe	6	59.9	8.5	20.6	15.1	82.0	192.8	6.49×10^{-4}
KH04	$\tilde{H}$ = o	6	84.8	-136.7	3.61	41.1	28.5	130.6	5.89×10^{-4}
	$\tilde{H}$ = 200 Oe	6	73.6	24.1	3.71	40.3	62.1	164.9	1.41×10^{-4}
KH06	$\tilde{H}$ = o	5	30.4	- 21.5	1.92	78.1	62.3	8.0	1.49×10^{-3}
	$\tilde{H}$ = 200 Oe	5	-35.3	- 61.3	1.70	89.7	9.6	15.7	4.07×10^{-4}
KH07	$\tilde{H}$ = 0	6	29.1	- 50.3	1.59	84.5	40.9	37.3	1.90×10^{-4}
	$\tilde{H}$ = 200 Oe	6	-56.5	- 79.4	1.54	88.5	-13.8	12.6	1.10×10^{-4}
KH08	$\tilde{H}$ = o	5	10.6	- 45.5	3.28	50.2	38.1	23.2	1.18×10^{-4}
	$\tilde{H}$ = 200 Oe	5	-45.0	- 46.0	2.65	58.9	13.6	0.1	6.24×10^{-5}
KH09	$\tilde{H}$ = o	5	66.7	- 60.0	2.05	73.3	45.5	85.1	2.22×10^{-4}
	$\tilde{H}$ = 200 Oe	5	-25.5	-118.8	1.98	75.9	-31.0	54.8	1.55×10^{-4}
KH10	$\tilde{H}$ = o	5	66.5	- 25.2	32.4	13.6	67.7	91.2	1.83×10^{-4}
	$\tilde{H}$ = 200 Oe	5	-53.2	-112.0	9.41	26.3	-35.5	29.8	6.37×10^{-5}
KH11	$\tilde{H}$ = o	5	- 9.5	- 96.5	2.29	66.4	- 8.1	48.7	1.73×10^{-4}
	$\tilde{H}$ = 200 Oe	5	-55.0	-138.0	10.5	24.8	-56.3	37.3	2.29×10^{-4}
KH12	$\tilde{H}$ = o	5	-63.9	-151.5	82.6	8.5	-66.7	16.5	8.31×10^{-4}
	$\tilde{H}$ = 200 Oe	5	-64.5	-142.7	53.6	10.5	-60.6	17.0	8.00×10^{-4}
KH99	$\tilde{H}$ = o	2	-17.3	-174.3	11.6	81.6	-62.0	126.7	1.24×10^{-4}
	$\tilde{H}$ = 200 Oe	2	-52.7	-179.6	880.6	8.4	-86.9	132.5	1.14×10^{-4}

*, $\tilde{H}$ = o denotes an original NRM. $\tilde{H}$ = 200 denotes the NRM after a-c demagnetization with H = 200 Oe.
N, number of samples.
I, Inclination of mean direction of NRM.
D, Declination of mean direction of NRM.
k, Fisher's precision parameter.
α_{95}, Semiangle of core of 95% confidence for mean direction.

Table 2. K-Ar ages of Hanamagari and Kirizumi lava flows

Sample	Wt (gr)	(Ar^{40})rad moles/gr	(Ar^{40})air / (Ar^{40})total	K (%)	t (m.y.)
KH04-5	7.685	1.164×10^{-12}	97.1	0.650, 0.643	1.01
	6.942	1.405×10^{-12}	96.5		1.22
KH06-2	8.787	4.416×10^{-12}	74.5	0.806, 0.797	3.10
	8.985	4.573×10^{-12}	85.1		3.17
KH10-3	13.42	5.078×10^{-12}	67.6	0.935, 0.936	3.04
	11.39	5.122×10^{-12}	73.5		3.07

$\lambda_e = 0.585 \times 10^{-10} y^{-1}$, $\lambda_\beta = 4.72 \times 10^{-10} y^{-1}$, $K^{40}/K = 1.19 \times 10^{-4}$ mole/mole

Appendix

Petrographic description of lavas of the Hanamagari and the Kirizumi groups

		KH04	KH06	KH10
phenocryst	plagioclase	+++ slight alteration	+++ partly altered to clay mineral, carbonate etc.	+++ slight alteration
	hypersthene	++ fresh	+ fresh	++ fresh
	augite	++ fresh	+ fresh	++ fresh
	opaque mineral	+ oxide coating	+	+
groundmass	texture	coarse-grained intersertal	fine-grained pilotaxitic	coarse-grained intersertal
	plagioclase	+++ fresh	+++ fresh?	+++ fresh
	orthopyroxene	++ fresh	+ fresh?	?
	clinopyroxene	++ fresh	+ fresh?	++ fresh
	silica-feldspar mesostasis	+++	+++ ?	+++
	opaque mineral	+	+	++
	clay mineral	+	?	+

+++ most abundant
++ abundant
+ less abundant

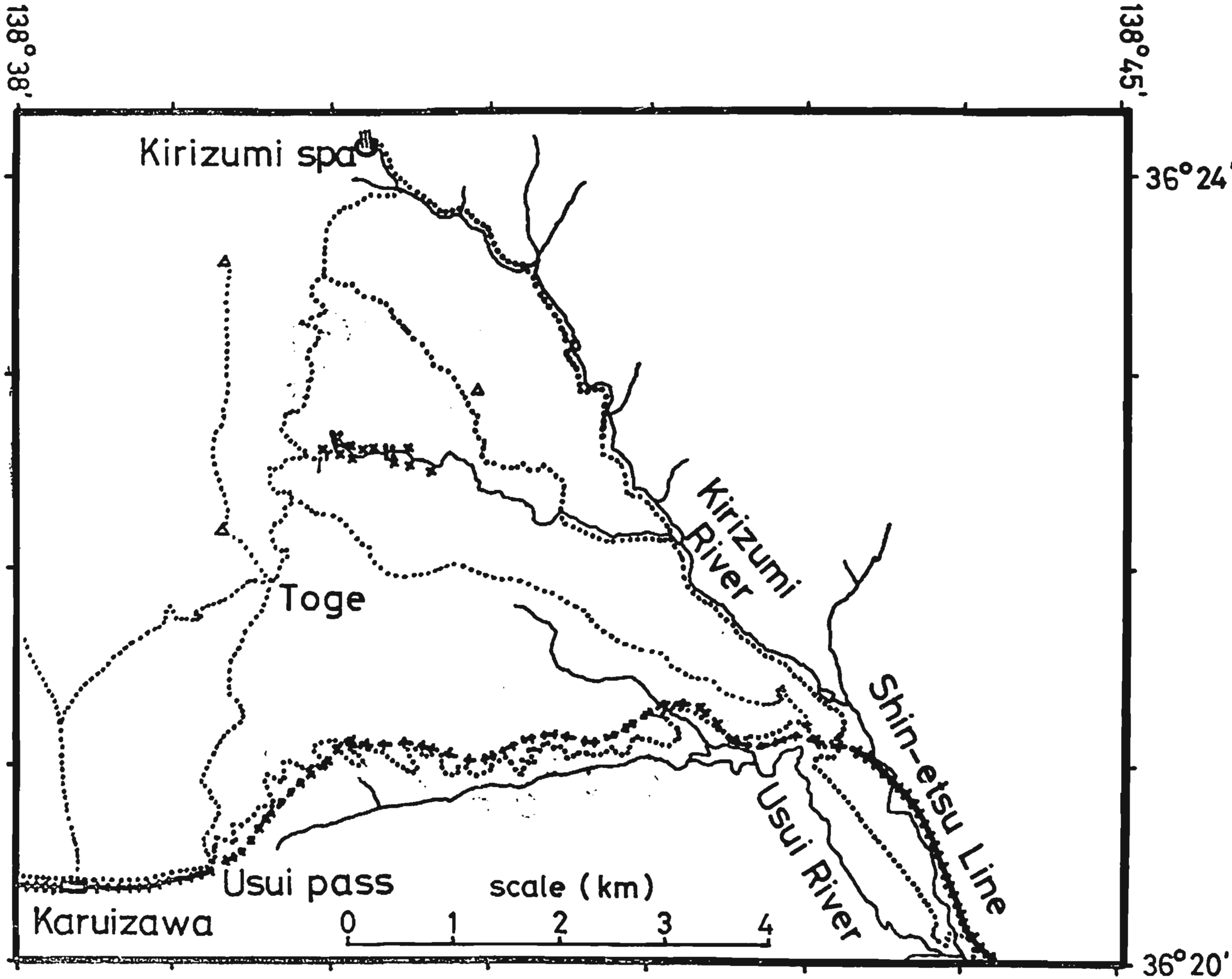

138°38'
138°45'
36°24'
36°20'
Kirizumi spa
Toge
Kirizumi River
Shin-etsu Line
Usui River
Usui pass
Karuizawa
scale (km)
0 1 2 3 4

Fig. 1

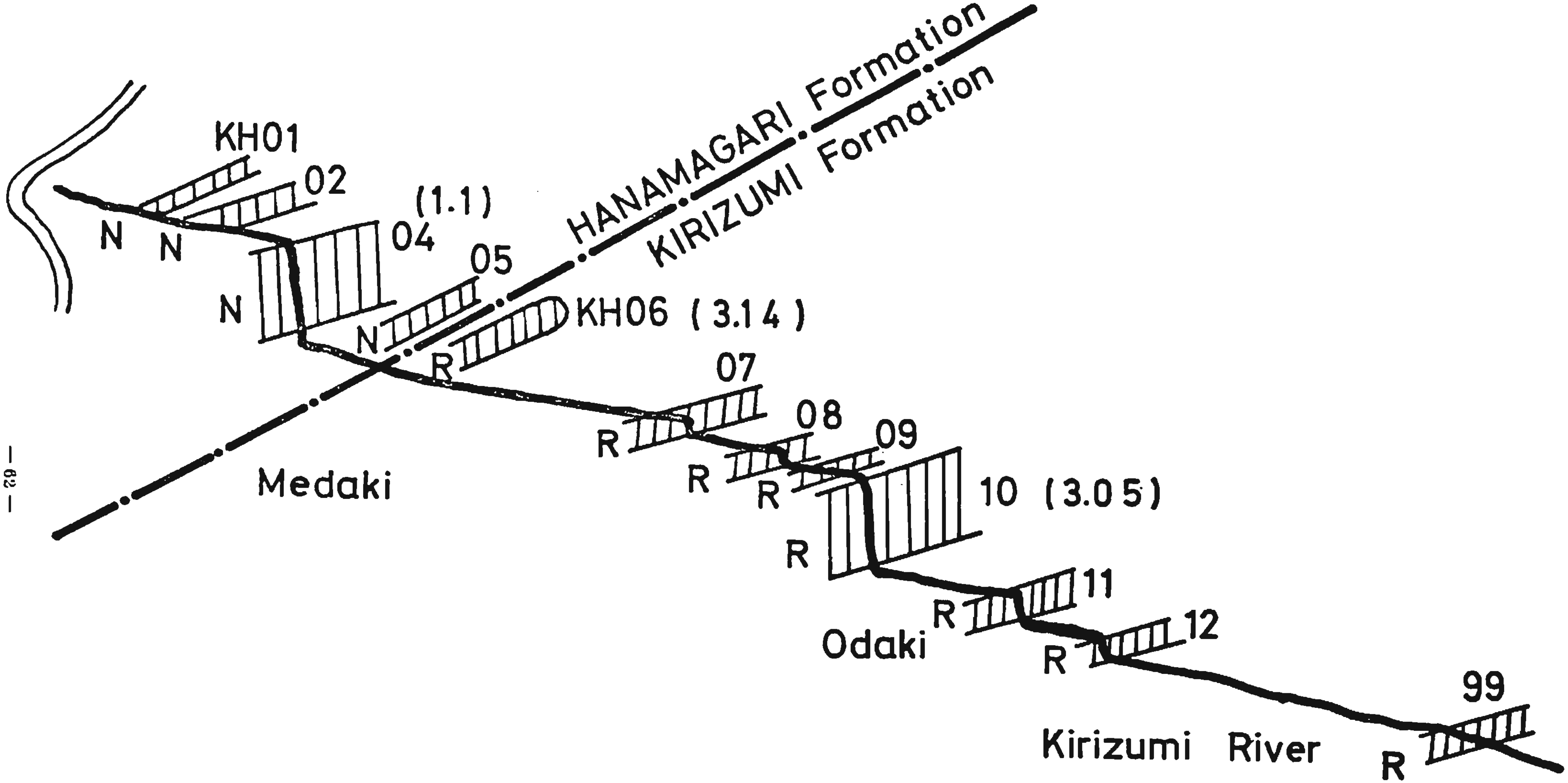

KH01
02
(1.1)
04
05
KH06 (3.14)
07
08
09
10 (3.05)
11
12
99
N
N
N
N
R
R
R
R
R
R
R
R
HANAMAGARI Formation
KIRIZUMI Formation
Medaki
Odaki
Kirizumi River

Fig. 2

10. Mass Spectrometric Studies on Double β-decays

N. Takaoka, J. Okano and K. Ogata

Faculty of Science, Osaka University

In order to extend our double β-decay investigations, the isotopic analyses of xenon from tellurium minerals and of krypton from selenium mineral were carried out with a high-sensitivity mass spectrometer. For xenon analyses, old tellurium minerals of different four localities were used, that is, tetradymite ($Bi_2\ Te_2S$) from the Oya mine, bismuth telluride (Bi_2Te_3) from the Suwa mine, native tellurium (Te) from the Teine mine and tellurium mineral from the Rendaiji mine. In order to find the temperature where the xenon isotope amonalies would appear, the gas extraction was performed by 100°C stepwise heating at 200 - 1000°C range. In the stepwise heating the temperature was raised stepwise typically by 100°C and kept constant for an hour. Fraction of rare gases extracted at each temperature was purified and then sealed up in the respective ampoule. The amount of ^{131}Xe-excess was determined quantitatively by the isotope dilution technique with ^{128}Xe spikes. An age of the mineral was measured by a potassium argon dating method using biotite for the Suwa mineral. The concentration of tellurium in the mineral was determined by gravimetric analysis. The results obtained for each sample of tellurium mineral are as follows:

(a) In xenon from the Oya mineral, large definite excesses in ^{129}Xe, ^{130}Xe and ^{130}Xe were found in the fraction of xenon extracted at 600°C. These excesses appeared sharply as shown in Fig. 1. A rough estimate of the ^{130}Xe-excess based on the sensitivity of mass spectrometer gives $(1.5\pm0.3) \times 10^{-11}$ cc STP/g ^{130}Te, which is consistent with the previous result (Takaoka and Ogata, 1966). A half-life limit was set at 6×10^{22} years for ^{128}Te double β-decay, using the ratio of ^{128}Xe-excess to ^{130}Xe-excess and the half-life for ^{130}Te double β-decay (8.0×10^{20} years), and taking account of contribution of other nuclear processes to the ^{128}Xe-excess. The other excesses at the isotope ^{129}Xe and ^{131}Xe seem to be more complicated. For different samples, even if they were taken from the same mine, the excess-ratio of these isotopes are different from those for the other sample. So these excesses may be rather complex mixture of various nuclear products.

(b) In xenon from the Suwa mineral, large definite ^{130}Xe-excesses and small excesses in ^{129}Xe and ^{131}Xe were found in the fraction of xenon extracted between 400 and 600°C (Fig. 2). The total amount of the ^{130}Xe excesses is 3.32×10^{-12} cc STP or $(1.39 \pm 0.07) \times 10^{-11}$ cc STP/g ^{130}Te. An age of the mineral was determined to be 9.0×10^{7} years. Thus the half-life for ^{130}Te double β-decay was estimated $(7.71 \pm 0.38) \times 10^{20}$ years.

(c) In xenon from the Rendaiji mineral, there were small excess at the isotope ^{130}Xe in the fraction of xenon extracted at 400, 500, 600, 700 and 900°C. The total amount of the excesses is 4×10^{-13} cc STP/g ^{130}Te. An age of the mineral has not been determined by any physical method but was assumed $1.3 - 2.5 \times 10^{7}$ years (Miocene, Tertiary) from geological evidences. However a gas retention age of the mineral was estimated 3×10^{6} years form the above ^{130}Xe-excess, if the half-life for ^{130}Te double β-decay is 8.0×10^{20} years.

(d) In xenon from the Teine mineral, the stepwise heating fractionated the contaminating atmospheric xenon from radiogenic ^{130}Xe. Thus we could identify small excess in ^{130}Xe. The amount of the ^{130}Xe-excess is 9×10^{-13} cc STP/g ^{130}Te. An age of the mineral was assumed $0.1 - 6.3 \times 10^{7}$ years (Tertiary) from geological evidences. However a gas retention age was estimated to be 6×10^{6} years with the half-life for ^{130}Te double β-decay (8.0×10^{20} years). This age estimated falls into the assumed period.

From the half-life (8.37×10^{20} years) estimated from the previous result (Takaoka and Ogata, 1966) and the one (7.71×10^{20} years) estimated in this report with the Suwa mineral, we get the half-life for ^{130}Te double β-decay on the average,

$$T_{1/2} = (8.0 \begin{smallmatrix} + 0.4 \\ - 0.9 \end{smallmatrix}) \times 10^{20} \text{ years.}$$

Errors cited here include mean errors of the average value and the difference between the xenon age of the minerals and the argon ages of porphyrite and of biotite (about $- 5 \times 10^{6}$ years).

From these studies of ^{130}Te double β-decay, we can conclude that the double β-decay would occur predominantly with emission of two neutrinos. Since the absence of neutrinoless double β-decay is identical with the lepton-conservation (Lee and Wu, 1965), we can estimate the ratio of lepton-nonconservation to lepton-conservation in β-decay to be less than 3×10^{-3} :

$$\frac{\text{lepton-nonconservation}}{\text{lepton-conservation}} = \frac{\lambda_{eff} - \lambda_{2\nu}}{\lambda_{no\nu} - \lambda_{2\nu}}$$

$$= \frac{1/8 \times 10^{20} - 1/8 \times 10^{21\pm2}}{1/2 \times 10^{16\pm2} - 1/8 \times 10^{21\pm2}}$$

$$\leq \frac{2 \times 10^{18}}{8 \times 10^{20}}$$

$$\leq 3 \times 10^{-3}$$

For krypton anomaly (Takaoka et al., 1967), a preliminary experiment has been carried out to test whether it is possible to detect radiogenic ^{82}Kr which might have been accumulated in old selenium mineral as double β-decay products of ^{82}Se. An old selenium mineral from the Kushikino mine, containing naumanite Ag_2Se was used as a sample. An age of the mineral was assumed to be 1 - 13 $\times 10^6$ years form geological evidences. Extraction and purification of the krypton gas from selenium mineral was carried out by a similar method to that used in the case of Te-Xe. The extraction for sample No. 1 was done by heating it at 1100°C for 6.5 hr. The extraction from the sample No. 2 was made in two steps. In the first, the sample was heated at 700°C for 2.5 hr. In the second step, it was heated at 1100°C for 2.5 hr. In each the extracted gases were collected in the respective ampoule.

As a first stage of our programme, $^{82}Kr/^{83}Kr$ ratio of the extracted krypton were measured particularly and compared with those of atmospheric krypton measured under the same analytical conditions. Results are shown in Fig. 3. The ratios for the sample No. 1 and for the fraction of xenon extracted from the sample No. 2 at 700°C showed small excesses of 1.1 and 1.5%, respectively, compared with those of the atmospheric krypton. The ratio for the fraction of xenon extracted from the sample No. 2 at 1100°C showed no excess.

The amount of the ^{82}Kr-excess with the sample No. 1 was estimated to be 2.3×10^{-15} cc STP/g, based on the sensitivity of the mass spectrometer. Provided that this excess was due to ^{82}Kr double β-decay, the half-life of the decay was estimated $0.7 - 9 \times 10^{20}$ years preliminarily, assuming an age of the mineral between 1×10^6 and 1.3×10^7 years.

References

N. Takaoka and K. Ogata, (1966), Zeit. Naturf. 21a, 84.

T. D. Lee and C. S. Wu, (1965), Weak interactions (First section), Ann. Rev. Nucl. Sci., 15, 381.

N. Takaoka, J. Okano and K. Ogata, (1967), paper presented at International Mass Spectrometry Conference, Berlin, September 1967.

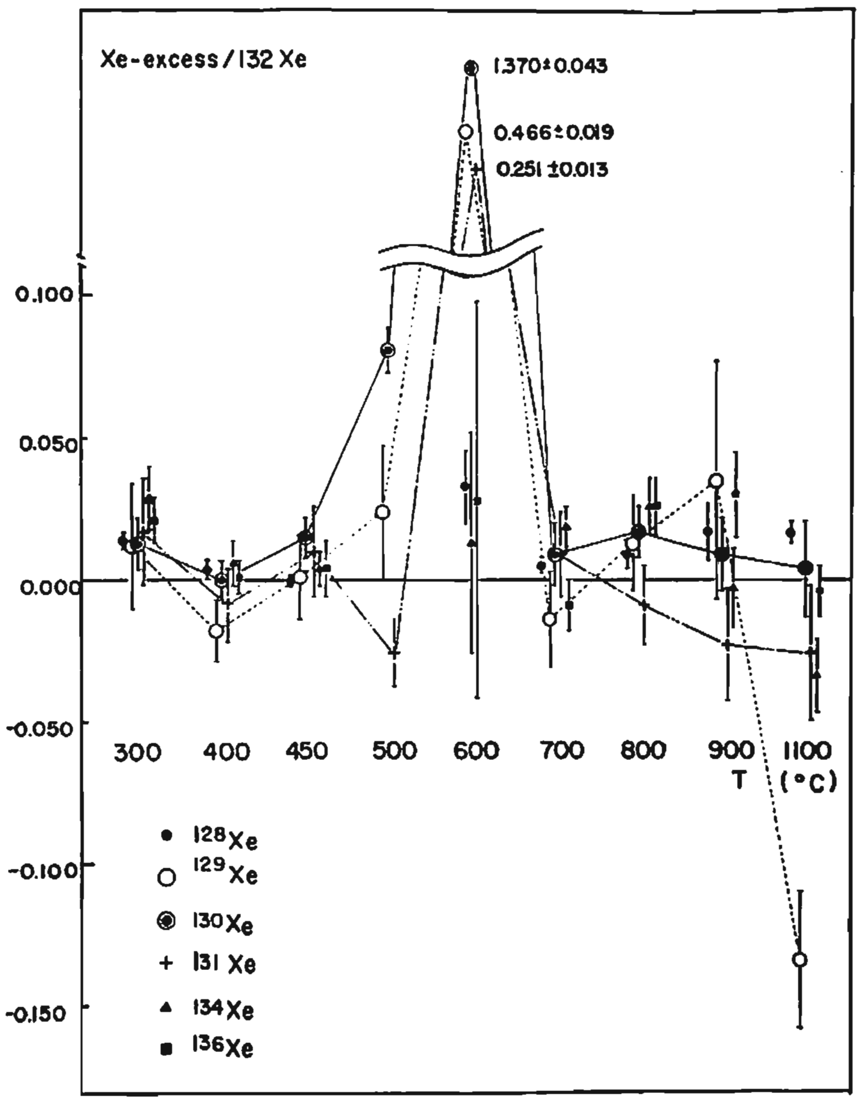

Fig. 1, Release patterns of Xe anomalies for xenon from Oya tellurium mineral. Temperature was raised stepwise by 50 °C at 400 - 500 °C and by 200 °C at 900 °C.

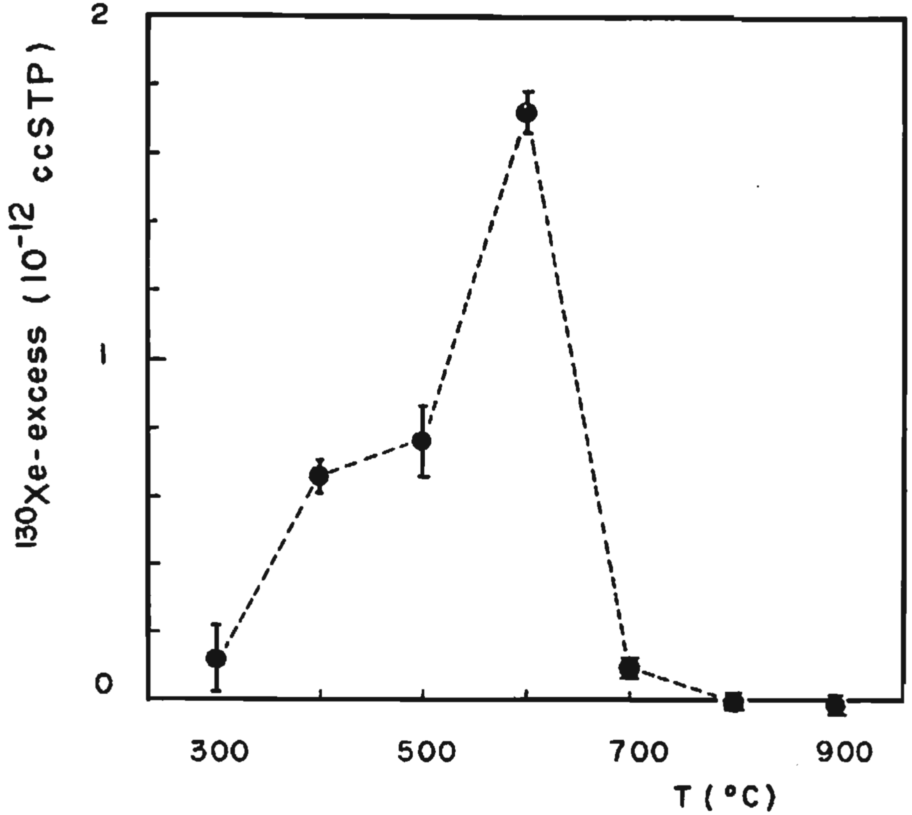

Fig. 2, Release of ^{130}Xe-excess from Suwa tellurium mineral.

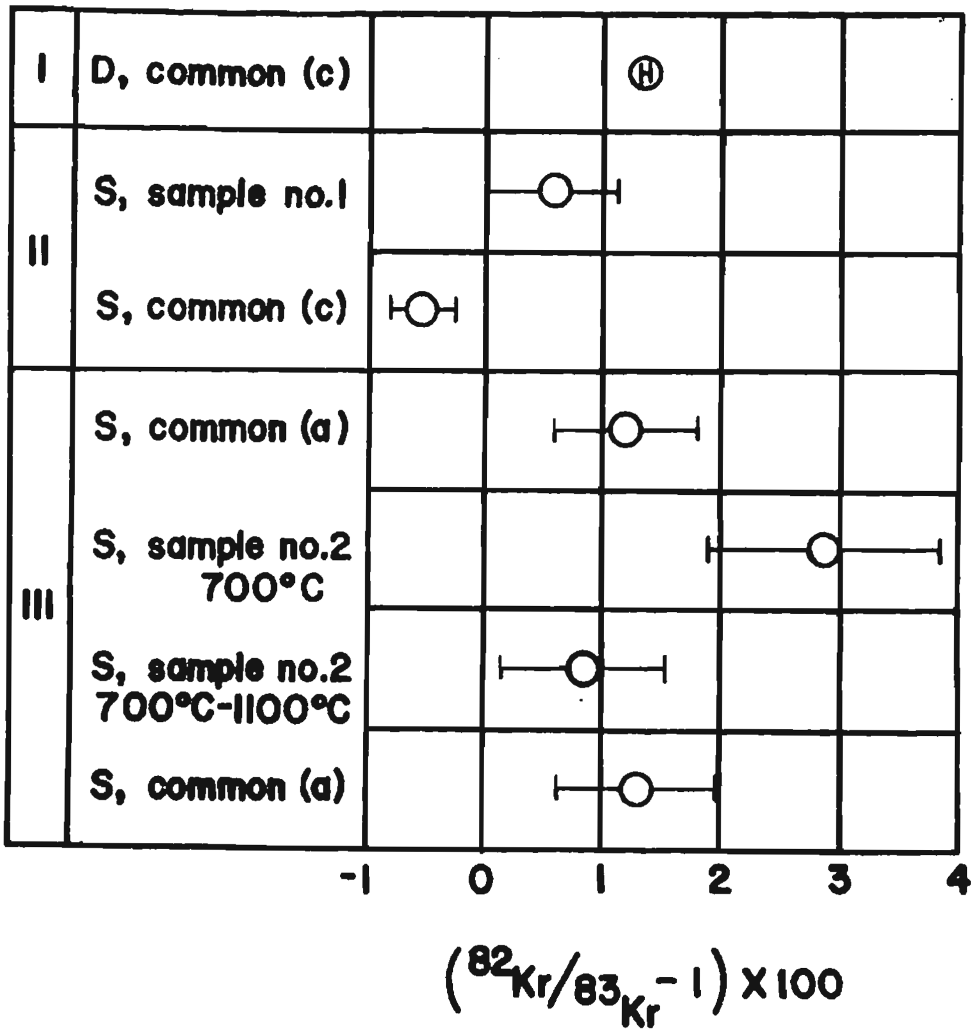

Fig. 3, ^{82}Kr / ^{83}Kr ratios obtained for sample krypton and for common krypton. The ratios are uncorrected peak-height ratios. I, II and III show series of measurements with experimental conditions hept closely constant within each series. D and S denote dynamic operation and static operation respectively. Common (c) and common (a) denote commertial krypton and purified air krypton respectively.

11. Results of Age Determination of Some Late Cenozoic Rocks in Southwestern Japan

Kimio Hirooka and Naoto Kawai

Faculty of Engineering Science, Osaka University

Radiometric K-Ar age determinations were undertaken with Late Cenozoic volcanic rocks which outcrop widely in southwest Japan and whose remanent magnetism was utilized in the palaeomagnetic studies so far by many authors (Matuyama 1929, Kawai 1951, Hirooka 1961, Ito 1963, 1965, Nishida et al. 1967).

Before the study, the rocks were carefully examined under the microscope and the following seven rocks (tabulated in Table 1) were selected as the suitable specimens for our K-Ar method. The localities from which these samples are taken are shown in Fig. 1.

Of the seven samples, the rocks with No. 514 and 713 and that with suffix Mikasa-b' have what we call normal remanent magnetism. In contrast, the rocks with suffix A-2, B-2 have reverse remanent magnetism. On the other hand, rocks with suffix Muroo-60 and Kumano-R possess an anomalous direction which is neither parallel nor antiparallel to that of the present geomagnetic dipole field, all being found in some direction between the two.

For measuring the amount of potassium, a flame photometer was used. The mean value for two measurements was assumed as its concentration.

In the case of Kumano-R, age determination was carried out using two diferent minerals, one being sanidine and the other biotite. The ages obtained in the two different ways turned out to be exactly the same. Two runs of whole rock measurements using the sample No. 514 indicate ages which are very close to each other, being about 0.8 m.y. This rock was found to have been covered with a lava reverseley magnetized. The geomagnetic field, therefore, seems to have switched from normal to reverse at some age younger than 0.8 m.y.

All ages determined are tabulated in Table 2.

This work was done under the United States-Japan scientific cooperative programme. The present authors would like to express their cordial thanks to Dr. G. B. Dalrymple of U.S. Geological Survey for his kind guidance to the dating work.

References

Hirooka, K. (1961), Graduation thesis of Geol. Mineral. Inst. Kyoto Univ., No. 429, 1-38.

Ito, H. (1963), 1963 Ann. Progress Rep. Rock Mag. Res. Group Japan, 87-90.

Ito, H. (1965), Bull. Shimane Univ. (Natural Sci.), No. 15, 26-32.

Kawai, N. (1951), J. Geophys. Res., 56, 73-79.

Nishida, J., M. Shimada and S. Sasajima (1967), Mem. Coll. Sci., Kyoto Univ., Ser. B, 34, 1-8.

Matuyama, M. (1929), Proc. Imp. Acad. Japan, 5, 203-205.

Figure Caption

Fig. 1. Map of southwestern Japan in which collecting sites are shown by numbers.

1. Saigo-Cho (514)
2. Kochidani (Muroo-60)
3. Aodani-Cho (713)
4. Mikasayama (Mikasa-b')
5. Nachikatsuura-Cho (Kumano-R)
6. Genbudo (A-2)
7. Wakurayama (B-2)

Table 1

Sample Name	Sampling Locality	Rock Type	Direction of magnetization	
			Dec.	Inc.
514	Saigo-Cho Tottori Pref.	basalt	12°	50°
Muroo-60	Kochidani Nabari-Shi	dacite	265°	-63°
713	Aodani-Cho Tottori Pref.	basalt	19°	60°
Mikasa-b'	Mikasayama Nara-Shi	andesite	36°	22°
Kumano-R	Nachikatsuura-Cho Wakayama Pref.	granite porphyry	313°	-39°
A-2	Genbudo Hyogo Pref.	basalt	152°	-40°
B-2	Wakurayama Matsue-Shi	andesite	185°	-56°

Table 2

Sample Information		K_2O Analyses (weight %)			Argon Analyses			Calculated
Sample	Material dated	(1)	(2)	Average	Sample weight (grams)	Ar^{40}_{rad} (moles/gram)	$\frac{Ar^{40}_{rad}}{Ar^{40}_{total}} \times 100$	Age* (10^6 years)
514	basalt	1.98	1.99	1.98	8.878	2.351×10^{-12}	46.7	0.801 ± 0.048
	basalt	1.90	1.90	1.90	8.783	2.407×10^{-12}	55.5	0.857 ± 0.035
Muroo 60	sanidine	11.32	11.32	11.32	1.340	2.202×10^{-10}	91.4	13.1 ± 0.4
713	basalt	0.612	0.599	0.606	5.450	4.979×10^{-12}	15.2	5.84 ± 0.51
					5.439	5.479×10^{-12}	32.5	
Mikasa b'	andesite	2.34	2.33	2.34	5.902	4.620×10^{-11}	10.8	13.3 ± 2.3
Kumano-R	sanidine	11.37	11.12	11.24	1.663	2.384×10^{-10}	94.3	14.3 ± 0.4
	biotite	8.19	8.27	8.23	1.033	1.745×10^{-10}	58.4	14.3 ± 0.4
A-2	basalt	1.80	1.79	1.80	5.272	4.280×10^{-12}	51.4	1.61 ± 0.08
B-2	andesite	2.98	3.07	3.02	5.408	2.838×10^{-11}	50.3	6.34 ± 0.19

* Calculated using $\lambda_\varepsilon = 0.585 \times 10^{-10}$ yr^{-1} , $\lambda_\beta = 4.72 \times 10^{-10}$ yr^{-1} , $K^{40}/K = 1.19 \times 10^{-4}$ mole/mole.

The $\pm$ is an estimate of the standard deviation of precision

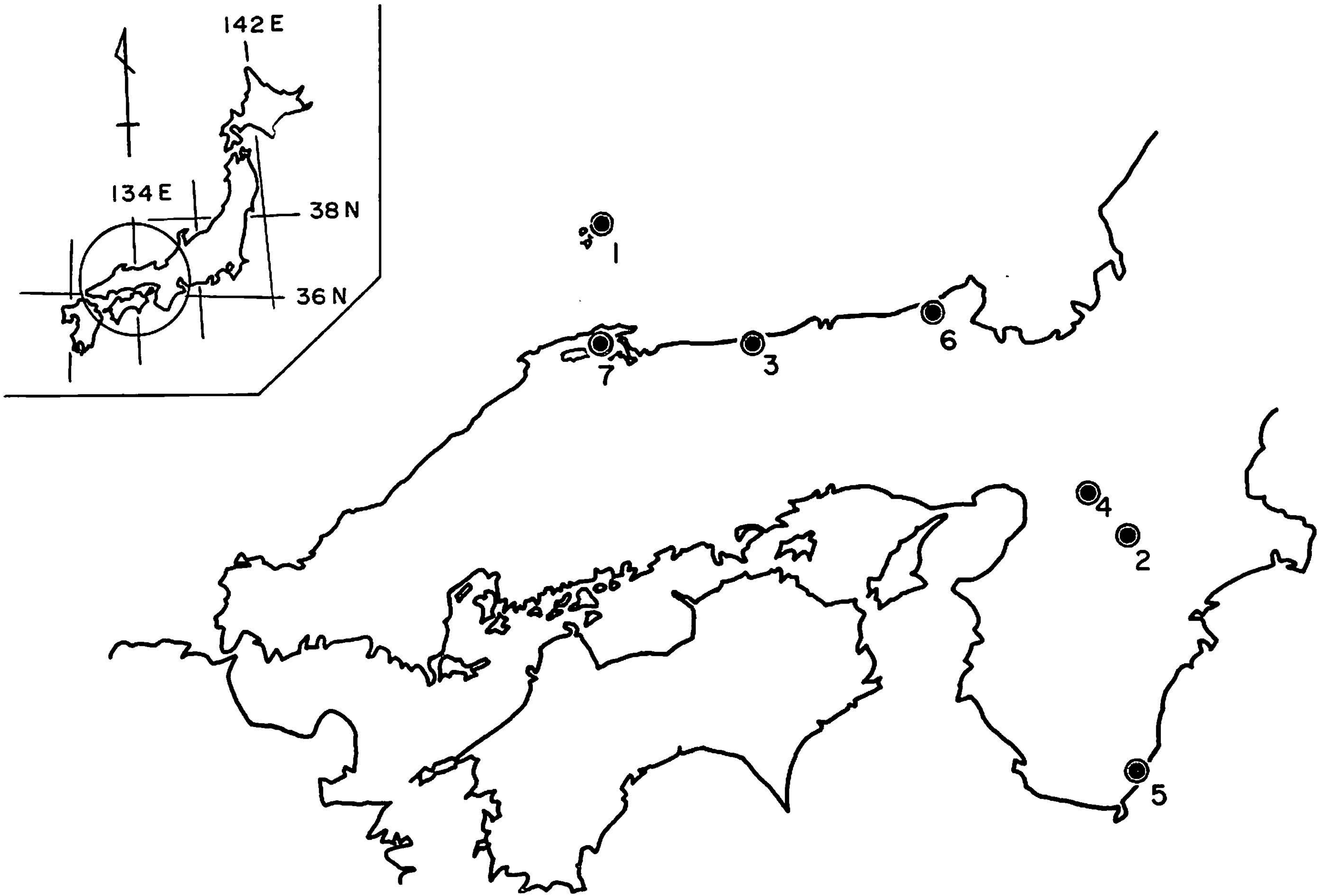

Fig. 1

12. Preliminary Report on the Magnetic Study of the Tephra in Diluvial Deposits, Yamaguchi Prefecture, West Japan

Haruo Domen

Faculty of Education, Yamaguchi University

In Ube district of the coastal area of Suo-Nada of the Seto Inland Sea, of Yamaguchi Prefecture, West Japan, the so-called 'Ube volcanic ash' layer correlated to the Yame clay and the Aso pyroclastic flow in the Northern Kyushu and also to the Musashino loam in the Kwanto district have been widely distributed.

Over twenty samples of the volcanic ash were taken from several sites in Ube district mentioned above and those remanent magnetizations were determined in order to be the specimens for palaeo-/or archaeo-magnetic investigations in connection of the tephrochronology.

In general speaking, the questioned ash layer has deposited having the thickness from few centimeters to few meters and is divided into two groups such as the upper layer that is brown in color and lower one in white. These two groups seem to be successively deposited almost at the same time in geologic time scale.

The N.R.M. data obtained preliminarilly show that the dip angle of the mean direction of the remanent magnetic vectors of white group, lower deposit is shallower than that of the brown group, upper one, but more-over on the dispersion around the mean direction of the remanent magnetizations of the white group is greater than that of the brown group. It may suggest that these two groups have had different types of the mode of the depositions.

The proposed study on this ash may be interesting subject not only of the palaeo-/archaeo-magnetism of the earth; which subject the present author would like to call 'meso(geo)magnetism' for convenience' sake because of the few data on the samples of some ten thousand years before present have been published up to date, but also of the tephrochronology and geology of the Diluvial deposits in this district and in the western end of the Honshu Island of Japan.

18. Secular Variation in the Non-dipole Parts of the Earth's Magnetic Field

Takesi Yukutake

Earthquake Research Institute, University of Tokyo

The non-dipole field occupies merely a fraction of the total earth's magnetic field, but it plays a very important part in the secular change having periods from decades to thousand years. It has been indicated that the freely decaying non-dipole field can exist more than a thousand years (Yukutake 1968a). Archeomagnetic results seem to confirm this, suggesting that the secular variations obtained from archeomagnetism are well illustrated by the westward drifting of the non-dipole fields (Yukutake 1962, 1967, Burlatskaya et al. 1965). However, the archeomagnetic data are available only at limited numbers of localities and not sufficient to trace the change of the whole distribution of the non-dipole field.

In order to investigate the detailed changes, the non-dipole fields were computed from the Gauss-Schmidt coefficients at various epochs, extending back to the 16th century. It was ascertained that thus syntherized field could approximate the charted field with an uncertainty less than 10% for the analyses of the 20th century and about 20% for those of the 19th century (Yukutake 1968b). Although no examination was made for the earlier analyses, it is surmized that the approximation errors are approximately the same as those for the data of the 19th century.

Examples of the synthesized fields are shown for the vertical component in Fig. 1. It can be noted that the changes in the individual anomalies are not the same. A negative anomaly covering the African Continent, for example, shows a remarkable displacement during the period from 1700 to 1965, while a positive anomaly in Mongolia has been staying still on the same place during the period. The existing non-dipole anomalies can be classified into three groups; i.e. the anomalies drifting westwards, those remaining stationary at the same point but changing its intensity and those standing still without change in the intensity.

<u>The drifting anomaly</u>: African negative anomaly, South-Atlantic positive anomaly and a negative anomaly in the Southeastern Pacific belong to this classification. The African anomaly has been drifting westwards with a velocity of approximately 0.3°/yr, and the South-Atlantic anomaly with that of 0.15°/yr.

<u>The stationary anomaly with changing intensity</u>: The Mongolian positive anomaly, the Australian negative anomaly and possibly the North American positive anomaly belong to this. The Mongolian anomaly has been increasing its intensity at such a large rate as 50γ /yr since the 17th century. The North American anomaly, on the other hand, seems to have changed very slightly, only showing about a few hundred gammas decrease since the middle of the 17th century.

<u>The stationary anomaly with its intensity unchanged</u>: The Icelandic negative anomaly, the Central Pacific positive anomaly and the North Pacific negative one belong to this group. Common features to these anomalies are that they are somewhat smaller in size than the previous two anomaly groups, and that the intensities weaker. These anomalies firmly fixed to the mantle might be ascribed to the crustal or mantle origin rather than to the core.

The results obtained here have some practical importance for paleomagnetic study, besides the consequences they are likely to entail on hydromagnetism within the core. The non-dipole field has so far been assumed to be short-lived and rotating westward around the geographical axis (Bullard et al. 1950). When the directions of remanent magnetization of the samples at any locality are averaged over a fairly long interval such as several thousand years, which is sufficient for the non-dipole field to complete one rotation or to end its life, it has been admitted that the results do not include the effect of the non-dipole field and give the correct direction of the dipole field. However, if there exists an anomaly which does not change with time, the averaged results are still contaminated by the anomaly and will give systematic differences when samples are collected at different parts of the anomaly. Although the stationary anomalies are of smaller size when compared to the time varying ones, they are still much larger than the local anomalies in the crust which are duly taken into account for the current data process of paleomagnetism.

References

Bullard, E. C., C. Freedman, H. Gellman and Jo Nixon (1950), The westward drift of the earth's magnetic field, Phil. Trans. Roy. Soc. London A, 243, 67-92.

Burlatskaya, S. P., T. B. Nechaeva and G. N. Petrova (1965), The westward drift of the secular variation of magnetic inclination and variations of the earth's magnetic moment according to "Archeomagnetic" data, Izv., Earth Phys. Ser., 6, 31-42 (R), 280-385 (E).

Yukutake, T. (1962), The westward drift of magnetic field of the earth, Bull. Earthq. Res. Inst., 40, 1-65.

Yukutake, T. (1967), The westward drift of the earth's magnetic field in historic times, Jour, Geomag. Geoelectr., 19, 103-116.

Yukutake, T. (1968a), Free decay of non-dipole components of the geomagnetic field, Phys. Earth Planetary Inter., 1, 93-96.

Yukutake, T. (1968b), Synthesis of the non-dipole components of the earth's magnetic field from spherical harmonic coefficients, Bull.

Earthq. Res. Inst., 46. (in press)

Figure Caption

Fig. 1. The non-dipole fields synthesized for the vertical component for the epochs 1700, 1845 and 1965.

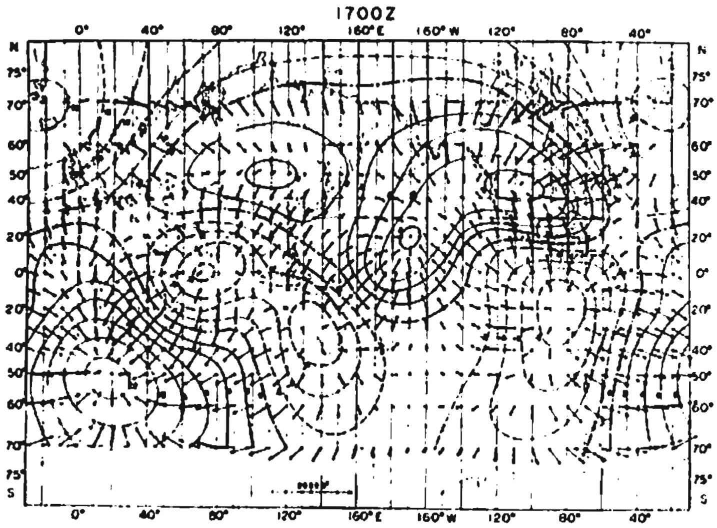
1700Z
0° 40° 80° 120° 160°E 160°W 120° 80° 40°
N 75° 70° 60° 50° 40° 20° 0° 20° 40° 50° 60° 70° 75° S

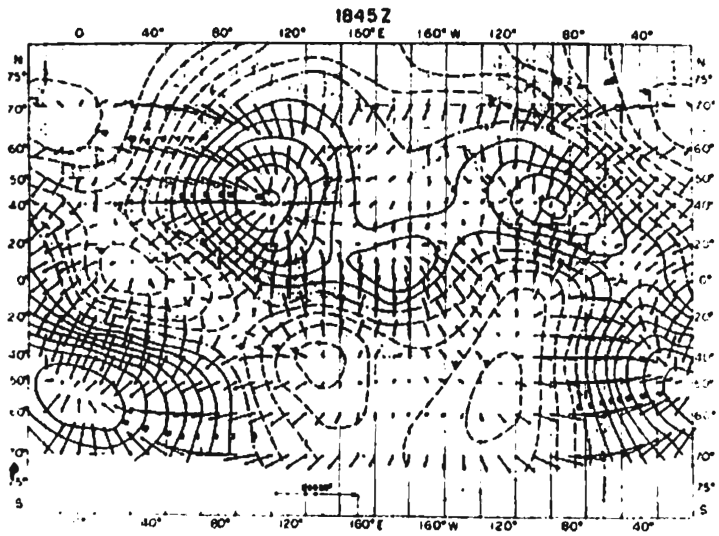
1845Z
0 40° 80° 120° 160°E 160°W 120° 80° 40°
N 75° 70° 60° 50° 40° 20° 0° 20° 40° 50° 60° 70° 75° S

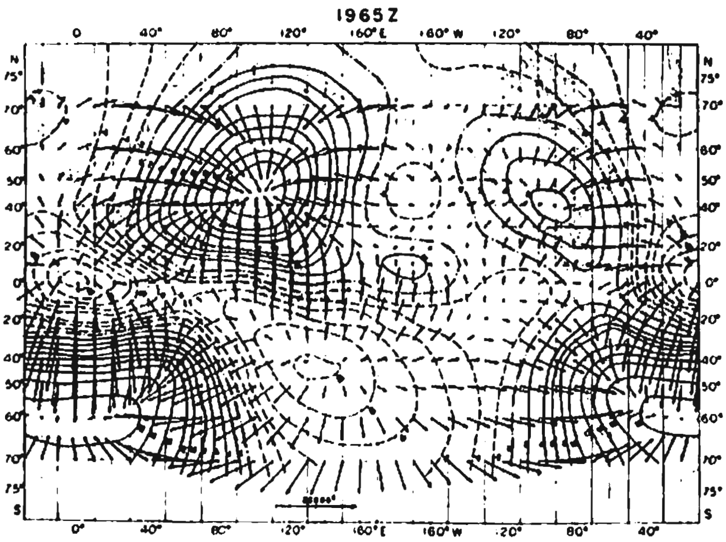
1965Z
0 40° 80° 120° 160°E 160°W 120° 80° 40°
N 75° 70° 60° 50° 40° 20° 0° 20° 40° 50° 60° 70° 75° S

14. Archaeo-secular Variation of the Geomagnetic Field in Japan

N. Kawai, K. Hirooka, K. Tokieda and T. Kishi
Faculty of Engineering Science, Osaka University

Over the past seven years the number of archaeological sites from which clays were sampled has increased to 40 in total number in the Tokai, Kinki and Okayama districts of Japan. Besides these archaeological observations two lava flows were also measured. Localities of these sampling sites are shown in Fig. 1.

The directions of magnetization of these oriented samples were measured directly, after the A-C demagnetization, or after the low temperature cleaning. Changes in both the declination and the inclination of the geomagnetic field in the historical time are shown in Fig. 2(a) and in Fig. 2 (b) respectively. The dotted curves in the two figures demonstrate the time changes of both the declination and the inclination to be expected from the quasihypotrochoidal movement of the geomagnetic dipole field proposed by Kawai and Hirooka (1967).

The solid curves in the same diagrams indicate the actual archaeo-secular variations we obtained from our observations. The curves obtained from our model of the wobbling dipole field and the curves obtained from the field observations resemble each other conspicuously.

Reference

Kawai, N. and K. Hirooka (1967), J. Geomag. Geoele. 19, 217-227.

Figure Captions

Fig. 1. Map of southwestern Japan in which collecting sites are shown by numbers.

1.	Mt. Sakurajima	8.	Suzuka City
2.	Bizen Cho	9.	Yokkaichi City
3.	Itami City	10.	Seto City
4.	Sakai City	11.	Nisshin Cho
5.	Kyoto City		Miyoshi Cho
6.	Shigaraki Cho	12.	Toyota City
7.	Hisai Cho	13.	Isobe Cho
	Taki Cho	14.	Ota Cho
	Tamaki Cho		

Fig. 2. Archaeo-secular variation in southwestern Japan shown in solid lines. The broken lines show the archaeo-secular variation calculated from the model of quasihypotrochoid motion of dipole axis.

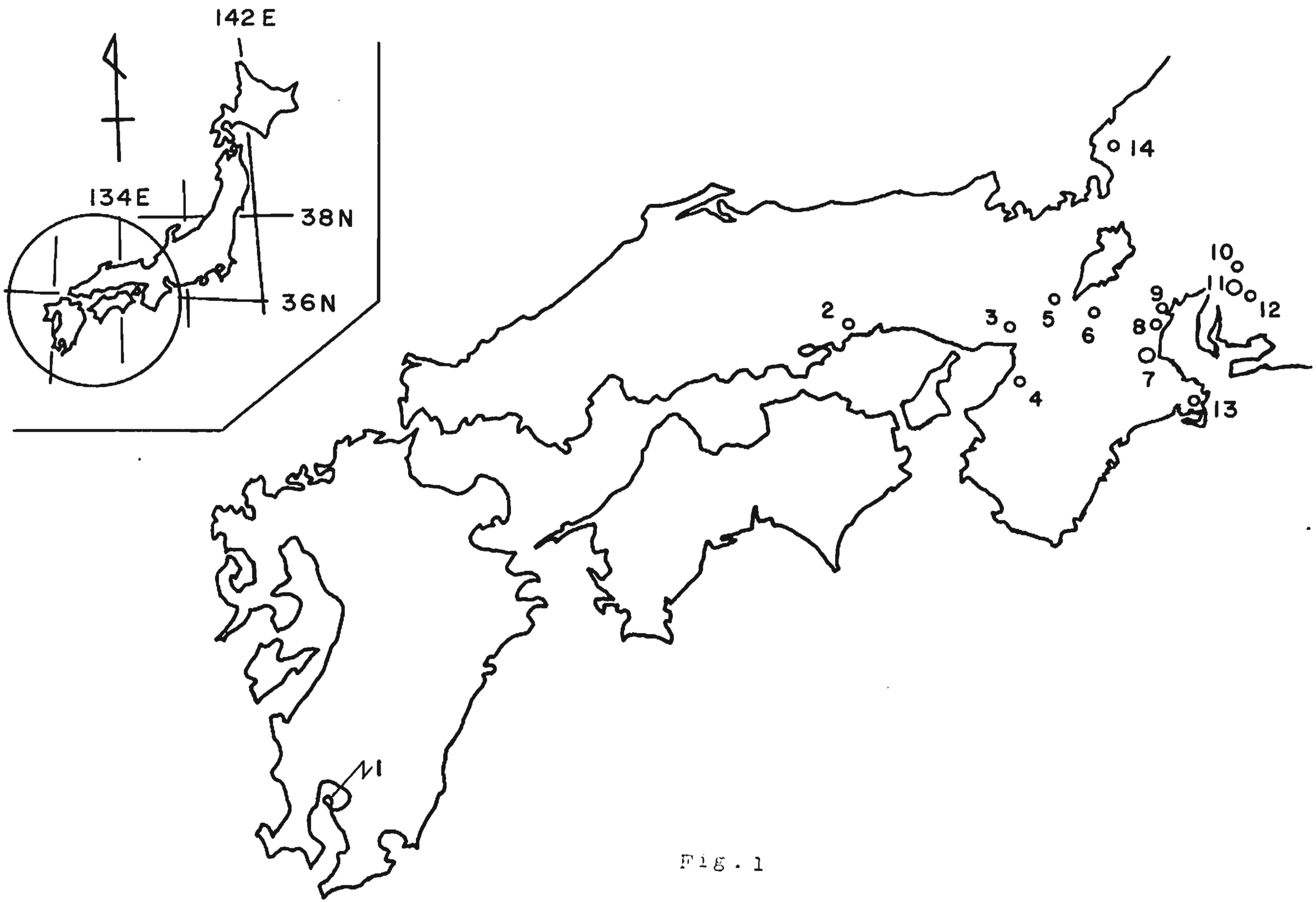

Fig. 1

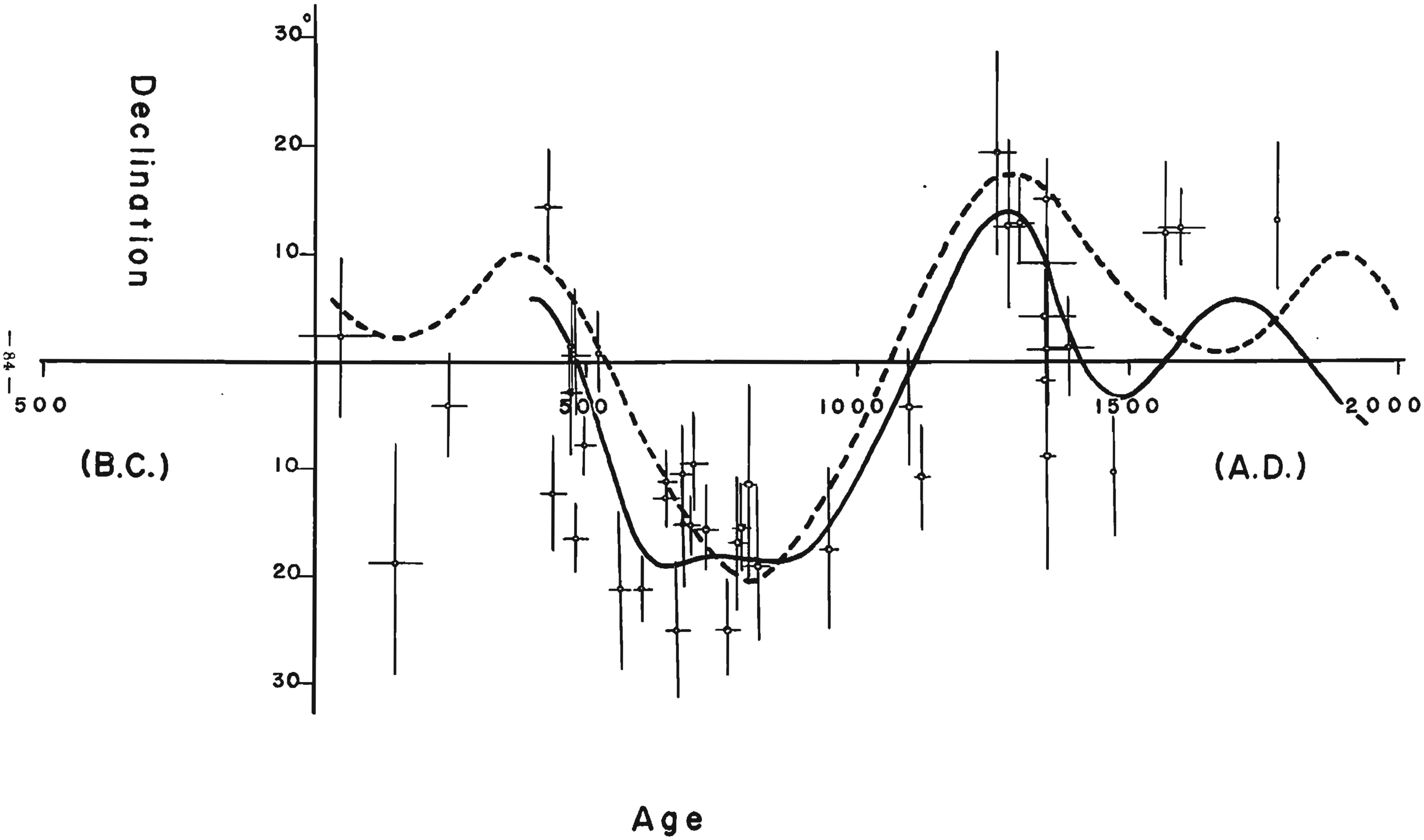

Fig. 2 (a)

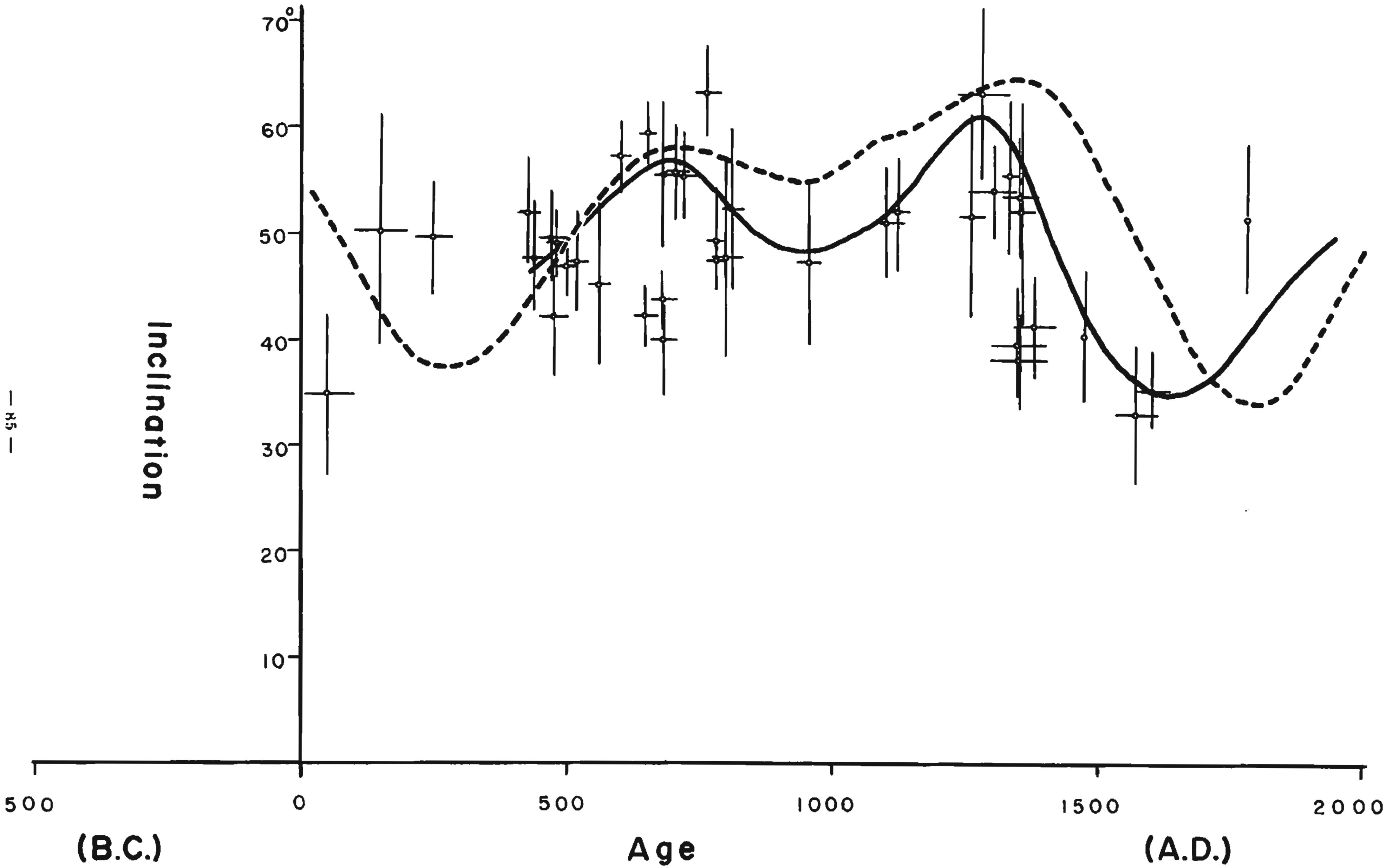
70°
60
50
40
30
20
10
Inclination
500
0
500
1000
1500
2000
(B.C.)
Age
(A.D.)

Fig. 2 (b)

15. A Preliminary Result on the Paleomagnetic Chronology of the Osaka Group

Kazuaki Maenaka and Shiro Ishida

Geological and Mineralogical Institute, University of Kyoto

and

Takuo Yokoyama

Mechanical Engineering, Doshisha University

The paleomagnetic chronology since the middle Pliocene basing on ancient geomagnetic polarity change has been recently established by several investigators (Cox et al. 1963, McDougall and Wensink 1966, Dalrymple et al. 1963), and it has been plausibly applied to the analyses of many ocean bottom sediments with success (Opdyke et al. 1966, Ninkovich et al. 1966, Harrison 1966, Watkins and Goodell 1967, Glass 1967).

In Kinki district, Plio-Pleistocene sediments such as, Osaka Group and its corresponding Kobiwako Group and Age Group have been extensively studied as a collaboration study by many stratigraphers. In order to set up a type Plio-Pleistocene geochronology in Japan, the authors have applied the paleomagnetic stratigraphic method into 30 volcanic ash layers of these sediments. The stratigraphic identification of samples was studied by Ishida and Yokoyama. (Ishida and Yokoyama, 1968). About 500 volcanic ash specimens are collected from 100 sites and their NRM were measured. Their NRM intensity is so weak that only a half of total specimens can be measured. The dispersion of NRM direction in each site is somewhat larger, as a whole, compared with that of volcanic rocks.

Considering from the storage test of NRM undertaken in the laboratory during months, it has been proved that the remanent stability is fairly reliable, though the partial a.c.-demagnetization has not been yet carried on all the specimens. The obtained NRM data are summarized in Table 1.

In this table, volcanic ash layers are listed according to the stratigraphic sequence in discending order from the upper to the lower. The direction of NRM obtained from the same stratigraphic horizon shows without exception fairly good agreement with one another. From the fact one can recognize the high accuracy of the stratigraphic work upon which the present sampling scheme has reliance. The preliminary result of the paleomagnetic stratigraphic correlation with the data proposed by Cox et al. (1963) and others (McDougall and Wensink 1966, Dalrymple et al. 1967), is briefly given in the last column of the table. From the result, the following important conclusions may be deduced.

1) All layers lying in higher horizon than Fukakusa layer which possess normal polarity may be safely correlated with the lower part of Brunhes Normal Epoch.

2) Almost all the ash layers ranging from Biotite tuff to Shimakumayama layer possess reverse polarity. We can assume with fair certainty that these layers are correlated with Matuyama Reverse Epoch.

3) A few interposed layers with normal polarity (Komyoike and Pink layers, A-054 and Naka layers) in the reversed epoch might be approximately correlated with Jaramillo or Gilsa event, and Olduvai event respectively. Further precise magnetic data are needed before the decisive correlation of these events, especially the direct age determination by the fission track method is highly expected.

4) The layers lying in the lower horizon than T-2 (Osaka Group) which possess normal polarity may be possibly correlated with Gauss Normal Epoch.

5) Basing on the present study of paleomagnetic stratigraphy, the age of Azuki tuff, one of the most important key beds in Osaka Group, is estimated at 0.7-0.9 m.y.. Again pumice tuff, another key bed in Osaka Group, is estimated at 2.1-2.4 m.y. on the same way.

References

Cox, A., R. R. Doell and G. B. Dalrymple (1963), Science, 142, 382.

McDougall, I. and H. Wensink (1966), Earth Planet. Sci. Letters, 1, 232.

Dalrymple, G. B., A. Cox, R. R. Doell and C. S. Gromme (1967), Earth Planet. Sci.Letters, 2, 163.

Opdyke, N., B. Glass, J. D. Hays and J. Foster (1966), Science, 154, 349.

Ninkovich, D., N. Opdyke, B. C. Heezen and J. H. Foster (1966), Earth Planet. Sci. Letters, 1, 476.

Harrison, C. G. A. (1966), J. Geophys. Res., 71, 3033.

Watkins, N. D. and H. G. Goodell (1967), Earth Planet. Sci. Letters, 2, 123.

Glass, B., D. B. Ericson, B. C. Heezen, N. D. Opdyke and J. A. Glass (1967), Nature, 216, 437.

Ishida, S. and T. Yokoyama (1968), in press.

Table 1

NRM data and magnetic stratigraphy of volcanic ash layers in Plio-Pleistocene sediments in Kinki district.

*Name of ash layer	No. of Specimen (No. of site)	Mean Direction D	Mean Direction I	α_{95}	**Polarity Epoch		Age (M.Y.)
Kasuri	3 (1)	64.3	37.0	-	N	BRUNHES	
Sakura	10 (2)	348.8	49.0	8.7	N	Normal Epoch	
Fukakusa	5 (1)	28.5	55.1	8.8	N		0.7
Biotite tuff	3 (1)	162.3	-18.0	30.3	R		
Azuki	18 (3)	170.6	-54.6	8.9	R		
Kamikatsura	4 (1)	307.6	- 2.8	19.1	I		
Yamada	3 (1)	185.4	-40.9	26.6	R		
Komyoike	4 (1)	331.5	40.2	15.5	N	MATUYAMA	
Pink	25 (6)	0.8	41.4	6.9	N	Reverse	
Yellow	20 (4)	174.9	-52.8	8.8	R	Epoch	
A-027, A-218	12 (2)	191.6	-37.0	10.0	R		
A-054,	4 (1)	352.9	53.6	17.8	N		
Naka	3 (1)	352.3	67.1	7.1	N		
Pumice	6 (2)	160.4	-48.0	35.7	R		
Shimakumayama	3 (1)	189.1	-34.7	40.9	R		2.4
T-2 (Osaka)	9 (2)	3.3	58.6	10.0	N		
T-1 (Osaka)	4 (1)	1.8	47.7	34.3	N	GAUSS	
T-5 (Agé)	4 (1)	22.2	41.3	25.4	N		
Hozoin	4 (1)	14.1	58.2	10.2	N	Normal	
Sagami	7 (1)	6.9	54.5	27.3	N	Epoch	
T-2 (Agé)	3 (1)	182.7	-45.3	17.0	R		
Ichiuno	4 (1)	343.7	46.6	32.3	N		

* Reference 9

** Reference 1-3

16. Palaeomagnetic Study on the Pliocene Lava near Mt. Daisen and the Miocene Lava at Hamada Area

E. Asami, T. Kishi and A. Kurotani

Physical Institute, Faculty of Literature and Science, Shimane University

In the San-in Province of west Japan are found various volcanic rocks of Tertiary and Quaternary. On the two of those, the Pliocene andesite lavas at Hirusen Area near Mt. Daisen, Tottori Prefecture and the Miocene andesite lavas at Hamada Area, Shimane Prefecture, palaeomagnetic studies were carried out by the present authors.

The age of extrusion of the lavas at Hirusen Area is generally estimated to be Pliocene from the geological point of view (Ota 1962a, 1962b). The stratigraphical sequence of the lavas is illustrated in Fig. 1, in which full circles represent the sampling sites. The authors collected many samples, measured the directions and intensities of their N.R.M. by means of an astatic magnetometer and performed a stability test. The directions of N.R.M. of the samples with stable magnetization thus obtained are plotted on the Wulff's net in Fig. 2. As seen in Fig. 1 and Fig. 2, the lavas (3) (5) (6) show normal polarity, while (1) (2) (4) reverse.

In the same way, the sampling sites of the Miocene lavas at Hamada Area (Yamada, 1960), are illustrated on (H) and the directions of the N.R.M. are plotted on (1) (2) (4) in Fig. 3. Stability test was performed by laboratory heat treatment up to the maximum of 300°C for an hour in the air, samples being set approximately parallel and antiparallel to the earth's field. For example, Fig. 4 shows the changes of the directions of magnetization due to such heat treatment of the specimens of the lavas (2). As seen in Fig. 4, two specimens with normal N.R.M. are unstable, while the rest with reverse one all stable. Many specimens of the lavas (4) with scattered N.R.M. are also all unstable; hence they are unsuitable for the purpose of studying palaeomagnetism. The same test shows that the lavas (1) are stable and (3) unstable. Thus, what can be mentioned as reliable data of palaeomagnetism of this area is that the lavas (1) show normal polarity, while (2) reverse.

However, the exact ages of extrusions of all lavas mentioned above are still unknown, because the radiometrical dating has not yet been carried out.

References

Ota, R. (1962a), Geological map of Akasaki and Daisen in the scale of 1:50,000. Geol. Surv., Japan, 37.

Ota, R. (1962b), Geological map of Yumoto in the scale of 1:50,000. Geol. Surv., Japan, 29.

Yamada, A. (1960), Geology of the vicinity of Hamada, Shimane Prefecture. Graduation Thesis, Dept. of Geol., Shimane Univ. (MS)

Figure Captions

Fig. 1. A map of Hirusen Area near Mt. Daisen.

Fig 2. The directions of N.R.M. of the Pliocene lavas at Hirusen Area. Wulff's net is used.

● : Lower hemisphere

○ : Upper hemisphere

Fig. 3. A map and the directions of N.R.M. of the Miocene lavas at Hamada Area.

Fig. 4. The changes of direction of magnetization due to the heat treatment up to 300°C.

0 : Room temperature, 1:100°C, 2:200°C, 3:300°C, being set antiparallel.

1': 100°C, 2':200°C, 3':300°C, being set parallel.

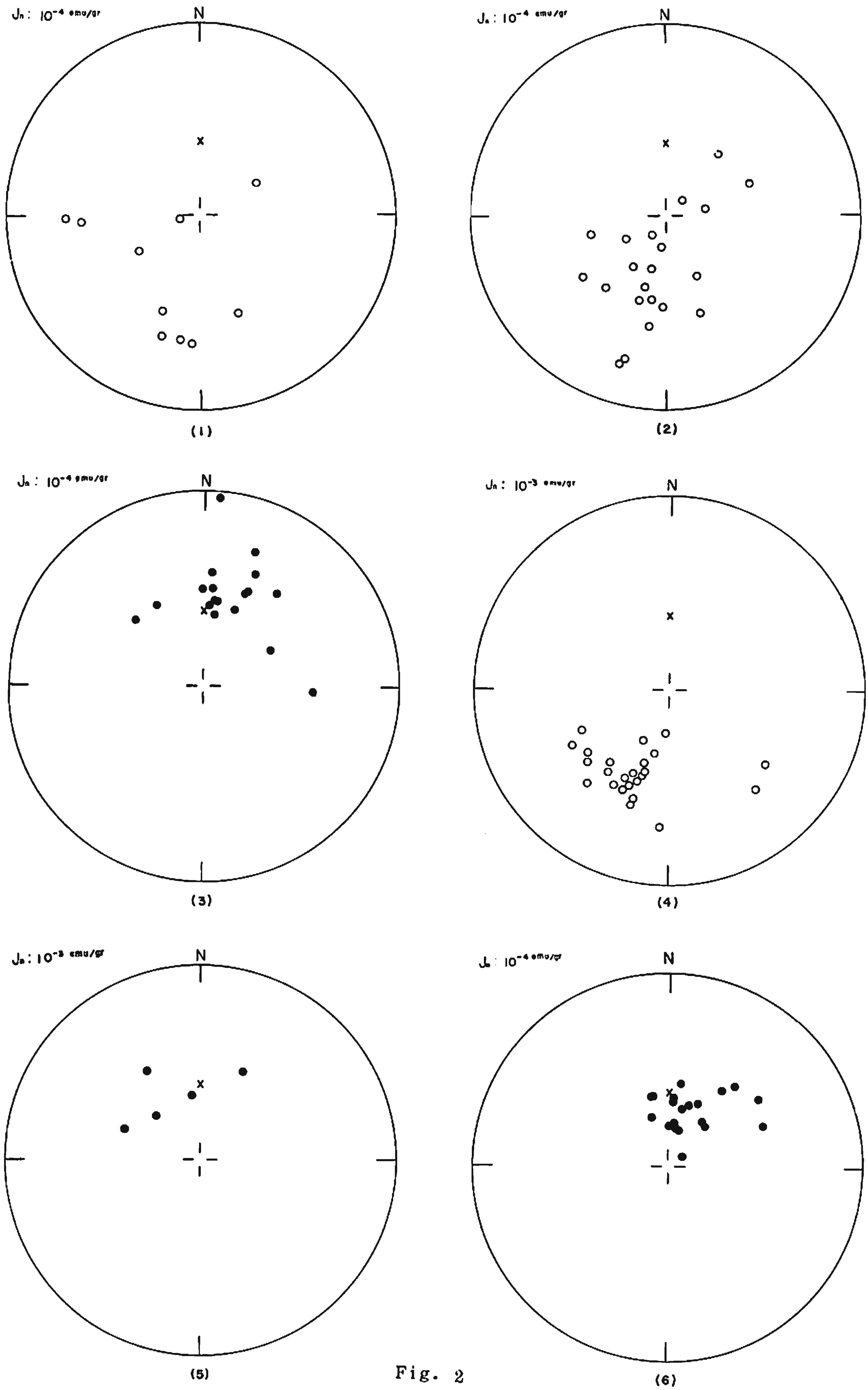

Jn : 10-4 emu/gr
N
(1)
Jn : 10-4 emu/gr
N
(2)
Jn : 10-4 emu/gr
N
(3)
Jn : 10-3 emu/gr
N
(4)
Jn : 10-3 emu/gr
N
(5)
Jn : 10-4 emu/gr
N
(6)

Fig. 2

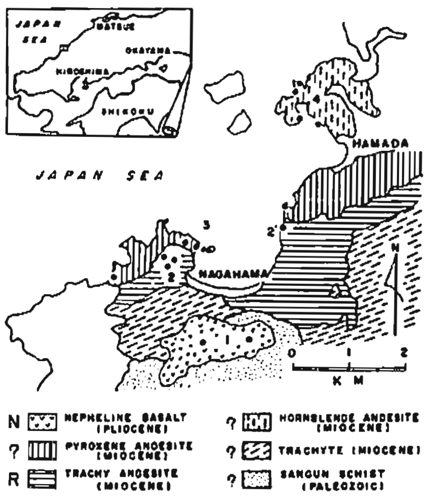

(H)

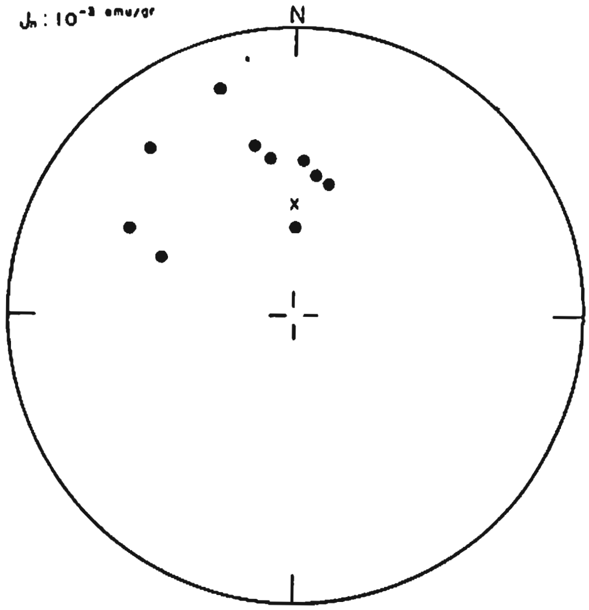

(1)

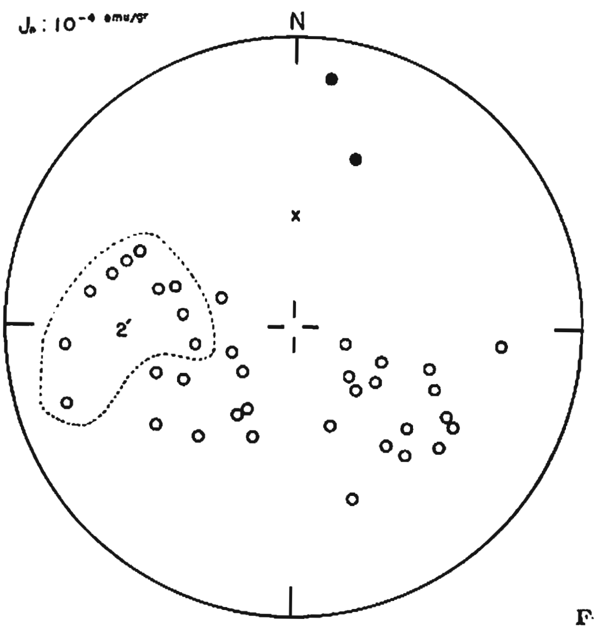

(2)

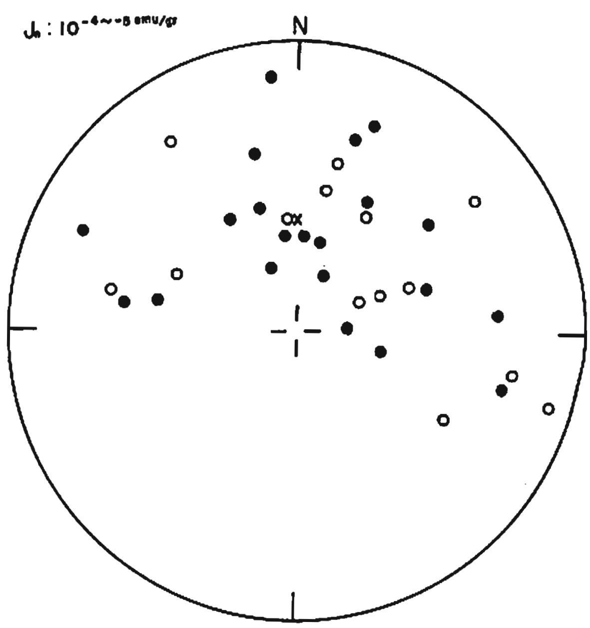

(4)

Fig. 3

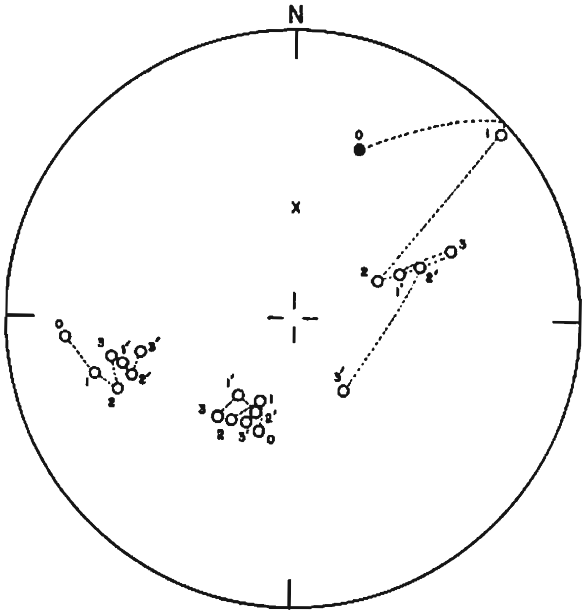

Fig. 4

17. Paleomagnetic Study in Northern Part of Hokkaido

Yasunori Nishida

Geophysical Institute, Hokkaido University

As already reported by the present author, the geomagnetic pole positions of Neogene are estimated by the rock specimens collected around Sapporo, Hokkaido, differ from those determined by the data obtained in the Main Island of Japan. And noteworthy characteristic of paleomagnetism around Sapporo is that the directions of magnetization of many rocks converge at the zenith of upper hemisphere of Schmidt's projection (Nishida 1966, Nishida and Yokoyama 1965).

Recently, the samples of igneous rocks were collected from the coastal region of Okhotsk, Hokkaido in order to prove whether the above characteristic is true there. The rock kinds comprise basalt, andesite and liparite. A-C demagnetization of the specimens were carried out after 2 months' storage tests. As the results of the stability tests, the localities, from which the specimens proved to be stable as paleomagnetic data, reached 5 in number. Three examples of the directions of the N.R.M. of these specimens are shown in Fig. 1. And various magnetic properties of the specimens which proved to be stable are shown in Table 1. The geological ages are also shown in Table 1.

Table 1. Various magnetic properties of the samples

Sample	Number of Samples	Geological Age	Mean Direction		α	Pole Position		Intensity
			I	D	(95%)	Lat.	Long.	(10 emu/gr)
A-1	3	Middle Miocene	62°	-17°	17°	78°N	59°E	5~6
A-2	7	Lower Pliocene	75°	68°	12°	47°N	177°W	3~46
A-3	3	Middle Pliocene	52°	37°	5°	60°N	136°W	4~27
A-4	9	Lower Pliocene	73°	-5°	5°	75°N	133°E	2~5
A-5	2	Lower Pliocene	69°	5°	13°	80°N	160°E	66~90

The magnetic north poles are plotted on the map as shown in Fig. 2, where the absolute ages of these specimens have not yet been determined and their sequences are uncertain. As the results, the following is clear that the virtual magnetic pole positions obtained from the data in the northern part of Hokkaido coincide with the pole path deduced from the data in the Main Island of Japan by many authors (e.g. Ito, 1965), though the pole obtained from the specimens collected around Sapporo travels over the eastern part of South America.

A possible interpretation is the relative crustal movements between Hokkaido and the Main Island of Japan. But it may be applicable only for the south western part of Hokkaido.

In either case, collection of samples from geographycally wide areas and from successive lava flows are necessary to discuss the general and more detailed paleomagnetic feature in Hokkaido.

References

Nishida, Y. (1966), Paleomagnetic Study around Sapporo in Hokkaido (1st Paper), Geophys. Bull. Hokkaido Univ., 15. (in Japanese)

Nishida, Y., Yokoyama, I., (1965) Annual Progress Report of the Rock Magnetism Research Group.

e.g. Ito, H. (1965), Paleomagnetic Study on a Granitic Rock Mass with Normal and Reverse Natural Remanent Magnetization, J. Geomag. Geoelect., 12.

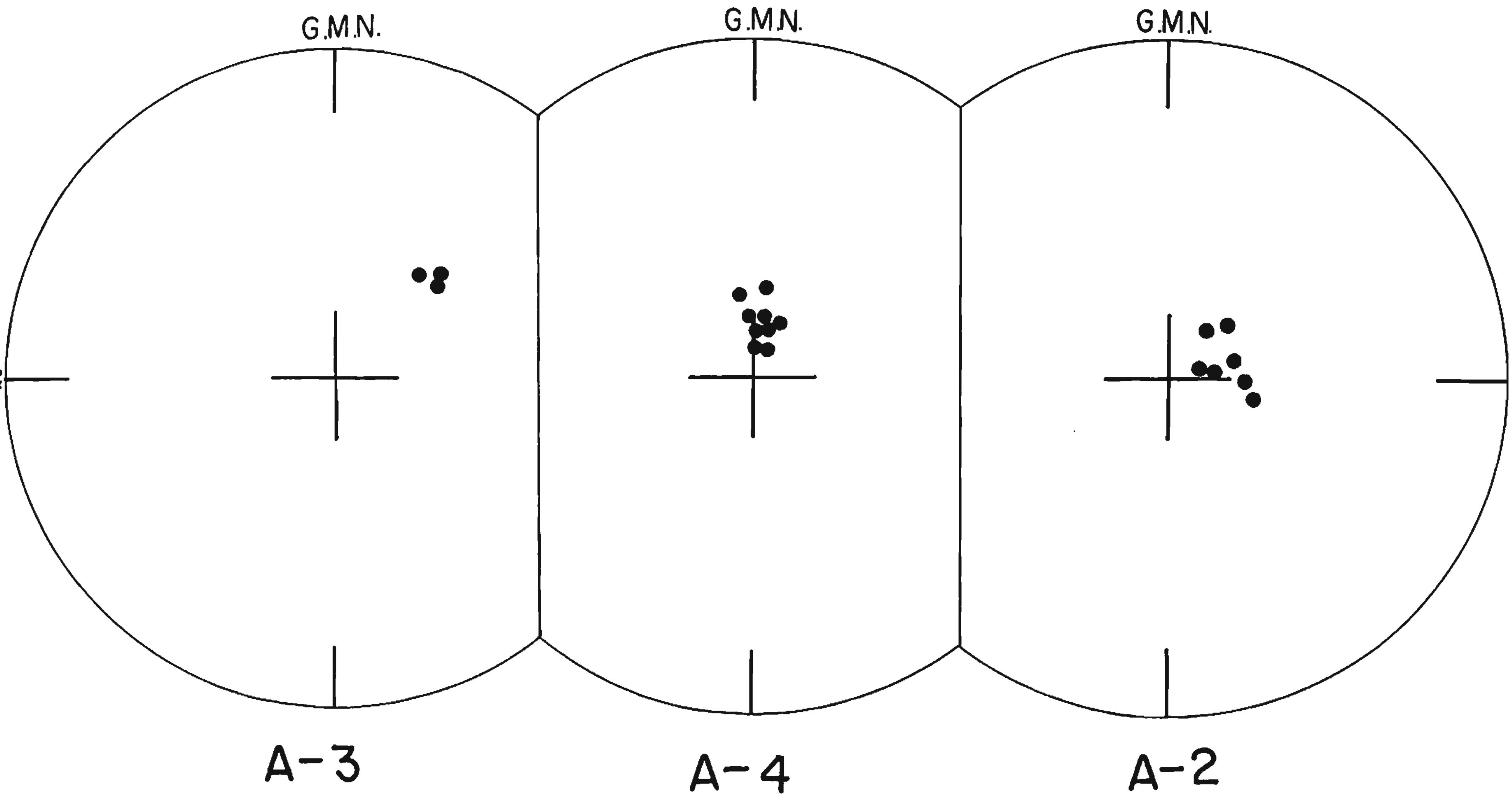

Fig. 1 Schmidt's projection of N.R.M. of the samples.

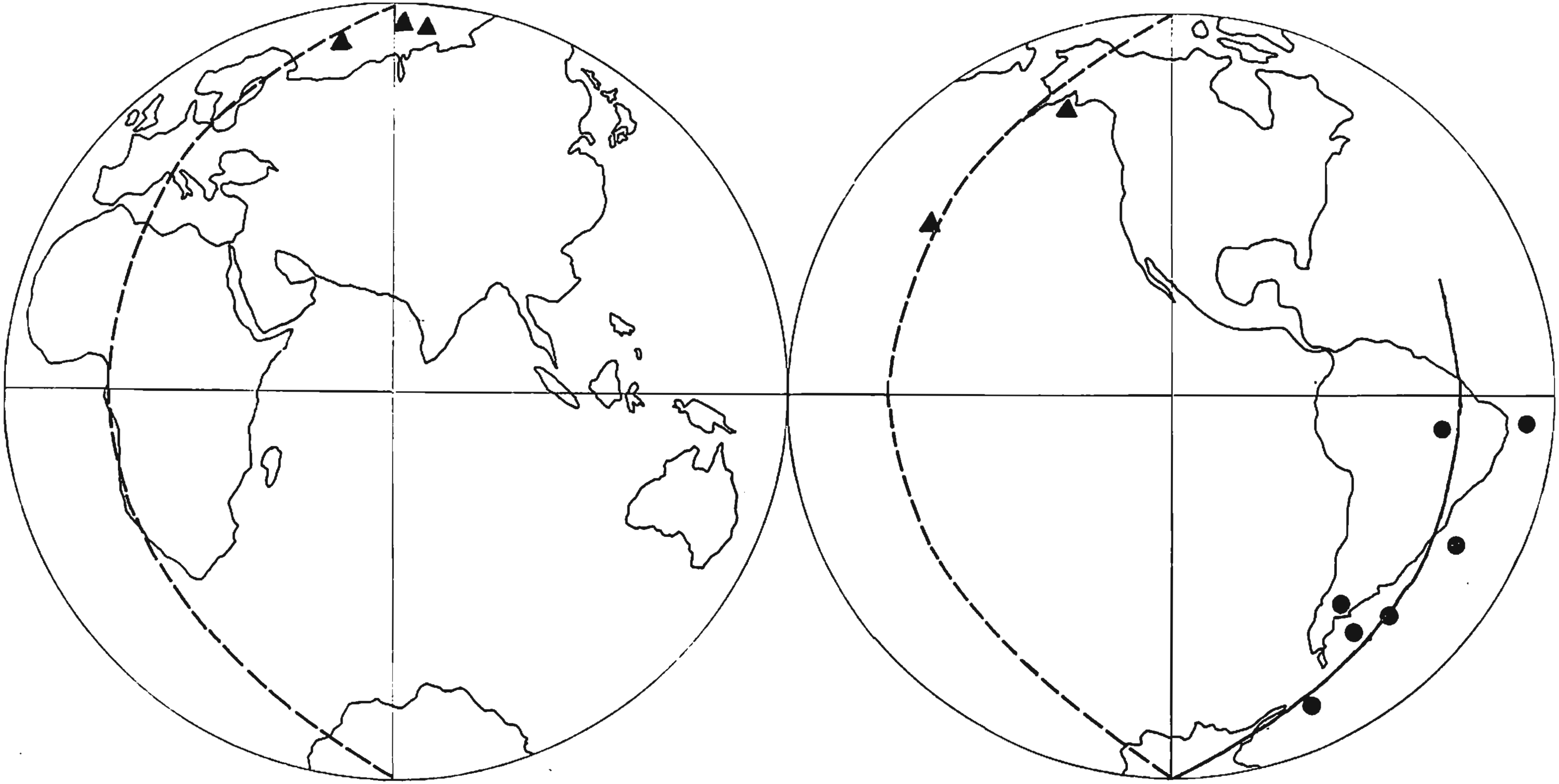

Fig.2 Pole positions obtained from the Mio–Pliocene data. Triangles denote the pole positions obtained from the data in the northern part of Hokkaido. Solid circles and solid line show the pole positions and the pole path deduced from the data in the south western part of Hokkaido. Dotted lines show the pole paths deduced from the data in the Main Island of Japan.

18. Geomagnetic Anomaly over Volcanoes and Paleomagnetism

Izumi Yokoyama

Geophysical Institute, Hokkaido University

Recently aeromagnetic data have been accumulated in our country, and on the geomagnetic maps, for example, the total force maps thus obtained, we find very often conspicuous anomalies, both positive and negative corresponding to the igneous bodies. Such anomalies may afford us very useful data for the study of paleomagnetism because the directions of their magnetizations are the statistical results over all rock-bodies and more reliable than the results obtained from a small number of the rock specimens, providing that these large igneous bodies were erupted during rather short geological times. It is necessary, however, to prove the relations between the magnetization of a mountain body as a whole and that of the rock specimens from its surface before we analyze the geomagnetic anomalies for the purpose of paleomagnetism.

Hitherto, several geophysicists have interpreted geomagnetic anomalies over volcanoes by "model method" and some of them assume that the volcanoes are the uniformly magnetized circular cones or ellipsoids above the surrounding topographies, and they compare the effective magnetization of a volcano with that of the rock specimens collected there. From the standpoint of volcanology, volcanoes generally have their bases or roots beneath the topographies and their locations are an important problem. Furthermore, the following condition should be fulfilled: The effective magnetization deduced from geomagnetic anomaly over a volcano should be smaller than J_n and larger than $F_0\kappa$, both of the rock specimens. The base for this condition is that volcanoes generally consist of lavas and the other porous ejecta, the former having strong J_n and the latter being effective in $F_0\kappa$ and J_n is far larger than $F_0\kappa$ as for igneous rocks: It is almost unreasonable that the effective magnetization equals to the mean value of J_n of the lava specimens.

Determination of paleomagnetic field by analyses of geomagnetic anomalies over volcanoes, the author fears, would involve risk because of uncertainties about uniform magnetization of volcanoes and about limits of volcanic bases. The most reasonal method to utilize the results of geomagnetic surveys over volcanoes may be to find the volcanic bodies which are clearly magnetized normally or reversely and thereafter, the rock specimens from these volcanic bodies should be studied paleomagnetically.

In Hokkaido, two volcanic regions, Kuttyaro and Sikotu, were aeromagnetically surveyed both by the U.S. Geological Survey. The present author and his colleague (Yokoyama 1966, Mori and Yokoyama 1967) made discussions on the geomagnetic anomalies in these regions. The total force map in the district of Kuttyaro is shown in Fig. 1 where we find several remarkable anomalies corresponding to the volcanic bodies. Some of them are listed in the following table:

Table 1

Volcano	Height a.s.l. (meter)	Age	Geomagnetic anomaly
Kikin-dake (KI)	995	Lower Pleistocene	Negative
O-Akan-dake (OA)	1371	Holocene	Positive
Nisibetu-dake (NI)	800	Pleistocene	Positive
Syari-dake (SH)	1545	Holocene	Positive
Etobi-yama (ET)	713	Pleistocene	Negative
Mokoto-yama (MO)	1000	Lower Pleistocene	Negative

On the other hand, the N.R.M.s and susceptibilities of many rock specimens from these two volcanic districts have been measured by the present author. The majority of these specimens were collected by R. Blank and Y. Nishida, to whom the author is very grateful. The directions of the N.R.M.s are expressed on Schmidt's projection as shown in Fig. 2 where the circles denote the specimens from Sikotu and the squares those from Kuttyaro. As already mentioned by Y. Nishida(1966), many rocks from these districts are magnetized in the zenith direction of the upper hemisphere. The rocks from Mokoto-yama being situated at the northern rim of Kuttyaro Caldera, are denoted by MO in Fig. 2 and are all magnetized in the upward direction. Unfortunately any oriented rock specimens from the other volcanoes listed in Table 1 have not been collected. However, it is very suggestive that we observe a small negative magnetic anomaly on Mokoto-yama, of which era is determined stratigraphically as lower Pleistocene, and that the Holocene volcanoes, O-Akan-dake and Syari-dake, manifest the very clear positive anomalies in the total force accompanied by small negative values at the northern parts of the volcanoes. We may say that these Holocene volcanoes are normally magnetized ignoring the precise directions of their magnetizations. In the nearest future, the author wishes to measure the magnetizations of the rocks from all volcanoes in the districts of Kuttyaro and Sikotu referring the geomagnetic anomalies there.

References

Yokoyama, I. (1966), Note on Aeromagnetic Survey with Special Reference to Volcanic Regions (Part 1), Jour. Fac. Sci., Hokkaido Univ., Ser. VII, 2, 337-357.

Mori, T. and Yokoyama, I. (1967), Geomagnetic Anomalies in the Eastern Part of Hokkaido (Preliminary Report) (in Japanese), Geophys. Bull. Hokkaido Univ., 17, 15-21.

Nishida, Y. (1966), Palaeomagnetic Study around Sapporo in Hokkaido (1st Paper) (In Japanese), Geophys. Bull. Hokkaido Univ., 15, 59-78.

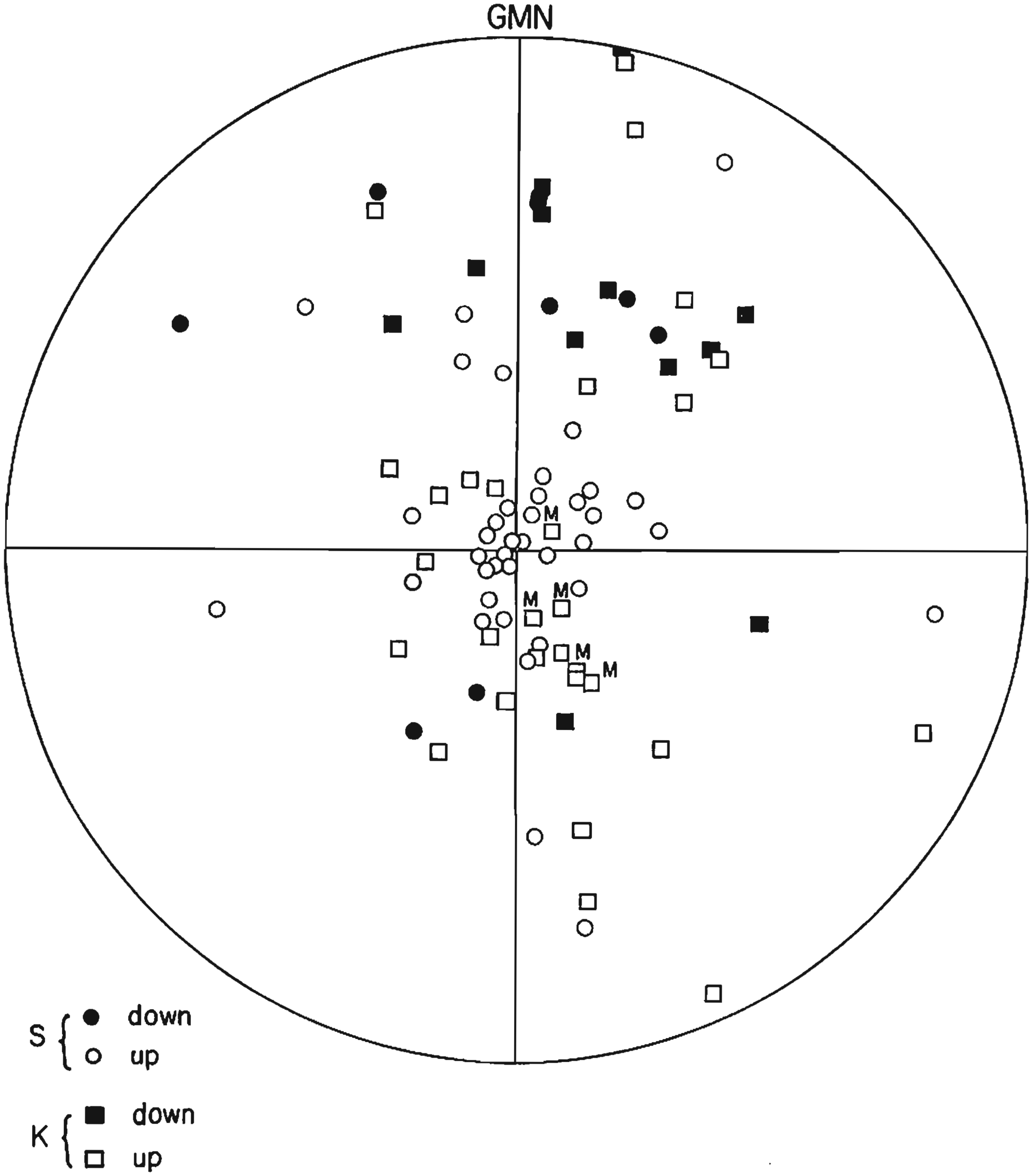

Fig. 2. Schmidt's projection of N.R.M.s of the specimens collected from the districts of Kuttyaro and Sikotu. M denotes the rocks from Mokoto-yama.

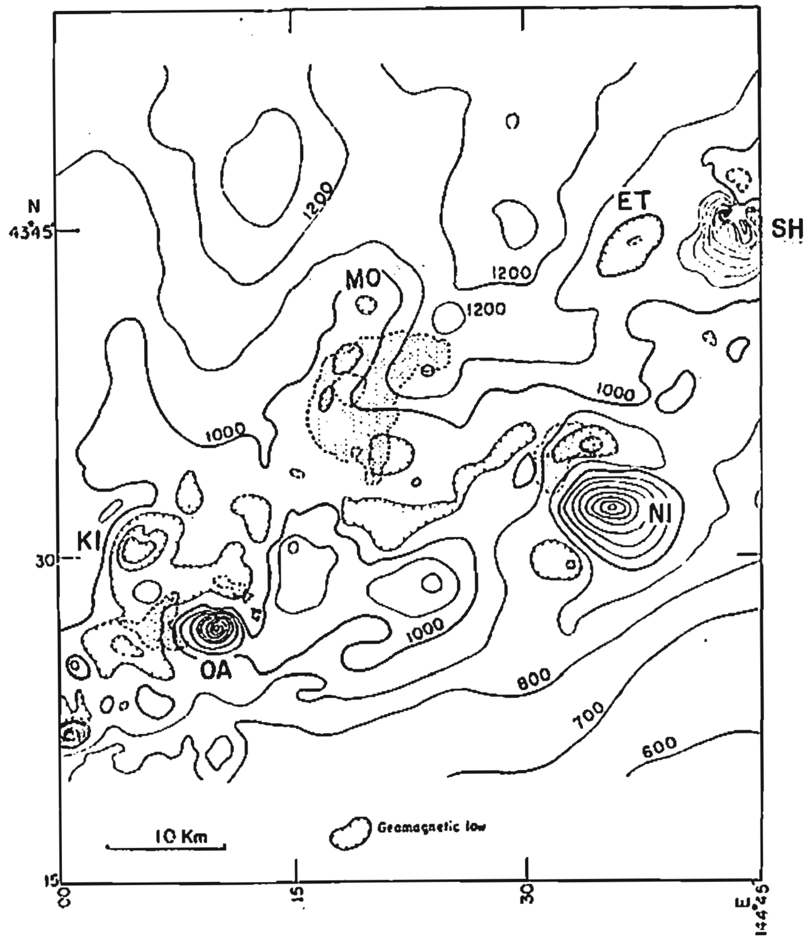

Fig. 1. Aeromagnetic map in total force over the district of Kuttyaro surveyed by the U.S. Geological Survey. Unit is gamma and the dotted parts denote lakes.

19. Field Intensity in the PreCambrian Period

Kazuo Kobayashi*

Geophysical Institute, University of Tokyo

Detailed magnetic and microscopic investigation was carried out to test the feasibility of paleomagnetic determination of the geomagnetic field intensity in the PreCambrian period. Natural remanent magnetization (NRM) of 13 samples from various localities in the Canadian Shield area of Canada and USA was investigated by Thelliers' stepwise heating method (Thellier and Thellier, 1959); thermal decay of the NRM, J_n was compared with the partial acquisition of TRM, J_T for several different temperature ranges between room temperature and the Curie temperature. With 4 samples among 13 J_T is nearly proportional to J_n for various heating temperatures unless they are higher than 550°C, while the other samples do not show such proportionality of J_T and J_n. The latters, therefore, were not used in the present study. Table 1 represents the petrographic descriptions, radiometric ages and references of relevant paleomagnetic articles in which the ages were given.

The ratios of J_n/J_T of the 4 samples were determined using the J_n-J_T diagrams such as shown in Fig. 1. The Curie temperatures, T_c were determined by thermomagnetic analyses in a magnetic field of 2800 Oe. Table 2 summarizes these magnetic characteristics. Thermal reversibility of the saturation magnetization was also demonstrated by these thermomagnetic analyses between room temperature and about 550°C. However, if the samples were heated at temperatures above 550°C, the thermomagnetic curves were no longer reversible, implying that a chemical change such as oxidation proceeded in the ferromagnetic minerals contained.

---

* Now at Ocean Research Institute, University of Tokyo

Analyses of microscopic remanent coercive forces after progressive heating indicated similar chemical stability of the samples; the mode of AC demagnetization of saturated IRM subsequent to the heat-treatment remained almost unchanged until the heating temperature exceeded $550^{\circ}C$. Possibility of the stress release or growth of exsolved phase due to annealing may thus be excluded.

Iron ore phases contained in the samples were microscopically examined with polished sections by reflected light, the results being described in Table 3. All the samples contain fresh (unoxidized) magnetite or titanomagnetite at least in a part of the rocks. In particular (titano) magnetite in samples Nos. 1 and 3 appears very fresh. Bulk grain sizes of titanomagnetite are moderately small in samples Nos. 1 and 4. Samples Nos. 2 and 3 have larger grains of titanomagnetite but the grains are divided into much finer dimensions by the grid exsolution lamellae of ilmenite or ulvöspinel. Thus, the effective grain sizes of magnetic constituents in these samples are all sufficiently small to behave as single domain or pseudo-single domain particles so that NRM consisting of TRM may be stable for the long duration of geological time (longer than 10^{9} years).

Since the ambient geomagnetic field reversed its direction almost periodically the viscous remanent magnetization induced during the preceding periods was demagnetized under the influence of the field during the subsequent period. At present only the effect of the field during the last normal epoch (since 0.7 my ago) may be detectable. However, recent paleomagnetic intensity study has shown that the viscous magnetization acquired for such a duration can be removed by heating at $150^{\circ}C$ to $200^{\circ}C$.

It may therefore be concluded that the values of J_n/J_T obtained so far represent the ratios of the intensity of the PreCambrian field at the sampling sites (Canada or USA) to that of the present field at our laboratory. Using the paleomagnetic pole positions given by others (references cited in Table 1), field intensity at the paleomagnetic equator, F was calculated and listed in Table 2. It is remarkable that the field intensity in the PreCambrian period was not much different from that at present (0.3 Oe). This may imply that in the middle or late PreCambrian the earth's core already reached a stage of development in which there existed a set of convective motions enough to generate magnetic field similar to the present one.

Acknowledgement

The author wishes to express his sincere thanks to Dr. E. J. Schwarz, Geological Survey of Canada and Prof. LeRoy Scharon, Washington University, St. Louis for their kindness to offer their samples for the author's experiment. This research was made in close cooperation with Dr. E. J. Schwarz.

References

Fahrig, W. F., E. H. Gaucher and A. Larochelle (1965), Palaeomagnetism of diabase dykes of the Canadian shield, Can. J. Earth Sci., 2, 278-298.

Hays, W. W., and LeRoy Scharon (1966), A paleomagnetic investigation of some of PreCambrian igneous rocks of southeast Missouri, J. Geophys. Res., 71, 553-560.

Larochelle, A. (1966), Palaeomagnetism of the Abitibi dyke swarm, Can. J. Earth Sci., 3, 671-683.

Thellier, E., and O. Thellier (1959), Sur l'intensité du champ magnétique terrestre dans le passe historique et géologique, Ann. Geophys., 15(3), 285-376.

Table 1. Petrography and radiometric age of samples

Sample No.	Locality	Rock Type	Petrographic Descriptions	Radiometric Age (my)	Reference
1	Matachewan, Canada	Amphibolite	Hornblende contained. Evidence of thermal metamorphism is found.	2485 (K-A)	Fahrig, Gaucher and Larochelle (1965)
2	Abitibi, Canada (NNE trending)	Quartz-bearing pyroxene gabbro	Pyroxene(augite) is partly altered. Opaques are slightly altered. Biotite and amphibole are contained.	1825 (K-A)	Larochelle (1966)
3	Muskox	Tholeiitic gabbro	Fresh augite is contained. Stillwater-type exsolution occurs along 001 in pigionite.	1155 (K-A)	Robertson, W. (in press)
4	Skrainka, Missouri, USA	Pyroxene gebbro	Augite and feldspar are partly altered.	1300 ± 100 (Sr-Rb)	Hays and Scharon (1966)

Remark: Microscopic examination of thin sections was made with the help of Dr. I. Kushiro.

Table 2. Magnetic properties of samples

Sample No.	Locality	J_n/J_T	F (Oe)	Paleomagnetic pole	T_c ($^\circ$C)
1	Matachewan	0.82	0.38	61.2°E, 62.9°N	(570)*
2	Abitibi (NNE trending)	0.72	0.33	122°W, 21°S	575
3	Muskox	0.66	0.30	191°E, 4.7°N	550
4	Skrainka	0.65	0.30	150°W, 5°N	575

Remark: As to symbols, see text.

* Value after irreversible oxidation by heating

Table 3. Opaque minerals revealed under reflection microscope

Sample No.	Locality	Magnetite or titano-magnetite	Maghemite or titano-maghemite	Ilmenite		Ulvöspinel	Pyrite
				Lamellae	Grain		
1	Matachewan	fresh, only partly to limonite	None	a little	None	None	Common
2	Abitibi (NNE trending)	partly weakly oxidized	marginal ?	None	Common	Common in net frame-work(exsolu-tion)in(100) magnetite	
3	Muskox	fresh	None	very plenty in net framework of magnetite (parallel to (111)planes)	Common	None	
4	Skrainka	very little remains, but still some are fresh	strongly altered to limonite	None	Common	None	Common

Remark: Reflection-microscopic observation was done with the aid of Prof. T. Tatsumi and Dr. I. Kushiro, Geological Institute

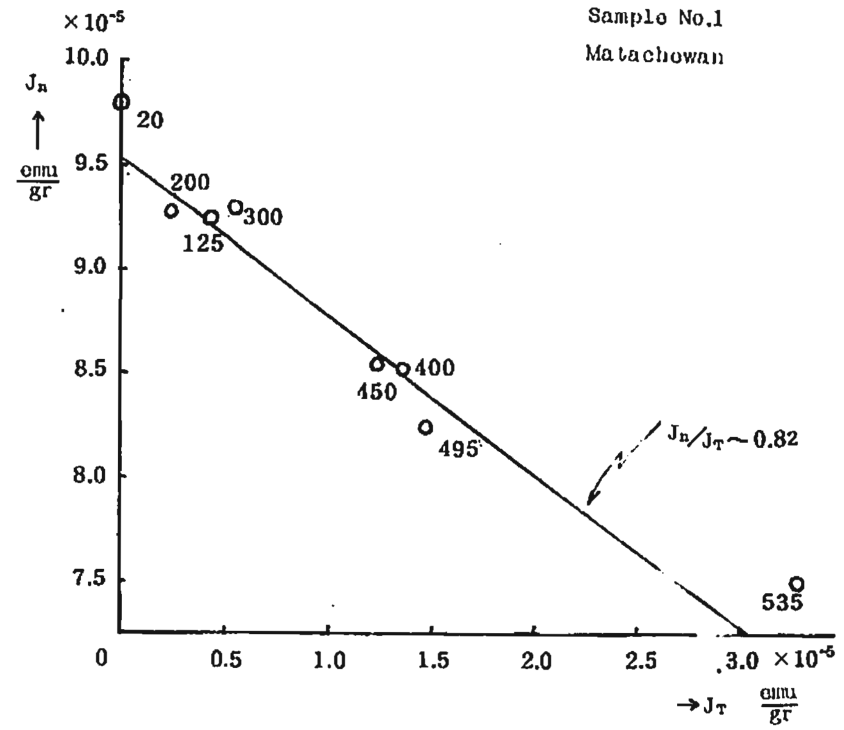

. F i g . 1 (a)

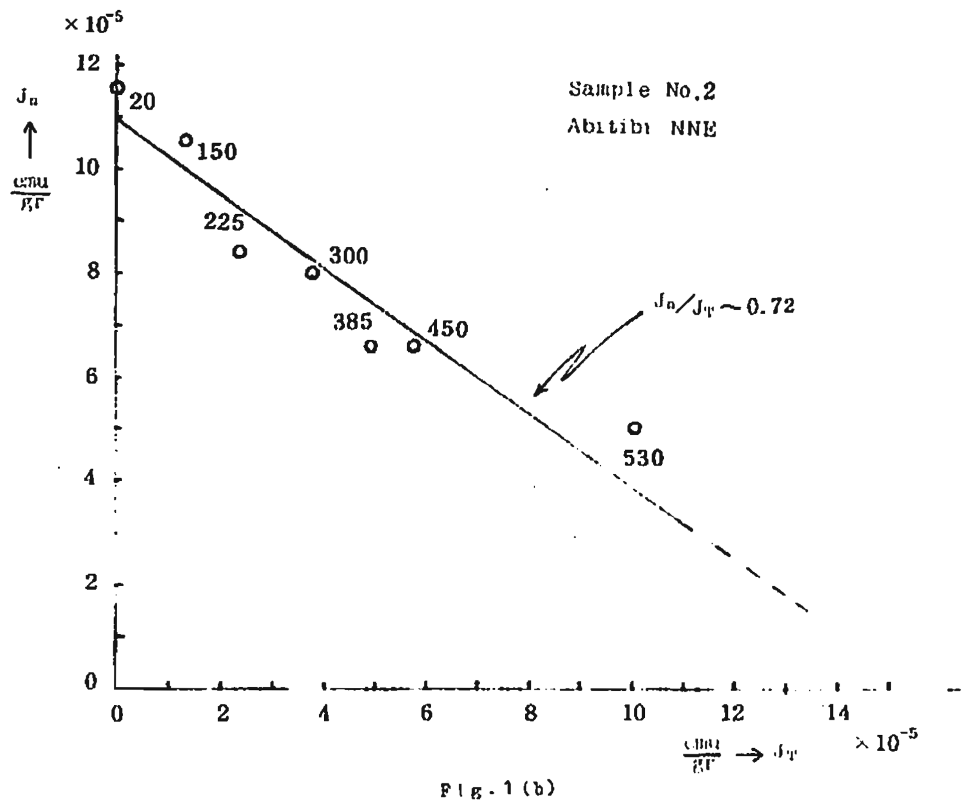

F i g . 1 (b)

Fig. 1 J_n - J_T diagrams of two Samples.

(a) Sample No. 1 Matachewan

(b) Sample No. 2 Abitibi NNE

Figures besides circles indicate heating temperatures.

All values of J_n and J_T were measured at room temperature.

20. Subaqueous Autobrecciated Lava

Hisashi Kuno

Geological Institute, University of Tokyo

It is well known that subaqueous flows of basalt magma form pillow lavas, often associated with palagonite. However little attention has been paid to a structure produced by more viscous andesite and dacite magmas entering into water. By recognition of some criteria which may distinguish subaqueous from subaerial flows, inference can be drawn as to whether a given pile of lavas was laid down under the water or on the land surface.

I have examined the structure of some historic and prehistoric flows which obviously entered into the water but later emerged therefrom, and also of subaqueous flows of Tertiary age. The result showed that subaqueous flows of andesitic composition have a characteristic autobrecciated structure which can be distinguished from the structures of brecciated part of subaerial lavas such as block lavas and aa lavas and also of nuee ardente deposits.

Subaqueous autobrecciated lava consists of polygonal blocks of various dimensions cemented by comminuted particles of the same material. Matrix of palagonite is sometimes present. Individual blocks are usually compact, although some vesicules are present, especially along the surface of larger blocks. The blocks are often traversed by joints which separate them into smaller polygonal blocks. In blocks ranging from 0.5 to 3 m in diameter, which are often angular in outline and sometimes roughly spheroidal, closely spaced joints parpendicular to the surface of the blocks are developed, indicating their quenching against the surrounding water. Thus a complete gradation can be observed from such large blocks with a joint pattern essentially similar to that of the pillow units to smaller blocks detached from the larger blocks and further to the fine particles of the matrix. The proportion of the fine particles to the blocks varies greatly in different parts of a single flow; sometimes even a gradation to a solid lava is observed.

Subaqueous autobrecciated lavas and pillow lavas are commonly observed in the older to younger Miocene volcanic formations of Izu Peninsula which occasionally contain marine fossils (the Yugasima and Sirahama Groups), whereas they have never been observed in the Pliocene and Pleistocene volcanic formations of the same region. Thus in this region, the submarine condition prevailed during the Miocene time, but the greater part of the present Izu Peninsula was above the sea during the Pliocene time. At the end of the Pliocene or the beginning of the Pleistocene, the southern part of the present peninsula was separated from the main land by a shallow sea where the fossiliferous Zyō formation was deposited. Upon this formation, the lavas of the Usami volcano were extruded. Some of the earlier lavas are normally magnetized, whereas the overlying lavas of the same volcano are reversely magnetized, indicating that the latter represent the close of the Matsuyama Epoch of Doell et al.

All the cone-shaped volcanoes of the peninsula were apparently build after the Zyō formation was elevated above the sea level. The absence of subaqueous autobrecciated lavas and pillow lavas in these cones precludes the possibility that even the lowest levels of the lavas now exposed on the land had once extruded under the water but have later emerged therefrom. This may imply that, since the early Pleistocene, no significant upheaval of the region have taken place. It is also possible that this is due to the rise of the sea level since the latest glaciation.

21. Piezomagnetization of Rocks

Takesi Nagata

Geophysical Institute, University of Tokyo

1. Dependence of magnetic susceptibility of rocks on uniaxial compression

The magnetic susceptibility (χ) of rocks under uniaxial compression $\underline{P}$ becomes anisotropic, the magnitude of χ along the direction of axis of $\underline{P}$ being empirically expressed as

$$\chi = \frac{\chi_0}{1 + \beta \underline{P}} \qquad (1)$$

where χ_0 denotes the isotropic magnetic susceptibility without the compression and β is a constant dependent on characteristics of samples. The magnitude of β for various rocks ranges between 0.8×10^{-4} and 1.3×10^{-4} cm^2/kg. (Kapitsa 1955, Nagata 1966).

2. Piezoremanent magnetization of rocks

Piezoremanent magnetization (PRM) is defined as the remanent magnetization after the application and release of uniaxial compression (P) in the presence of a magnetic field (H) and final removal of the magnetic field. The remanence after the above-mentioned procedures is denoted by Jr(H+P+PoHo). Similarly the ordinary IRM can be expressed as Jr(H+Ho). Then, the acquisition rate of PRM may be defined by

$$R(H,P) = \frac{Jr(H+P+PoHo)-Jr(H+Ho)}{Jr(H+Ho)} \qquad (2)$$

The dependence of R(H,P) of rocks on $\underline{P}$ is approximately represented by a linear relation for $30kg/cm^2 \leqq P \leqq 200kg/cm^2$ such as

$$R(H,P) = \alpha(P-30kg/cm^2), \qquad (3)$$

The observed values of α for typical basalts are given in the following table, together with coercive force (Hc), absolute intensity of IRM for Hex = 36Oe. and the AC-demagnetization coercive force $(\tilde{H}c)$, which is defined as intensity of $\tilde{H}c$ for $Jr(\tilde{H}c)/Jr(o) = \frac{1}{2}$ in the AC-demagnetization curve, $Jr \sim \tilde{H}$. The magnetically harder rocks have the larger value of α .

Table I

Acquisition rate of PRM and magnetic coercivity

Sample	Basalt A	Basalt C	Basalt B
α	1.10×10^{-2}	0.54×10^{-2}	0.36×10^{-2} /kg/cm²
Hc	245	—	71 Oe.
$\tilde{H}c$	98	58	22 Oe.
IRM(H=36Oe.)	7.27×10^{-4}	3.12×10^{-3}	3.09×10^{-2} emn/cc

Attention must be paid to the fact that α is very large for natural rocks.

3. Dependence of PRM on applied magnetic field

The acquisition rate of PRM defined by R(H,P) increases with a decrease in the intensity of applied magnetic field H. The results of measurements for the typical basaltic samples for the range of magnetic field from 18 to 54Oe have shown that the absolute value of PRM defined by J(PRM)= Jr(H+P+PoHo)-Jr(H+Ho) remains approximately invariant (or rather slightly increases with a decrease in the intensity of field) in the range. This result seems to be extremely important in connection with a problem of possible geomagnetic variation related to a breaking down of the earth's crust, because PRM in the geomagnetic field may have an appreciably large value.

4. Effect of hydrostatic pressure on Piezomagnetization

The saturation magnetostriction coefficients, λ_{100} and λ_{111} , and the magnetocrystalline anisotropy constants, K, and K_2, of magnetite change with changing hydrostatic pressure (Po). According to experimental results for the pressure range of 0 - 2 Kbar, both $|\lambda_{100}|$ and λ_{111} increase almost linearly with increasing hydrostatic pressure with rate of about 15%/Kbar, whereas both $|K_1|$ and $|K_2|$ decrease with increase of hydrostatic pressure with rate of about -5%/Kbar. (Nagata and Kinoshita 1967)

Since β in eq (1) can be theoretically represented by

$$\beta = 3\lambda_s \quad \chi o/Js^2$$

where $\lambda_s = \frac{2}{5}\lambda 100 + \frac{3}{5}\lambda 111$, the increase of λ_s with increase in $\underline{P}$ should result in an increase of β with $\underline{P}$. In case of rocks, β under P = P is numerically expressed as

$$\beta(P) = \beta(0)\ (1 + 0.16\underline{P})$$

where $\underline{P}$ is expressed in unit of Kbar.

References

Kapitsa, S.P. (1955), Izvestia Akad. Nauk, USSR, Geophys. Ser. 4. 489.

Nagata, T. (1966), J. Geomag. Geoele., 18, 73.

Nagata, T. and H. Kinoshita (1967), Phys. Earth. Planetary Interior, 1, 44.

22. Magnetic Cleaning By Use of Hydrostatic Pressure

M. Shimada, S. Kume

College of General Education, Osaka University

and

M. Koizumi

Institute of Scientific and Industrial Research,

Osaka University

A method of cleaning an unstable remanent magnetization has been developed by the authors and its example is shown in this report. The principle of this method is based on a demagnetizing effect of remanence under hydrostatic pressures (Kume, 1962; Girdler, 1963).

A single crystal of magnetite was used in the present experiment. Isothermal remanent magnetization was given to the sample by the application of magnetic field of 700 Oe as primary magnetization and then secondary magnetization was given by the application of field of 100 Oe. The angle between the primary and the secondary magnetization was 90°. The directions of these two magnetization were parallel to [111] and $[11\bar{1}]$ of cubic symmetry. The resultant magnetization, which was on (110) plane, deviated from the primary magnetization by about 40°.

Hydrostatic pressures up to 10 kbar were applied to the sample using a piston-cylinder type vessel. An assemblage of the high pressure cell will be reported elsewhere. After an application of a certain magnitude of pressure, the sample was taken out of the vessel and the direction and the intensity of magnetization were measured. The result of measurements is shown in Fig. 1.

It is observed that the secondary magnetization is completely demagnetized by the application of pressure of 10 kbar. The fact that only the unstable component is demagnetized and the stable component survives indicates a possibility of utilization of hydrostatic pressure in magnetic cleaning.

When this method is compared with ordinary ways such as A.C. or thermal demagnetization, it seems to possess some advantages. For instance, it does not require any nonmagnetic space, it takes only a few minutes to complete a run of demagnetization of soft component. However, enough care should be paid on generation of stress inside a sample as stress can be a cause of change in magnetic properties of a material.

References

Girdler, R.W. (1963), Ann. Géophys., 19, 118.

Kume, S. (1962), Ann. Géophys., 18, 18.

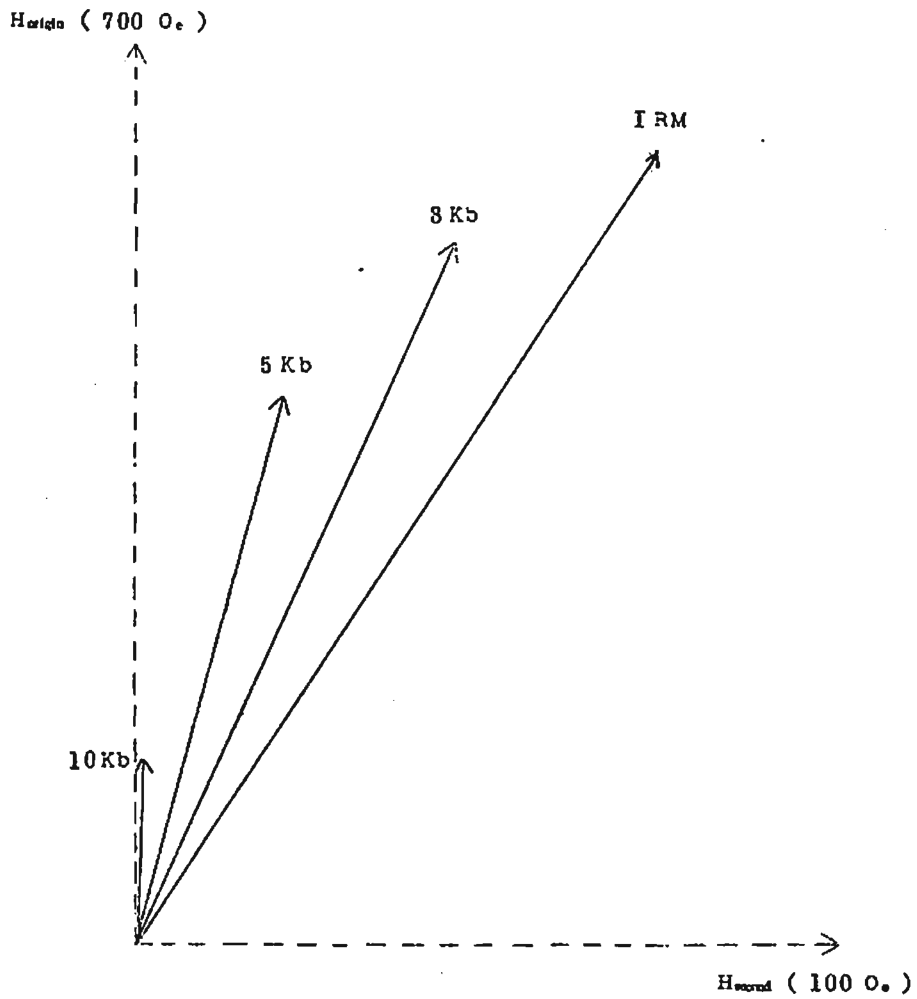

Fig. 1. Change in the direction and intensity of isothermal remanent magnetization of a single crystal of magnetite. It is observed that the unstable component completely disappears by the application of hydrostatic pressure of 10 kbar.

23. Change in Remanent Magnetization of Nickel Metal due to Compression

Hajimu Kinoshita and Mitiyasu Ohnaka

Geophysical Institute, University of Tokyo

Stress stability of remanent magnetization of pure nickel metal was investigated. The magnetization of a specimen of nickel metal under a uniaxial compression was measured by using an astatic magnetometer. The pressure, ranging from zero to almost 1.3 kb, was repeatedly exerted on the specimen. The initial remanent magnetization was TRM, PRM and IRM, which was produced in a cylindrically shaped nickel metal after an axial compression of up to 3 kb in nonmagnetic space. The specimen, having a diameter of 10mm and a length of 10mm, was cut from a pure nickel metal rod (purity 99.9%), and was previously annealed at 1000°C for 7 days in vacuum before measurement.

TRM was induced in the specimen by cooling down through the Curie temperature of pure nickel (375°C) in a magnetic field of 1.0 Oe perpendicular to the cylindrical axis. IRM and PRM were produced by a magnetic field of 50 Oe in the same direction as that of TRM. The magnetized specimen was put in the plane of rotation of the lower megnetic moment of the astatic magnetometer, as shown in Fig.1. The specimen was fixed between the press anvils with its magnetization in direction perpendicular to that of the astatic magnet system, in order to obtain an optimum condition for our measurements. In the present measurements, it was assumed that the direction of magnetization of the specimen was not changed by compression. An absolute value for the remanent magnetization was obtained by rotating the sample just before and after compressional treatments.

Changes in the remanent magnetization due to repeated compression are shown in Figs.1 and 2 for IRM, PRM and TRM at the same time on a normalized ordinate scale, where the compressional stress along the abscissa is plotted in units of kilo bar. From the results, it is clear that the TRM is very stable against compression compared with the IRM and PRM. The change in TRM with repeated compression can be characterized by its large recovery value, though with a small irreversible reduction in magnetization. Most unstable against compression, is IRM, which showed a nearly complete irreversible change in remanent magnetization due to compression at even 0.1 kb.

References

Lee, E.W. (1955) Magnetostriction and Magnetomechanical Effects, Rep. on Progress in Phys., 18, 184-229.

Bogdanov, A.A. (1966) On Effects of Elastic Stresses upon Domain Structure of Magnetite, Izv. Akad. Nauk CCCP, Phys. Zemli, No.1, 42-46.

Figure Captions

Fig. 1. Relative change in the remanent magnetization TRM with respect to repeated compression P. A schematic arrangement of the sample and astatic magnetometer is shown at the top of the figure.

Fig. 2. Relative change in PRM and IRM with repeated compression.

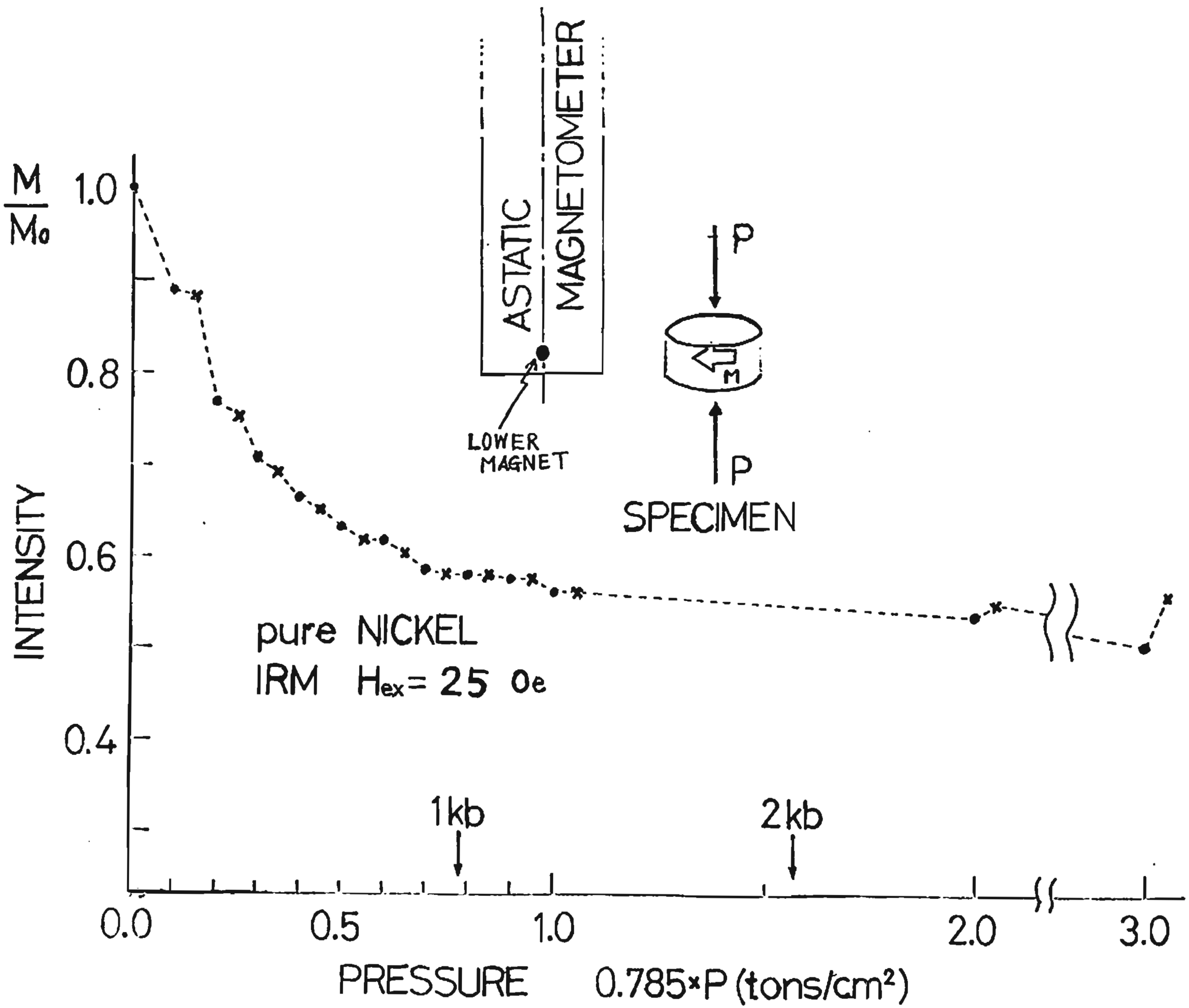
M/Mo
INTENSITY
1.0
0.8
0.6
0.4
ASTATIC MAGNETOMETER
LOWER MAGNET
P
M
P
SPECIMEN
pure NICKEL
IRM Hex= 25 Oe
1kb
2kb
0.0
0.5
1.0
2.0
3.0
PRESSURE 0.785×P (tons/cm²)

Fig. 1

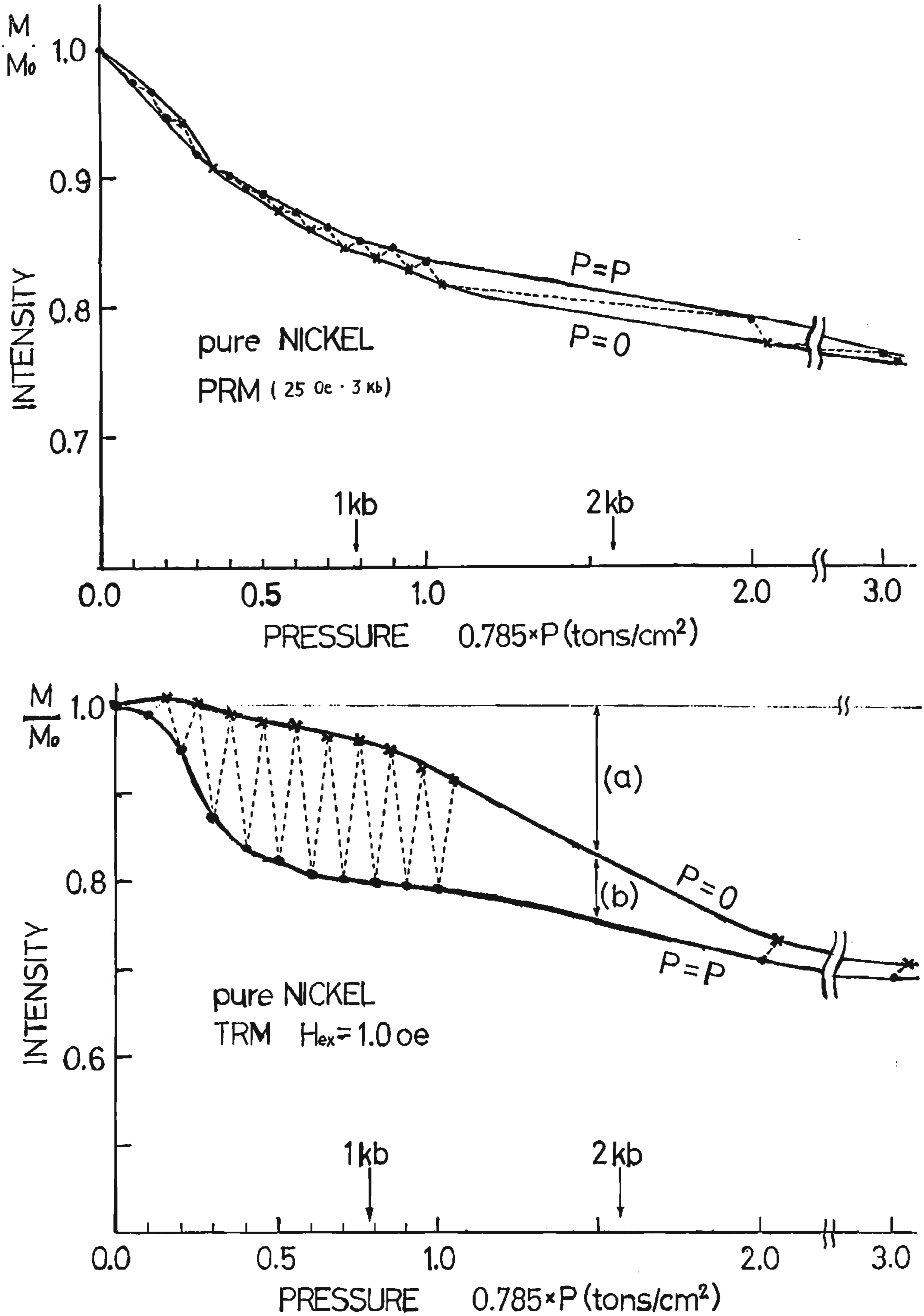
M/Mo
INTENSITY
1.0
0.9
0.8
0.7
P=P
P=0
pure NICKEL
PRM (25 Oe · 3 Kb)
1kb
2kb
0.0
0.5
1.0
2.0
3.0
PRESSURE 0.785×P (tons/cm²)
M/Mo
INTENSITY
1.0
0.8
0.6
(a)
(b)
P=0
P=P
pure NICKEL
TRM Hex=1.0oe
1kb
2kb
0.0
0.5
1.0
2.0
3.0
PRESSURE 0.785×P (tons/cm²)

Fig. 2

24. Change in Intensity of TRM of Lavas under Weak Compression

Mitiyasu Ohnaka and Hajimu Kinoshita
Geophysical Institute, University of Tokyo

TRM, i.e., NRM of lava flows is considered to change its intensity and direction under the influence of external mechanical forces. In order to study the variation in TRM and NRM (called TRM below) under purely uniaxial compression, we compressed a disk of volcanic rock having TRM whose direction is either parallel or perpendicular to the pressure axis. The pressure ranged in the present experiment from 0 to c a. 1 kb. The disk specimen was put between a pair of nonmagnetic press anvils without a container. A highly sensitive astatic magnetometer was attached about 5 cm from the press anvil in order to measure the change in magnetization of the rock under compression. A schematic arrangement of the apparatus is shown in Fig.1 a. In the experiment, arrangement A or B is chosen so that the magnetometer has an optimum position for the present measurements. The same procedure was carried out once again after rotating the sample 180° relative to the compression axis.

In Fig.1 b, the raw results of measurement are shown, where the zigzag curves represent variation of the magnetization of compressed rock, which are plotted on an arbitrary scale along the ordinate. The resultant change in the magnetization of the sample under compression was obtained by subtraction of the lower values from the upper ones read from the above curves. Two measurements are shown in Fig.2 a and b. The samples used here were from the basaltic lava flow of Mt. Fuji, collected at Mishima (ML-0852) and from that of Mt. Mihara, collected on Ohsima island (OL-106). ML-0852 and OL-106 were measured by using arrangements A and B (Fig.1), respectively.

As shown in the figure, the original magnetization increases in the direction perpendicular to that of the compressional axis and decreases in the parallel direction. Moreover, the resultant remanent magnetization after the release of stress decreases without exception. The change in the magnetization of ML-0852 is complicated, with the variation of TRM under pressure changing sign at about 0.265 kb. This type of change in the magnetization has also been observed by Kapitza (1955) on the measurements of the initial susceptibility of basaltic rocks. This behaviour may be explained as the result of relaxation of an internal stress due to the application of an external mechanical force, as mentioned by the above author.

Our present results can be used to estimate the seismomagnetic variation of the geomagnetic field, combining the results of pressure effects on the magnetic susceptibility, and the PRM effect of volcanic rocks.

We thank Professors Takesi Nagata and Kazuo Kobayashi for their helpful discussion. We are also grateful to Professors Hisashi Kuno and Kazuaki Nakamura for their kind suggestions on sample collections.

References

Kapitza, S.P. (1955) Magnetic Properties of Erupted Volcanic Rocks under Compression, Izv. Akad. Nauk CCCP, No.6, 489-504.

Kern, J.W. (1961) The Effect of Stress on the Susceptibility and Magnetization of a Partially Magnetized Multidomain System, J.G.R, 66, 3807-3816.

Nagata, T. and H. Kinoshita (1965) Studies on Piezo-Magnetization (I), J.G.G, 17, 121-136.

Figure Captions

Fig.1 a. A schematic arrangement of sample under measurement.

Case A: for measurement of TRM parallel to the pressure axis.

Case B: for TRM perpendicular to the pressure axis.

b. An example of raw data. The lower curve is obtained through the same compressional procedure with the sample rotated 180° after obtaining the upper curve.

Fig.2 a. Variation of TRM under compression measured with arrangement A. Sample: Fuji lava, ML-0852.

b. NRM with arrangement B. Sample: Mihara lava, OL-106.

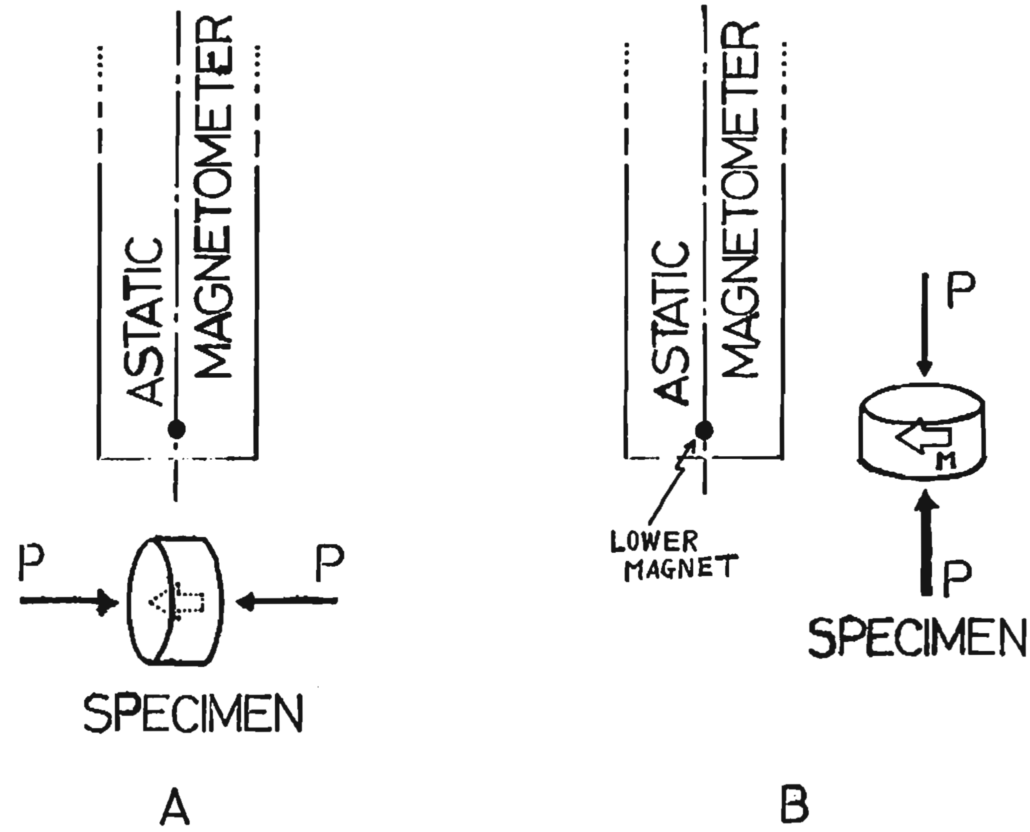
ASTATIC MAGNETOMETER
P
P
SPECIMEN
A
ASTATIC MAGNETOMETER
LOWER MAGNET
P
M
P
SPECIMEN
B

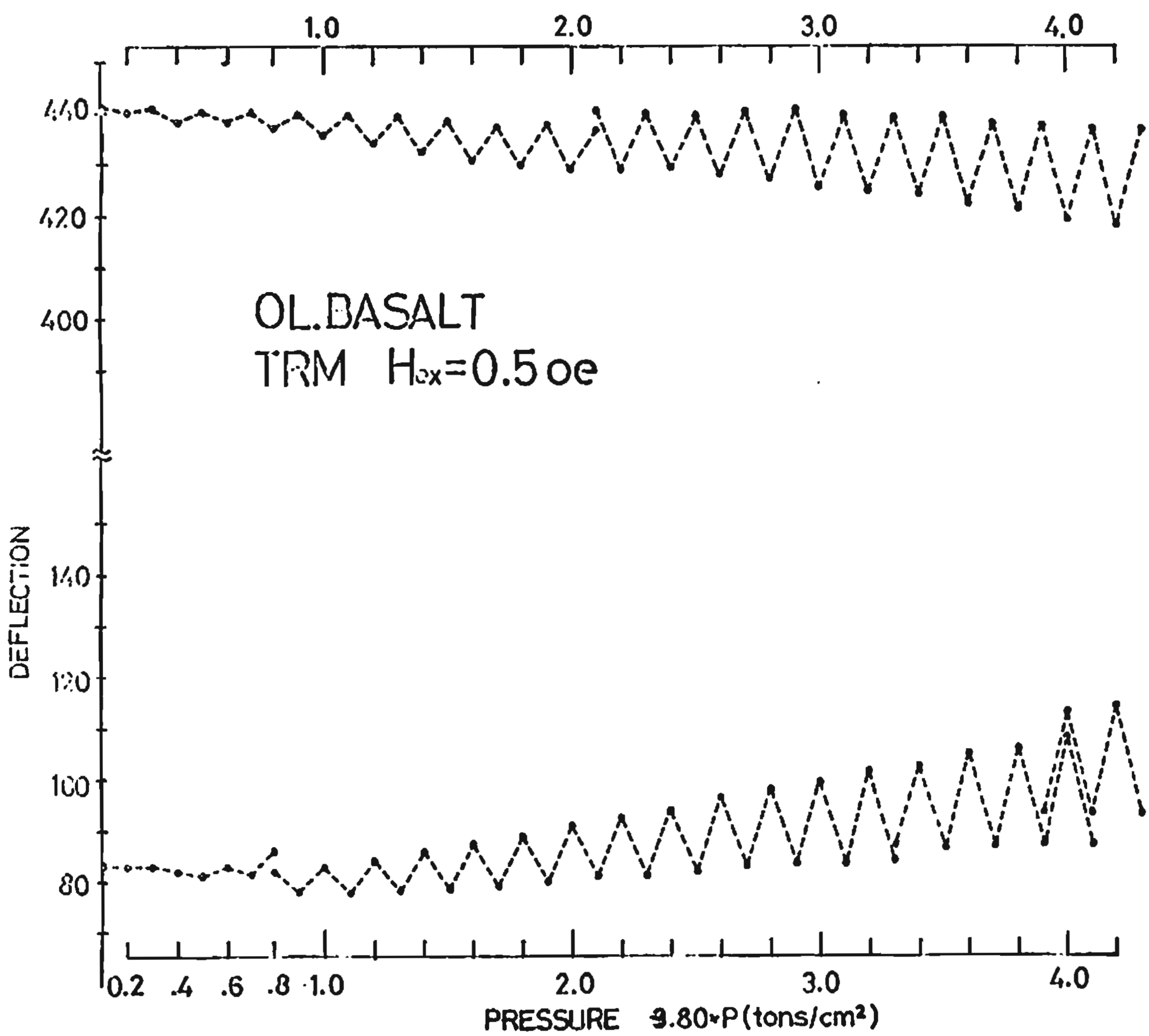
OL.BASALT
TRM Hex=0.5 oe
DEFLECTION
PRESSURE 9.80×P(tons/cm²)

Fig. 1 (b)

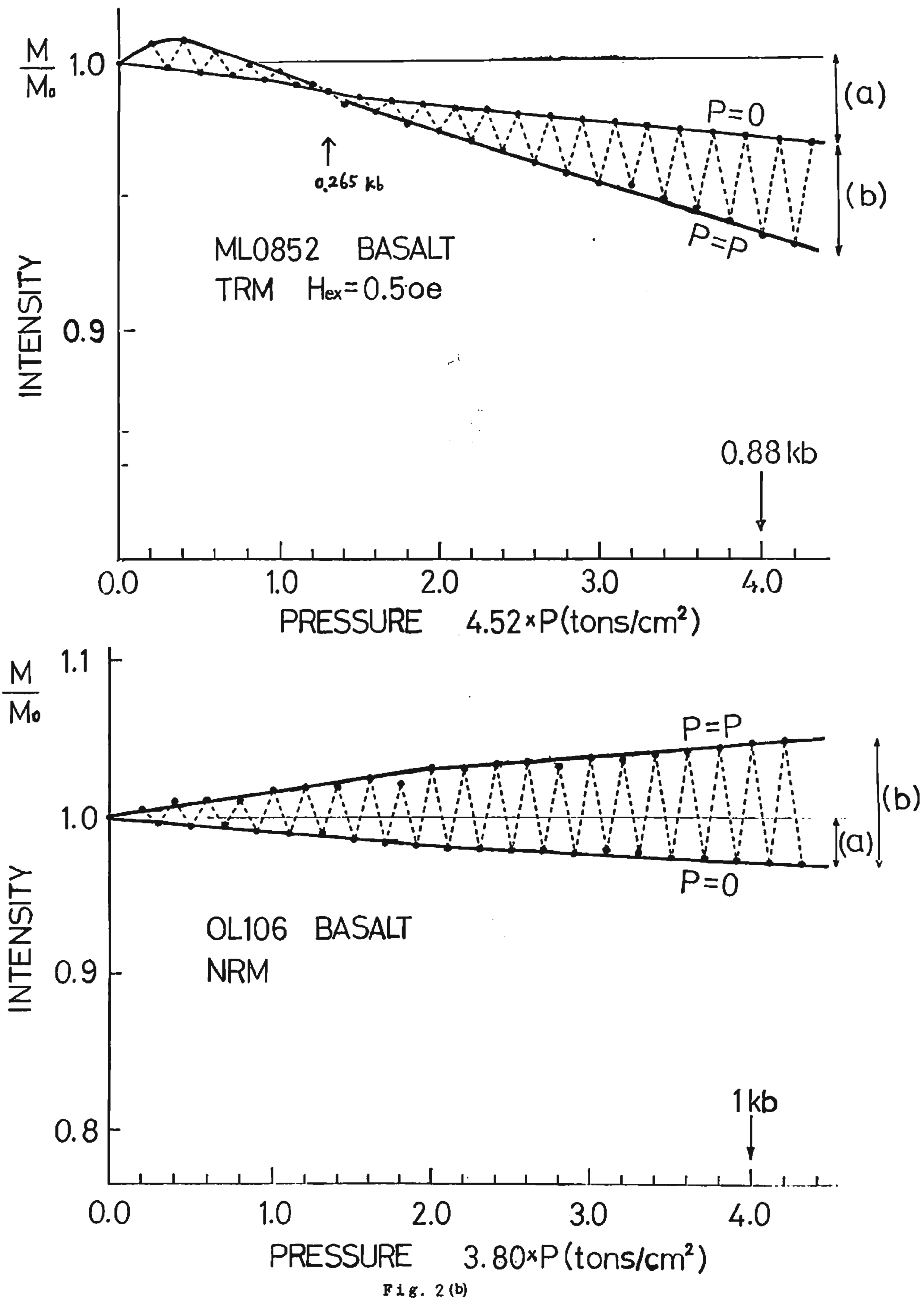
M/M0
1.0
0.9
(a)
(b)
P=0
P=P
0.265 kb
ML0852 BASALT
TRM Hex=0.5oe
INTENSITY
0.88 kb
0.0
1.0
2.0
3.0
4.0
PRESSURE 4.52×P(tons/cm²)
M/M0
1.1
1.0
0.9
0.8
P=P
P=0
(b)
(a)
OL106 BASALT
NRM
INTENSITY
1 kb
0.0
1.0
2.0
3.0
4.0
PRESSURE 3.80×P(tons/cm²)

Fig. 2 (b)

25. Dependence of Remanent Magnetization of Volcanic Rocks upon Moderately High Axial Pressure

Mitiyasu Ohnaka

Geophysical Institute, University of Tokyo

Effects of moderately high axial pressure on the remanent magnetization of volcanic rocks are studied. Remanent magnetizations used in the present study are NRM, TRM(induced in H=0.5 Oe), IRM 1(H=459 Oe), IRM 2 (H=172 Oe), and IRM(H=57 Oe).

Magnetization ($M=\chi H+M_0$) changes reversibly with applied stress if the stress does not exceed an elastic limit of the material. Above the yield point of the material, however, its magnetization generally changes irreversibly. Experimental results on the change in remanent magnetization of volcanic rocks due to purely uniaxial compression are also given in this annual report.

In the present experiment we used a cylindrical high pressure vessel, which is then tightly fitted to the specimen cut in a shape of circular cylinder, 10 mm in diameter and 10 mm in height. Hence, the specimens under such axial compression should be considered to be subject not only to uniaxial pressure (p_1) along its cylindrical axis, but also to confining pressure (p_2) from the side wall of the vessel due to an elastic deformation. Though the confining pressure thus occurred must inevitably reduce the intensity of the pressure within the material (i.e. deviatoric stress $p_1 - p_2$), the stress destribution in the specimen under the compression may be approximated by uniaxial compression. On the other hand it is well known that a brittle rock specimen under purely uniaxial compression becomes ductile, with the increase of the confining pressure. In accordance with this observation, actually, in the present experiment we found that some specimens were not fractured at all even under the external uniaxial compression of 5 kb.

An axial nonmagnetic press used in the present study was made of stainless steel and copper-berylium alloy. Specimens were packed in a nonmagnetic cylindrical high pressure vessel and compressed up to 5 kb with ceramic press anvils made of aluminum oxide.
Measurements of the remanent magnetization of rocks were carried out by an astatic magnetometer in the geomagnetic field after removal of the external compression.

Rock specimens were cut from a basaltic lava of Mt. Fuji collected at Mishima. IRM and TRM were induced either parallel or perpendicular to the cylindrical axis of the specimen. Dependence of remanent magnetization of rocks upon intensity of the axial pressure was examined. The specimens were situated in such a way as the remanent magnetization of the specimen always has a certain direction with respect to that of the geomagnetic field.

Dependence of the intensity of remanent magnetizations upon pressure P are shown in Fig. 1, where $//P$ and $\perp P$ denote the direction of the remanent magnetization parallel and perpendicular to the axis of uniaxial compression, respectively. The curves are well expressed by $M = M_O/(1+ \beta_r P)$, where β_r and P denote numerical constant and pressure measured in units of kb respectively. Being β_r much less than unity, we get first derivative of M with respect to P as

$$\frac{d}{dP}\left(\frac{M}{M_O}\right) = - \beta_r \,(1+ \beta_r \cdot P)^{-2} \simeq - \beta_r$$

From the above eqution, it can be seen that the numerical constant β_r is a measure of stability of the remanent magnetization against the compression P. dM/dP versus P relations are shown in Fig. 2 and values of β_r are summarized in Table 1.

From the experimental results mentioned above, changes in the intensity of remanent magnetization can be summarized as follows;

1) $M(P) = M_0/(1 + \beta_r \cdot P)$, for $\beta_r > 0$

2) TRM is usually more stable than IRM.

3) Unstable component of IRM decays almost completely below P = 1 kb.

4) TRM and NRM show a simillar character.

5) Demagnetization of the component of magnetization parallel to pressure axis is systematically more effective than that of the component perpendicular to pressure axis.

6) Numerical constants β_r of various remanent magnetizations are summarized in the following Table 1.

Table 1

Remanent Magnetization	Magnetizing Field (Oe)	Intensity (emu/gr)	Direction of Remanence	Numerical Constant β_r (1/kb)
IRM 1	459	$3 \cdot 10^{-1}$	// P axis	$(3.4 \pm 0.8) \cdot 10^{-1}$
IRM 1	459	$3 \cdot 10^{-1}$	⊥ P axis	$(2.9 \pm 0.7) \cdot 10^{-1}$
IRM 2	172	$1 \cdot 10^{-1}$	// P axis	$(7.2 \pm 1.5) \cdot 10^{-1}$
IRM 2	172	$1 \cdot 10^{-1}$	⊥ P axis	$(5.6 \pm 0.9) \cdot 10^{-1}$
IRM 3	57	$1 \cdot 10^{-2}$	// P axis	$(14.3 \pm 3.4) \cdot 10^{-1}$
IRM 3	57	$1 \cdot 10^{-2}$	⊥ P axis	$(12.4 \pm 4.0) \cdot 10^{-1}$
TRM	0.5	$5 \sim 6 \cdot 10^{-3}$	Arbitrary	$(2 \sim 7) \cdot 10^{-2}$
NRM		$5 \sim 6 \cdot 10^{-3}$	Arbitrary	$(2 \sim 7) ; 10^{-2}$

Changes in the direction of the remanent magnetization of rocks under compression are summarized as follows;

1) IRM induced in H=459 Oe is very stable and does not show any change up to P=5 kb.

2) IRM induced in the other field such as in H=172 and 53 Oe is considerably unstable.

3) Both TRM and NRM are stable.

4) No systematic difference between $M_{//P}$ and $M_{\perp P}$ can be found.

5) Mean variations in the direction of remanent magnetizations due to compression of 1 kb are summarized in the following Table 2.

Table 2

Remanent Magnetization	Magnetizing Field (Oe)	Intensity (emu/gr)	Change in Direction per 1 kb (deg./kb)
IRM 1	459	$3 \cdot 10^{-1}$	0.0
IRM 2	172	$1 \cdot 10^{-1}$	2.4
IRM 3	57	$1 \cdot 10^{-2}$	23.0
TRM	0.5	$5 \cdot 10^{-3}$	1.4
NRM		$6 \cdot 10^{-3}$	1.4

The auther wishes to express his hearty thanks to Dr. H. Kinoshita for his valuable suggestions and advices in the course of the work. Thanks are also due to Professor M. Ozima who read the manuscript and gave some suggestions.

References

T. Nagata and H. Kinoshita (1965), Jour. of Geomag. & Geoelect., 17, 121-135.

H. Kinoshita and M. Ohnaka (1968), in this report.

M. Ohnaka and H. Kinoshita (1968), in this report.

Figure Captions

Fig. 1 Change in the intensity of IRM, TRM and NRM due to compression in nonmagnetic field, Sample; Fuji basalt collected at Mishima, Notations; see text.

Fig. 2 The rate of the change in remanent magnetization with respect to pressure, calculated from curves in Fig. 1.

Fig. 3 Changes in the direction of IRM, TRM and NRM due to compression, A & B ; IRM 1, C & D ; IRM 2, E & F ; IRM 3, T ; TRM, N ; NRM Samples; Fuji basalt.

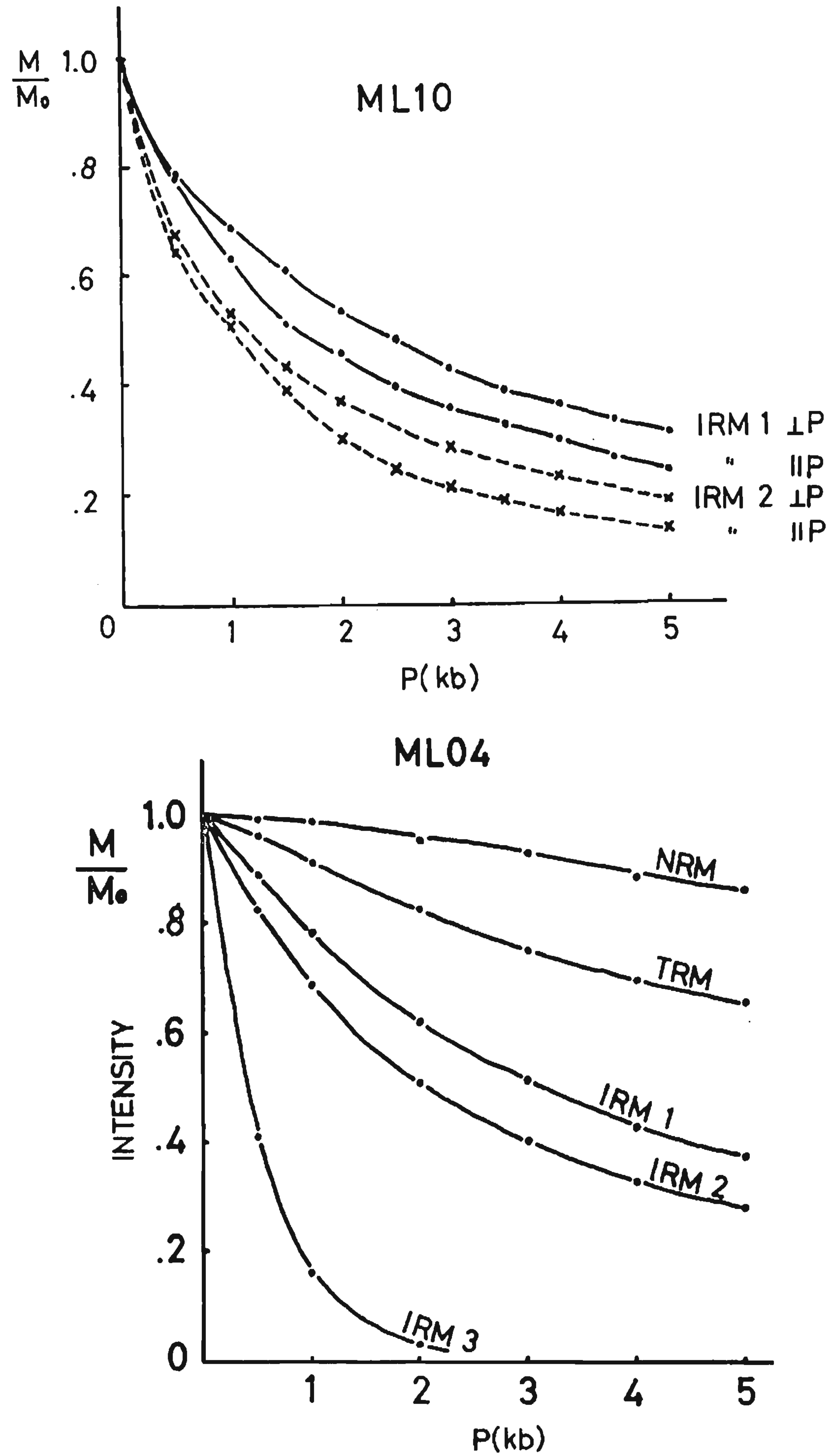
ML10
M/Mo
1.0
.8
.6
.4
.2
0
1
2
3
4
5
P(kb)
IRM 1 ⊥P
" ∥P
IRM 2 ⊥P
" ∥P
ML04
M/Mo
INTENSITY
1.0
.8
.6
.4
.2
0
1
2
3
4
5
P(kb)
NRM
TRM
IRM 1
IRM 2
IRM 3

Fig. 1

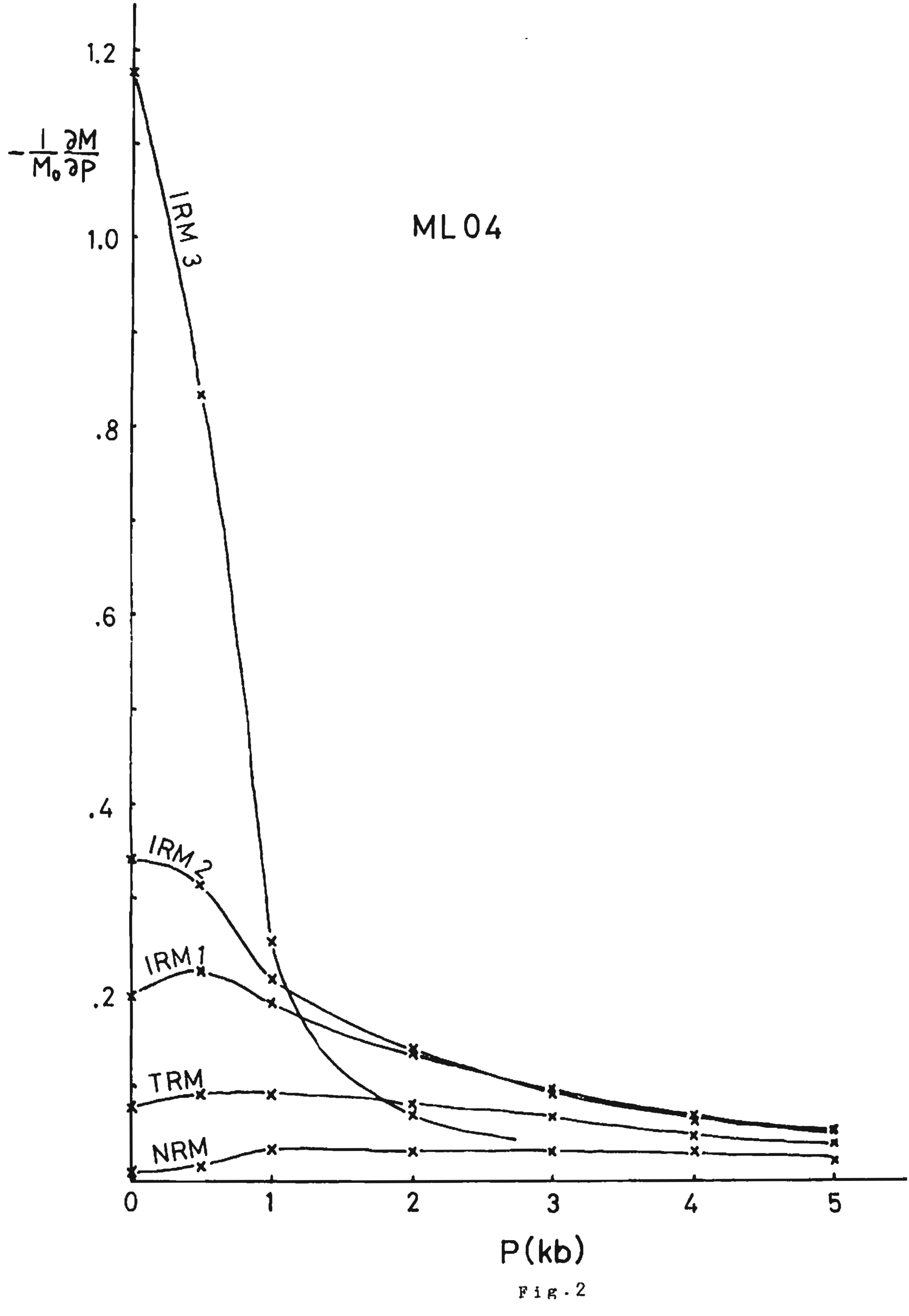

1.2
$-\frac{1}{M_0}\frac{\partial M}{\partial P}$
1.0
.8
.6
.4
.2
ML 04
IRM 3
IRM 2
IRM 1
TRM
NRM
0
1
2
3
4
5
P(kb)

Fig. 2

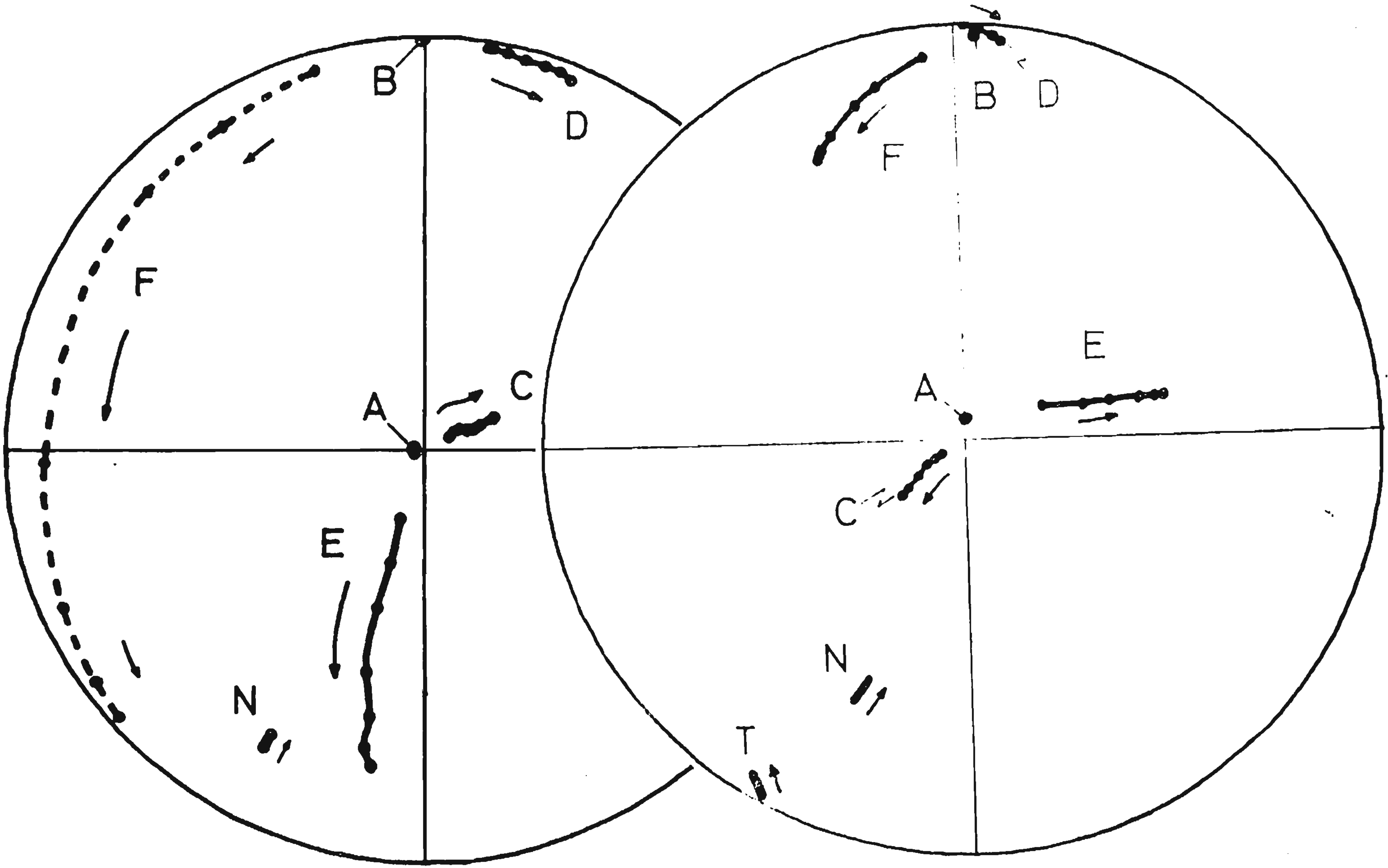

ML 018 ML 080

Fig. 3

26. Deformation Studies in Rock Magnetism

R. S. Carmichael

Department of Physics, Faculty of Engineering Science

Osaka University

The investigation of the effect of deformation on magnetic minerals and rocks serves two purposes for the study of rock magnetism. First, it indicates aspects of the magnetomechanical character of earth materials such as magnetite and hematite. An understanding of the effect of applied stress on the characteristics of low-temperature magnetic transitions and memory (Kawai and Ono 1966, Carmichael and Fuller 1967), susceptibility (Nagata and Kinoshita 1965, Nagata 1966a), magnetostriction and magnetocrystalline anisotropy (Kinoshita and Nagata 1967, Sawaoka and Kawai 1967), and remanence (Carmichael, 1968) of such minerals indicates their fundamental magnetic nature. The interpretation of some of the magnetomechanical effects for single-domain behaviour has been given as dependent essentially on magnetostatic energy and bulk magnetostriction (Nagata, 1966b). For a multidomain situation, a more appropriate approach might be the response of a multidomain configuration to anisotropy energies present during changes in the internal stress state-changes caused by rearrangement of structural defects (Carmichael, 1968). Secondly, the basic knowledge may be applied to help reveal a specimen's environment during formation, such as the paleomagnetic field, and its subsequent history. An interesting example of the latter that merits further investigation is the use of deformation-induced anisotropy of mechanical (Karp and Donath, 1966) or magnetic (Graham, 1966) properties to determine the orientation and magnitude of stresses acting in the geologic past. Such a study would be useful for rocks affected by dynamic metamorphism. Knowledge of the magnetic anisotropy imposed by deformation might make some metamorphic rocks more useful for paleomagnetism than they currently are.

Relatively few rocks now sampled for paleomagnetism were formed at the Earth's surface and remained undisturbed by any change in their stress environment. Most were formed in the upper region of the crust and exposed after uplift and erosion, or formed at the surface and then underwent one or several cycles of burial and erosion. A consideration of Curie temperatures and the Earth's thermal gradient indicates that titanomagnetites and ilmenohematites should retain appreciable magnetization down to a pressure regime of 4 to 6 kbar. A pressure of 10 kb is expected at the depth of the Moho (Wyllie, 1963). Some rocks have thus probably been subjected to several kbar of lithostatic confining pressure, either at the time of acquisition of their initial remanent magnetization, or afterwards with further burial. In addition, there may be directed stresses resulting from tectonic movements on a local or regional scale. These may occur repeatedly throughout the geologic history of the sample, with different magnitudes and orientation of principal stresses.

The presence of isotropic confining pressure should not be assumed to imply a condition of isotropic strain. No crystal lattice structure, including the cubic, is mechanically and magnetically isotropic. For example, Young's elastic modulus of cubic magnetite is about 10% greater in the [111] direction than in the [100] at room temperature (Fine and Kenney, 1954), the difference increasing with higher temperature. The anisotropy of mechanical properties would be expected to be more pronounced in a structure with lower symmetry, such as hematite. The magnetization, in magnitude and symmetry, is a function of exchange interaction and thus interatomic distances. Because of anisotropy of linear compressibilities, a uniform confining stress produces an anisotropic internal strain and thus magnetic anisotropy. This directional dependence of strain-induced changes in the interatomic distances makes the effect of confining pressure somewhat analogous to that of a directed stress. A better knowledge of the induced strain anisotropy may assist in interpreting the magnetic anisotropy of crystals under hydrostatic pressure.

Moderate, strictly elastic stress gives magnetomechanical effects which are particularly large for a multidomain magnetostrictive material such as coarse-grained titanomagnetite. For example, significant changes in the magnitude, and even the direction, of the "natural" remanent magnetization of specimens with an appreciable fraction of magnetically "soft" moment can be produced by experiments as simple, if undesirable, as dropping a sample on a table or handling it roughly during shipment. Application of elastic uniaxial compression gives irreversible changes of remanence in multidomain magnetite crystals (see Fig. 1). Increasing compression cycles causes a uniform decrease in an initial saturation isothermal remanent magnetization (IRM). The rate of decrease and limiting value are dependent on the magnitude of the ambient magnetic field. Sufficient deformation in a reversed field will induce a reversed remanence, again with a limiting value. In fact, the ultimate moment is independent of the magnitude of the initial IRM-from zero to the saturation value. A further point (Shapiro and Ivanov 1966, Carmichael 1968) of considerable significance is that even elastic stressing of a sample in a field produces a remanent magnetization larger and more relatively stable than the IRM from the field present during deformation, and more stable than the larger IRM giving the same initial moment as that given by the deformation. This is shown by the alternating-field demagnetization in Fig. 2. It is noted that the deformation moment has a significantly different spectrum of microscopic coercivities (obtained by differentiating the demagnetizing curves) than simple IRM. The given deformation in a field of 22 oe has produced a fraction of remanence with a coercivity of 100 oe--equal to that produced by an IRM from about 200 oe.

Thus the deformation moment, particularly in a multidomain material, is not virtually the same as IRM in stability and mode of acquisition, as if often assumed. All aspects of the behaviour represented in the Figures can be satisfactorily explained by the structure-dependent model referred to previously.

The effects due to plastic deformation should be even more pronounced, probably affecting the direction as well as magnitude of the remanent moment. This is because the higher stresses and irreversible structural changes cause an increased magnetomechanical interaction of the material's physical state with its magnetic domain pattern. Further, such structure-sensitive properties as coercive force are changed. The combination of long time, stresses, and mechanical and magnetic viscous effects, acting on rocks in the upper crust, would be expected to cause some irreversible plastic deformation. This might not be macroscopically observable. It is comforting that the major deformation effects seem to be associated predominantly with the softest, and thus least stable, magnetization. Thus a proper partial demagnetization should render rocks subjected to moderate deformation fit for paleomagnetic studies. However, the use of virgin "natural" remanence to draw conclusions as to paleomagnetic pole position and paleointensity of the Earth's field, without first ensuring that there is not a significant fraction of soft magnetization, may be a hazardous undertaking at best. This is especially true when the rocks are taken from a locality of apparent past tectonic activity. When an appreciable portion of a collection must be granted anonymity for being "unstable" or "unreliable", there may be good reason to suspect the past influence of applied stress even if only elastic.

Many of the past experiments that have been conducted to investigate the effect of deformation on magnetization and magnetic properties of minerals and rocks have been limited in their faithful representation of conditions in the Earth's crust. Present work is aimed at combining known conditions of hydrostatic pressure, ranging up to 10 kb, and directed stress to induce plastic deformation. The accompanying changes in such magnetic parameters as coercivity and remanence will be observed. The apparatus being used is a modification of that described by N. Kawai and A. Sawaoka elsewhere in this volume. The nonmagnetic pressure bomb is portable, allowing it to be removed from the press to other apparatus for measurement.

It is a pleasure to acknowledge the Japan Society for the Promotion of Science for support of the author during this work.

References

Carmichael, R. S. (1968), Phil. Mag., in press

Carmichael, R. S. and M. D. Fuller (1967), Nature, 216, 365

Fine, M. E. and N. T. Kenney (1954), Phys. Rev., 94, 1573

Graham, J. W. (1966), in The Earth Beneath the Continents, ed. by J. S. Steinhart and T. J. Smith, A.G.U.

Karp, E. and F. A. Donath (1966), Transactions A.G.U., 47, 187

Kawai, N. and F. Ono (1966), Physics Letters, 21, 279

Kinoshita, H. and T. Nagata (1967), J. Geomag. Geoele., 19, 77

Nagata, T. (1966a), J. Geomag. Geoele., 18, 73

Nagata, T. (1966b), J. Geomag. Geoele., 18, 81

Nagata, T. and H. Kinoshita (1965), J. Geomag. Geoele., 17, 121

Sawaoka, A. and N. Kawai (1967), Physics Letters, 24A, 503

Shapiro, V. A. and N. A. Ivanov (1966), Akad. Nauk. SSSR, Izv. Fizika Zemli, 10, 97

Wyllie, P. J. (1963), in High Pressure Physics and Chemistry, Vol. 2, ed. by R. S. Bradley, Academic Press

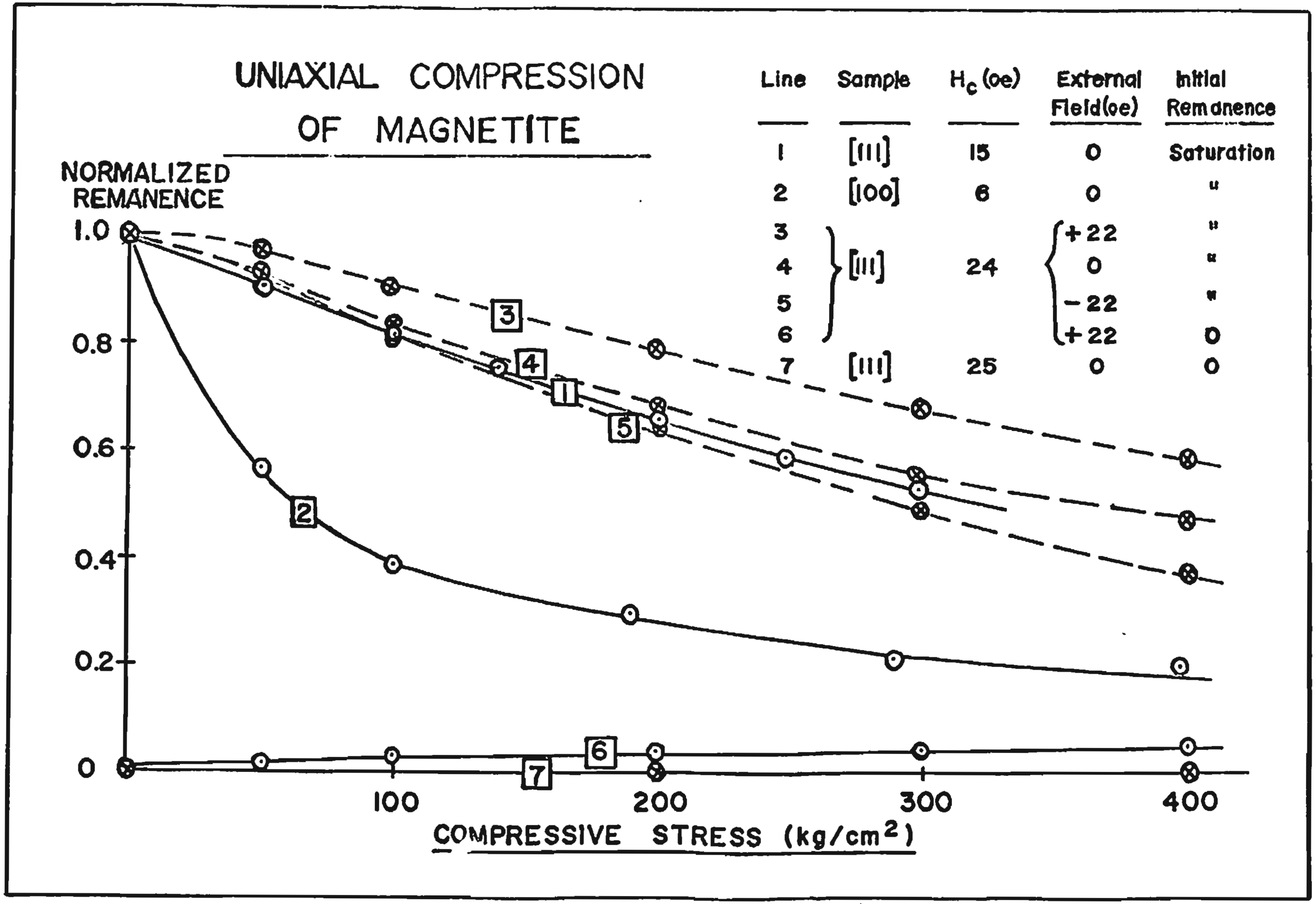

Fig. 1. Change of remanence produced by uniaxial compression of magnetite single crystals. Remanence normalized with respect to initial saturation IRM. Stress applied in non-magnetic press; field applied with solenoid.

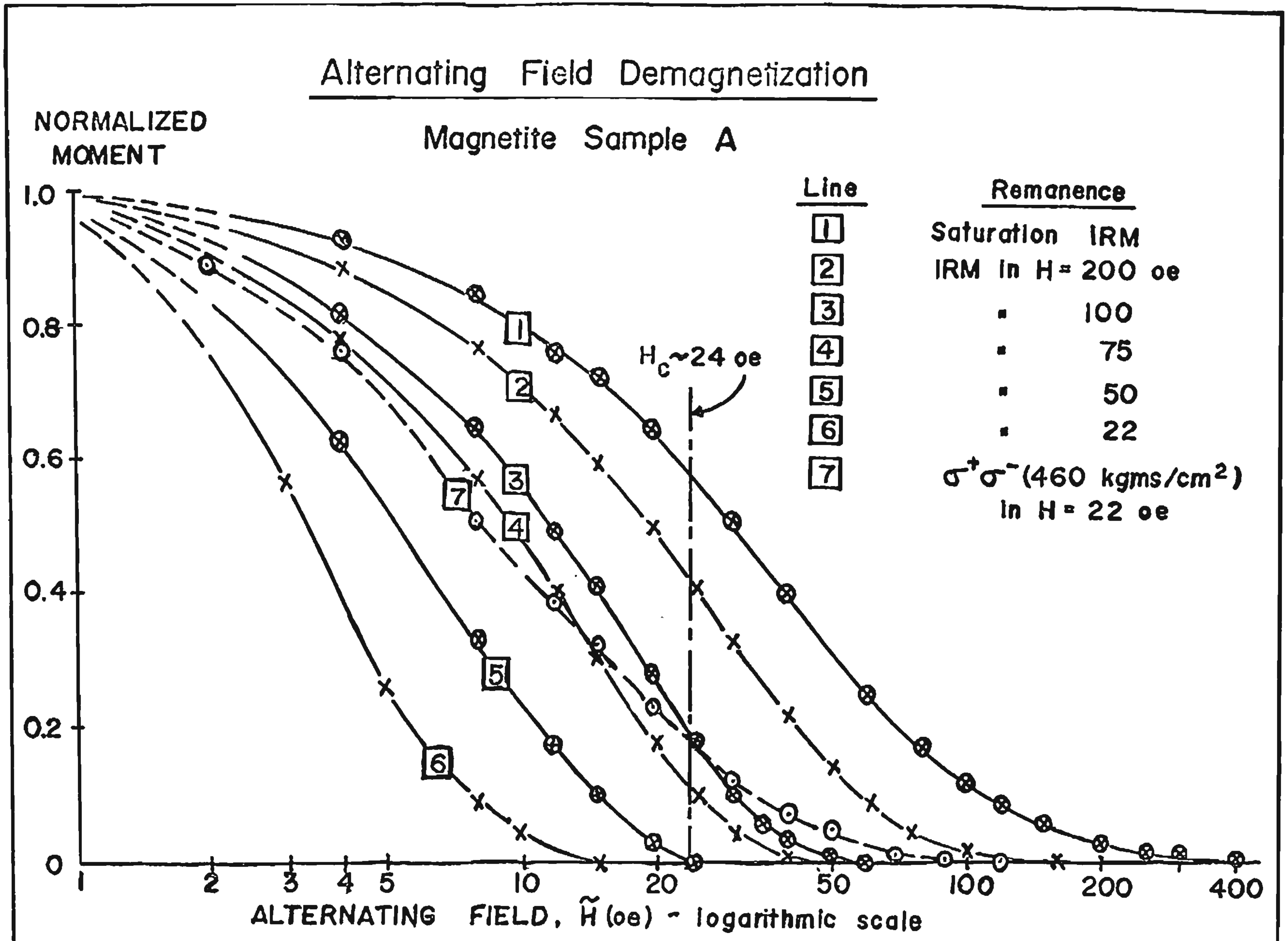

Fig. 2. Alternating-field demagnetization of remanences for magnetite [111] single crystal. Normalized with respect to initial moment. Deformation by 460kg/cm² (Line 7) produces same moment as IRM from field of 60 oe.

27. Magnetic Properties of Ferromagnetic Minerals of Pumice in Tephra 1

K. Momose, Kunio Kobayashi,

K. Minagawa and M. Machida

Department of Geology, Faculty of Science,

Shinshu University

Correlation of tephra horizon is usually difficult unless such coarse materials as pumices or scoriae are visible by their occurrence within the tephra section.

Ordinary pumices and scoriae would, however, consist of a rather unvaried assemblage of a few kinds of mineral, because most of volcanic products erupted in the Late Quaternary are andesitic in composition. Examination of mineral composition is inevitably not always valid to identify origination or sources of materials.

We now are examining, by means of natural titaniferous magnetite contained in pumices, whether or not the thermo-magnetic properties prove to be characteristic to each pumice. More than 200 samples were measured with respect to thermomagnetic properties of natural titaniferous magnetite of which the grain-size averages 0.1 mm.

As to five sheets of pumice (including scoria) deposits which within the tephra section of the Ontake volcano range from $5\sim6\times10^4$ to 2.7×10^4 years ago, titanomagnetic mineral contained in each bed, respectively shows, from lower to upper, the pertinent Curie temperature being 555°C, 450°C, 425°C, 400°C and 240°C. With the decrease of the Curie temperature, is indicated also an increase in cell dimension of the titanomagnetites in question.

The Curie temperature of titanomagnetite contained in 9 sheets of pumice in South Kanto district which mostly are supposed to have originated from

Hakone volcano, ranges from 290°C to 350°C. The relation revealed between magnetic properties and cell dimensions of titanomagnetite in taphra demonstrates a similar relation standing between the former and titanomagnetite in volcanic rocks, as previously obtained from the solid solution in the $TiFe_2O_4$ - Fe_3O_4 series (Akimoto and Katsura 1959).

Recently Aoyagi and Iwasaki (1967) have called our attentions to the fact that in tephra TiO_2 decreases in amount with an increase of grain-size --- especially above 0.1 mm in diameter of titanomagnetite, whereas the amount of TiO_2 is nearly the same between the grains smaller than 0.1 mm.

Another measurements were undertaken to examine the mode of the thermomagnetic curve in relation to Ti-content and the grain-size of titanomagnetite. Titanomagnetite of the pumice fall deposits Pm-I from Ontake volcano was sieved and fractionated into 5 classes, i.e. $\phi \geq 0.25$ mm, $\phi = 0.25 \sim 0.5$ mm, $\phi = 0.15 \sim 0.11$ mm, $\phi = 0.11 \sim 0.07$ mm, $\phi = 0.07 \sim 0.06$ mm (Fig. 1).

(i) No significant relation is observed between the size of particles and the pertinent Curie temperature of titanomagnetite, all of which being lower than 450°C.

(ii) The smaller the grain is, the easier titanomagnetite is apt to be oxidized during heating process, so that the sample whose grain-size is between 0.074 ~ 0.060 mm may possibly have somewhat a lower Curie temperature than 450°C.

As Akimoto and Katsura (1959) discussed, a volcanic rock sample may be composed of numerous kinds of titanomagnetite having different Curie temperatures, thermomagnetic separation method is to be employed for our future study.

From the measurement thus made, one thing is clear that the pumice-fall deposit Pm-I from Ontake volcano can be identified in South Kanto district, by its characteristically high Curie temperature different from those of the so-called "Kanto Loam". Secondly, titanomagnetite in pumice sensitively reflect the varying composition of associated magma through volcanic activity, hence the magnetic properties of titanomagnetite may well afford a basis for identification of the origination of pumice.

Professor Akimoto, Drs. Kazuo Kobayashi and H. Kinoshita undertook some experiments for this study, also kindly took part in the discussion. To these persons we are greatly indebted.

References

Akimoto, S. and Katsura, T. (1959), Journ. Geomag. Geoelectr., 10, 69.

Aoyagi, R. and Iwasaki, I. (1967), Quat. Res., 6, 44.

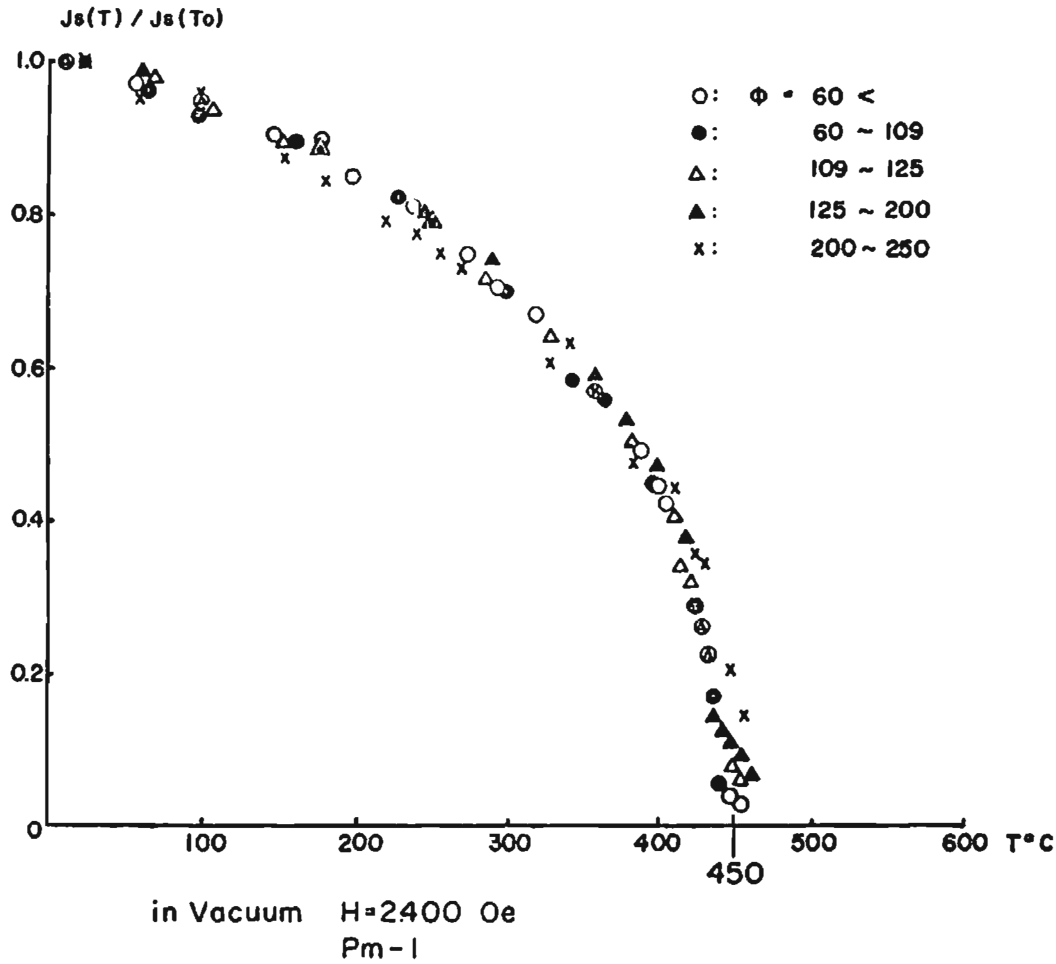

Fig. 1 Thermomagnetic curves of titanomagnetite of the pumice-fall deposit Pm-I in various grain-size fractions.

28. A Simply Designed Home-Made Micro Balance and Its Application to a Palaeomagnetic Study

Haruo Domen

Faculty of Education, Yamaguchi University

A home-made micro balance simply designed which is able to weigh the mass of a small specimen of the order from one gram to one milligram. To weigh may be available for only few minutes. And this micro balance is very useful to be a main part of a thermo-magnetic analyzer, say a Curie-point meter.

In recent, commercial automatic micro balances have been greatly developed in the products but still these are so dear for the reconstruction to the various purposes in the laboratory use. Since more than several years ago, the present author has built by himself and used for rock magnetic investigation some of micro balances which be made of the fused quartz, such as Kawai's genuine balance (see Clark's paper in 'methods in palaeomagnetism' 1967, Elsevier). The simplest designe amongst them is illustrated in this paper.

The main system of the presented micro balancc is constructed by a spiral, a rigid beam and a point indicator as shown in figure 1. In this figure A is a spiral of ca. 6 cm in diameter made of the fused quartz beam which has a diameter of about 1 mm. B, the center of the spiral A which is to be supported by a rotating shaft with a revolving dial. C is a rigid stem with some knots, at where be hung down a sample holder in the suitable distances from A, and a sharp end pointer D is an indicator against a mirror fixed on the side wall of a container in which the whole system of this micro balance may be settled. A, B, C and D are made of single beam of the fused quartz and are all in the same vertical plane.

The quartz rod shaft which supports the center of the spiral, B, is available to be revolved by means of a revolving device and the rotating angles of the shaft may be read as the numerals. Using a dial borne a circular scale with an aid of a vernier, it is easy to read one tenth of the minimum scale-division of the main circular scale of revolving dial.

The sensitivity of this micro balance mainly depends on the dimension of the spiral A; such as a diameter of the spiral, the number of turns, a diameter of the quartz beam itself and so on. When a sample holder loaded a specimen desired to be weigh had been hanged down at a suitable knot (k_1, ... 4, in figure 1) on the beam C, the spiral might be expanded, then the pointer D has moved downwards. The dial should be revolved and the pointer D has to be restored manually to the initial position; the rest point of the whole system before loading the specimen is easily recognized by the mark scratched on the attached mirror against D.

The calibration of weighing may easily be made in advance such a way that the known weights, i.e. a set of the weights for a chemical balance, has been placed on the sample holder basket at every knot of the stem C. The calibration curves, say the weights v.s. the scale readings, are obtained for each knot and weighing is wonderfully so swift; it takes only less than three minutes and also so convenient; the weighing of one-milligram-specimen at the end knot k_1, the nearest neighbor to the pointer D, is available and a one-gram-weighing on k_4, at the root of C.

An application of the micro balance thus made is to use as a balance for the thermo-magnetic analyzer. The present author has put this micro balance system on an electro-magnet assembly and the long stem with a weighing basket at its end which is also made of the fused silica, takes the place of the ordinal sample holder and then the basket with the ferromagnetic grains come from a palaeomagnetic sample is hung down into an electric furnace with a water jacket set at the gap of a pair of the pole pieces of the magnet and it is able to measure the changes of the saturation magnetization intensity of the specimen with the rising temperatures; that is to say the magneto-thermal analysis may easily be made. Typical thermo-magnetic curves obtained by means of this simply designed micro thermo-magnetic balance are illustrated on figure 2.

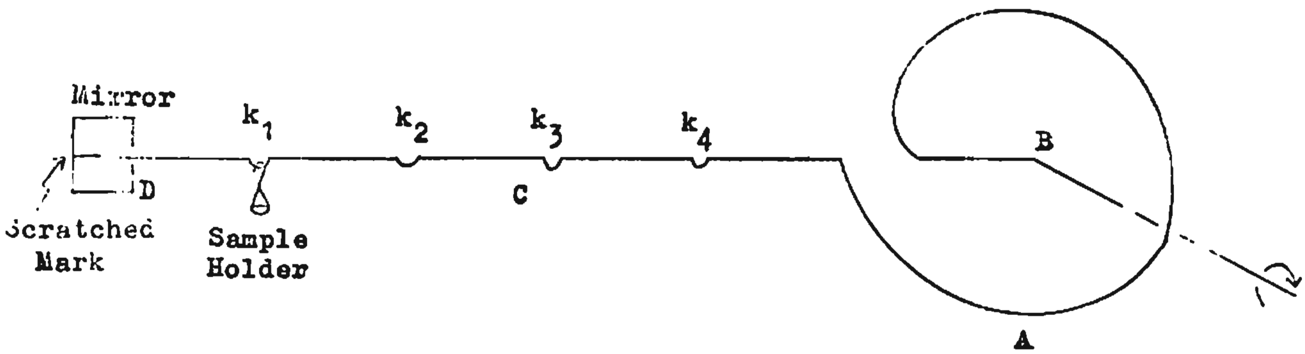

Fig. 1. Schematic view of the main system made of the fused quartz.

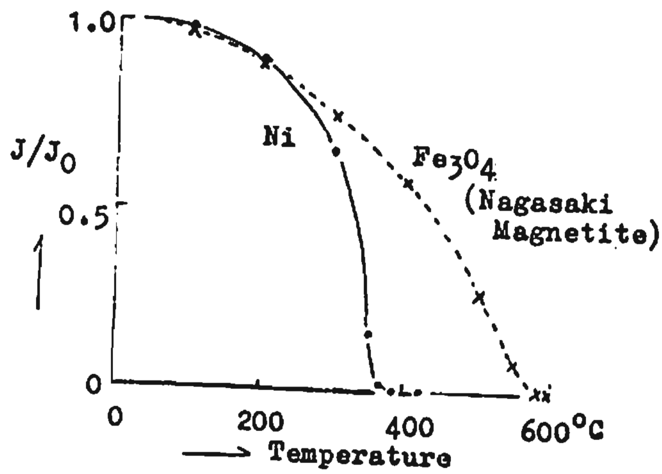

Fig. 2. Typical examples of the thermo-magnetic curves obtained by means of the home-made micro balance.

29. Some Techniques on Magnetic Measurements under Hydrostatic Pressure

N. Kawai and A. Sawaoka

Department of Physics, Faculty of Engineering Science,

Osaka University

A technique was developed to make magnetic observations of materials possible under hydrostatic pressure up to 12 kilobars in a wide temperature range from liquid helium temperature up to 200°C. We made two kinds of non-magnetic pressure vessels in which the materials to be measured were inserted. For measuring susceptibility or saturation magnetization, the pressure vessel was connected to a torsion pendulum and its deflection in a magnetic field was measured. For measuring remanent magnetism, the vessel was placed under an astatic magnetometer, and the latter's deflection was observed. For measuring anisotropy of ferro-magnetic single crystals, the vessel was connected to an air-bearing torque magnetometer having an unbonded strain gauge detector, and its torque moment in a uniform magnetic field was determined.

Detachable Type Non-magnetic High Pressure Vessel (Kawai and Sawaoka, 1967)

For the material of the above-mentioned pressure vessel, we employed hardened Cu-Be alloy whose Be concentration is 1.82 in Wt. %. In Fig. 1 (a) are shown the details of the vessel we have made. Kerosene and electric transformer oil in a 1:1 mixture were used for the pressure transmitting medium. The mixture was compressed with a Bridgman type intensifier and was sent through the stainless steel pipe A into the sample space of the vessel. When the oil pressure inside the vessel reached the value desired for the experiment, the pipe jacket B was unscrewed, and the connector A was disconnected from the vessel. Internal oil pressure was maintained by the action of the cone shaped nonreturn valve D. The pressure in the vessel was carefully calibrated with an attached manganin gauge, while the temperature was observed using a thermocouple. Lead wires were taken out of the vessel through the walls of plug G. In Fig. 1 (a) is also shown another cone valve E which was used to release the oil pressure.

Locking Type Non-magnetic High Pressure Vessel:

This vessel is a modification of the bomb which was first made by Itskevich (1962). Details of this vessel are shown in Fig. 1 (b). Pressure was produced in the sample chamber of the bomb by driving a piston C by a hydraulic press. After the desired pressure was attained, the piston locked tightly to the cylinder B with an attached screw nut B.

These two type of vessels can be connected directly to a torsion pendulum (Kawai and Sawaoka, 1967) for measuring magnetization and to an air-bearing torque magnetometer (Kawai and Sawaoka, 1967, 1968) for measuring magnetic anisotropy. They also can be placed under our astatic magnetometer when the effect of pressure on the remanent magnetism of materials was desired.

In Fig. 2 are shown some typical magnetization curves of Dy (Kawai and Sakakihara, 1968) with varying temperature under high pressure. In Fig. 3 are shown some typical torque curves of Fe_3O_4 (Sawaoka and Kawai, 1967) at room temperature under high pressure.

References

N. Kawai and A. Sawaoka (1967), Rev. Sci. Instrum., 38, 1770.

E. S. Itskevich (1962), P.T.É., No.4, 148.

N. Kawai and A. Sawaoka (1968), J. Phys. Chem. Solids., to be published, No. 3.

N. Kawai and M. Sakakihara (1968), to be submitted to the J. Phys. Soc. Japan.

A. Sawaoka and N. Kawai (1967), Phys. Letters, 24A, 503.

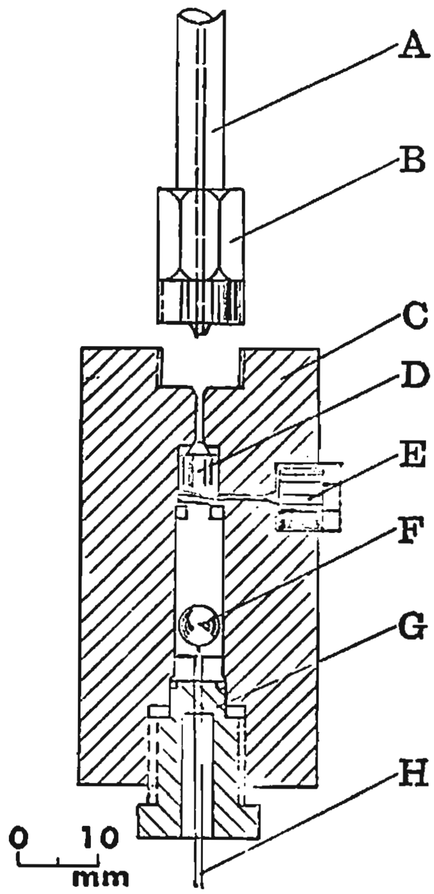

Fig. 1(a) Detachable Type Non-magnetic High Pressure Vessel.

A - stainless steel tube,
B - connector,
C - bomb,
D - cone type nonreturn valve,
E - cone type leak valve,
F - sample,
G - plug,
H - electric lead wires or thermocouple.

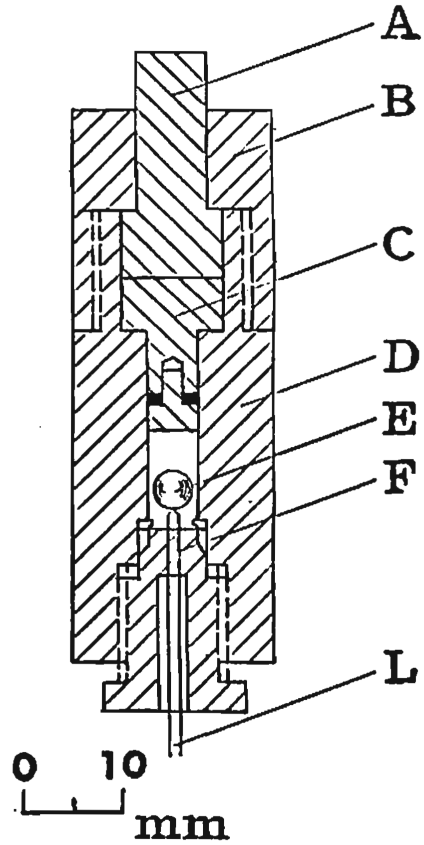

Fig. 1(b) Locking Type Non-magnetic High Pressure Vessel.

A - rod transmitting the force,
B - locking nut,
C - piston with mushroom type packing,
D - bomb,
E - sample,
F - plug,
L - electric lead wires or thermocouple.

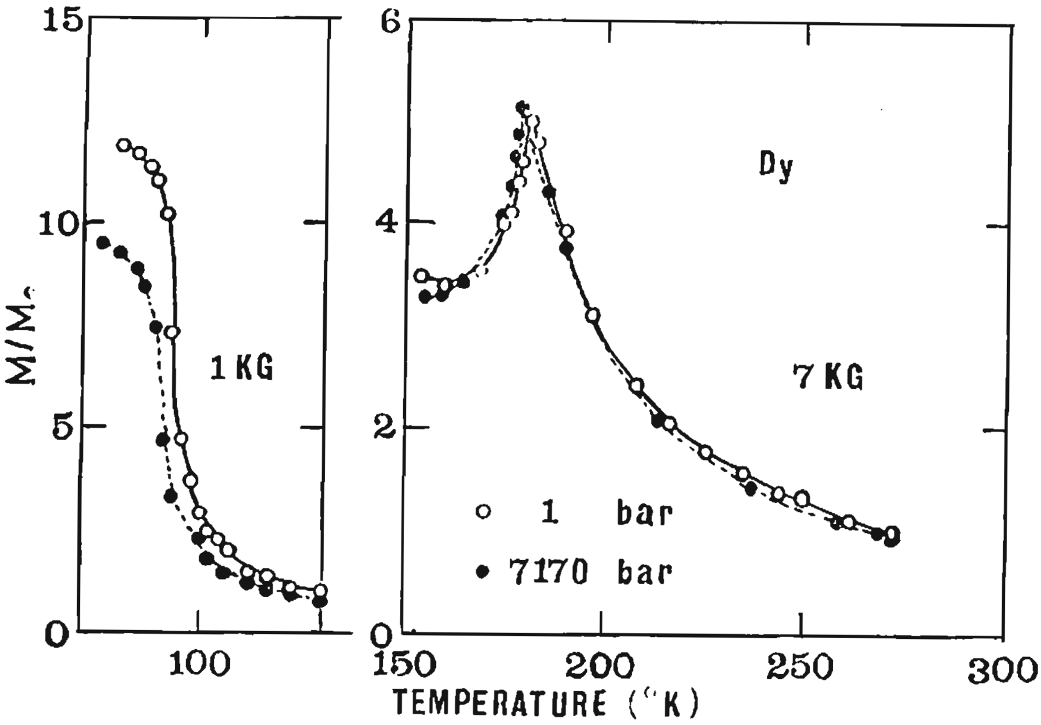

Fig. 2. Magnetization curves of dysprosium under hydrostatic pressure.

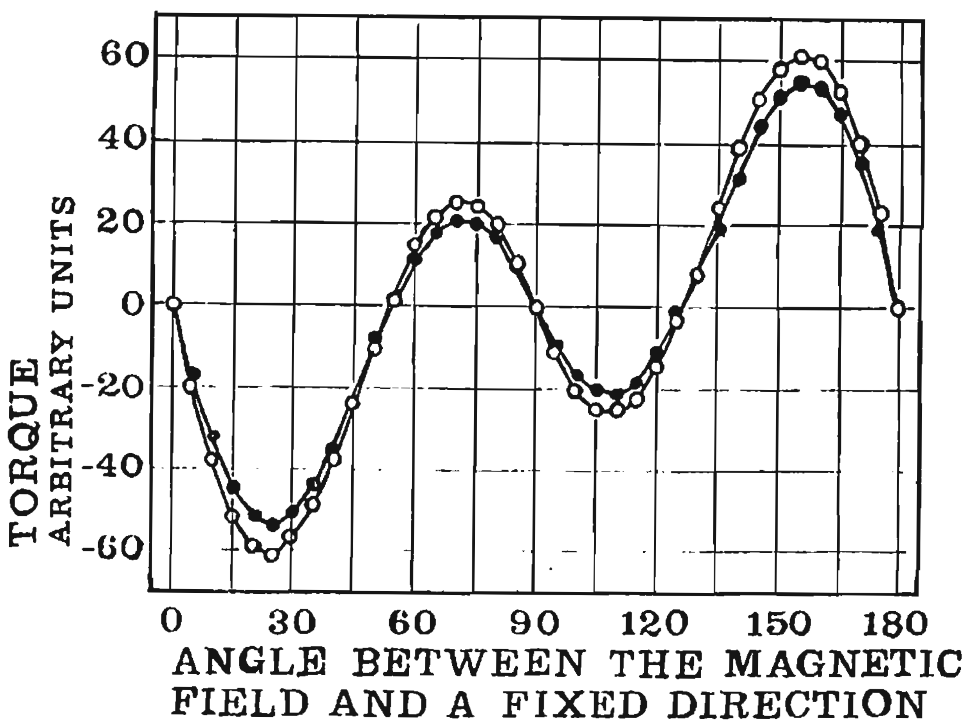

Fig. 3. Torque curves of magnetite(Fe_3O_4) single crystal in the (110) plane at room temperature under an applied field of 9600 Oe. The open and closed circles show the vales observed under 1 bar and 9240 bar, respectively.